Université de Montréal

Synthesis of a Biotin-functionalized biguanide for the identification of the tumor growth inhibition mechanism of Metformin

Par

Farzaneh Mohebali

Département de chimie

Faculté des arts et des sciences

Mémoire présenté à la Faculté des études supérieures et postdoctorales

En vue de l'obtention de grade de

Maîtrise ès sciences (M.Sc.)

en chimie

août 2017

Acknowledgments

At the beginning, I would like to show my appreciation for my advisor, Prof. Andreea Schmitzer for trusting and offering me this honorable opportunity to study and work as one of her group's member. She supported me throughout my thesis with her patience and knowledge. I also want to thank all the members of Prof. Andreea Schmitzer's group for their helpful suggestion and comments regarding this project.

I present my appreciation of the Department of Chemistry, Université de Montréal for providing the required facilities and suitable environment to pursue my Master's degree. I owe appreciation to all those who have supported me to reach the results of my thesis, especially Dr. A. Fürtös, K. Venne, and M-C. Tang from the Laboratory of Mass Spectrometry, Sylvie Bilodeau, Antoine Hamel and Cedric Malveau from the Laboratory of NMR Spectroscopy and Francine Belanger-Gariepy from the Laboratory of X-ray Analysis, at the Université de Montréal. I thank them for their assistance to perform many of the analyses herein.

I thank my family for their love and support. Last but not the least, I thank my husband for all of his support and efforts during the completion of this research.

Résumé

La metformine est largement utilisée pour réduire le taux de glycémie dans le cas des patients souffrant de diabète de type 2. Dans des études récentes, les chercheurs ont observé une association inverse entre l'utilisation de la metformine et le cancer dans différents tissus. L'inhibition du complexe I de la chaine respiratoire des mitochondries a été considéré responsable pour l'activité antinéoplasique de la metformine, mais le mécanisme par lequel la metformine conduit à inhiber le complexe I et, par conséquent, la prolifération des cellules cancéreuses, n'a jamais été entièrement démontrée ou comprise.

Dans cette thèse, nous nous somme proposé d'identifier le mécanisme d'action de la metformine et de sa cible dans les mitochondries, en fonctionnalisant la biguanide analogue de la metformine avec de la biotine. Des extraits de mitochondries ont mises en contact avec la metformine biotinylée et ont été séparés sur des colonnes d'affinité contenant de la streptavidine immobilisée. Les protéines éluées après les étapes de lavage ont été analysées par LC-MS/MS et leurs séquences analysées en utilisant l'algorithme BLAST (NCBI). Nous avons isolé et identifié par spectrométrie de masse (MS) une protéine de 8 KDa qui lie spécifiquement et directement la metformine. Cette protéine a été identifiée comme étant la sous-unité de la ATP synthase. Nos résultats suggèrent que la metformine inhibe la prolifération des cellules cancéreuses par l'inhibition directe de l'ATP synthase de la chaîne respiratoire mitochondriale.

Les travaux présentés dans cette thèse ont été réalisés dans le département de chimie, en collaboration avec le département de biochimie et médecine moléculaire de l'université de Montréal.

Mot-clés : metformine, biguanide, biotine, streptavidine, chromatographie d'affinité, anticancéreux, complexe I, ATP synthase, chaîne respiratoire des mitochondries

Abstract

Metformin is widely used to reduce high blood sugar levels in type 2 diabetes patients. In recent studies, researchers observed an inverse association between metformin use and cancer incidence in different tissues. Inhibition of the mitochondrial respiratory complex I has been proposed to be the cause of the antineoplastic activity of metformin, but the mechanism by which metformin inhibits the complex I and consequently stops proliferation of cancer cells was not fully identified and understood.

In this thesis, we present the functionalization of a biguanide. A metformin - biotin conjugate was synthesized and used to identify the mechanism of action of metformin and its target in mitochondria. Mitochondrial extracts were put in contact with the biotinylated biguanide and were passed over affinity columns containing immobilized streptavidin. The proteins eluted after the washing steps were analyzed by LC-MS/MS and their sequences analyzed using the BLAST algorithm (NCBI).

We isolated and identified by mass spectrometry (MS) an 8 KDa protein that specifically and directly binds metformin. This protein has been identified as the ATP synthase-subunit e. Our results suggest that metformin inhibits cancer cell proliferation through the direct inhibition of the ATP synthase of the mitochondrial respiratory chain.

The research presented in this thesis has been performed in the Department of Chemistry, in collaboration with the Department of Biochemistry and Molecular Medicine, at the University of Montreal.

Keywords: metformin, biotin, streptavidin, affinity chromatography, anticancer, complex I, ATP synthase, biguanide, mitochondria respiratory chain,

Table of Contents

List of Figures

List of Schemes

List of Tables

List of Abbreviations

ADA	American Diabetes Association
ADP	Adenosine triphosphate
ACC	Acetyl-CoA carboxylase
AF	Acid Formic
ATP	Adenosine triphosphate
AMP	Adenosine monophosphate
AMPK	5-activated protein kinase
A6L	protein encoded by mitochondria DNA
Bcl-2	B-cell lymphoma 2
BCA	bicinchoninic acid
br	Broad (spectral)
BFB	Biotin functionalized biguanide
BSA	Bovine serum albumin
^{o}C	Centigrade
CBP	A protein in the human cells
CHREBP	Carbohydrate responsive element binding protein
CREB	cAMP response element-binding protein
CM	Conditioned medium
d	Doublet
DNA	Deoxyribonucleic acid

DMEM	Dulbecco's modified eagle media
2D	Two dimension
Da	Dalton
DCD	Dicyandiamide
DCM	Dichloromethane
DMF	*N*,*N*-dimethylformamide
DMSO-d_6	Hexadeuterodimethyl sulfoxide
EDC	N-(3-Dimethylaminopropyl)-N′-ethylcarbodiimide
ECL	Enhanced chemiluminescence reagent
E. coli	*Escherichia coli*
EASD	European Association of study of Diabetes
FAS	Fatty acid synthesis
G6P	Glucose-6-phosphate
g/mole	Gram per mole
h	Hour
HK	Hexokinases
HER2/neu	A type of receptor tyrosine kinase
HRMS	High-resolution mass spectrometry
H. sapiens	Homo sapiens
IR	Infrared
IC50	The half maximal inhibitory concentration
IL-6	Interleukin-6
IFNγ	Interferon gamma

IL-2	Interleukin-2
IF1	Inhibitor factor 1
IRSI	Insulin receptor substrate 1
IGF1	Growth factor 1
J	Coupling constant
K_D	Dissociation constant
KDa	Kilo Dalton
KLF15	Kruppel Like Factor 15
LCMS	Liquid chromatography mass spectrometry
LM	Lauryl maltoside
M^{-1}	Litre per mole
LKB1	liver kinase B1
mM	Millimolar
mg	Milligram
min	Minutes
MHz	MegaHertz
mmol	Millimole
ml	Millilitre
MS	Mass spectrometry
MW	Molecular weight
miRNA	Small non coding RNA molecule
NAD	Nicotinamide adenine dinucleotide
NHS	N-hydroxy succinimide

NMR	Nuclear magnetic resonance
NF-kB	Nuclear Facture Kappa Beta
OSCP	Oligomycin sensitivity conferring protein
Pi	Phosphate
$PTEN^{+/-}$ mice	Lung tumor resistance
Prep HPLC	Preparative high performance liquid chromatography
ppm	Part per million
PBS	Phosphate buffer saline
Raptor	Regulatory protein of mTOR
Rag GTPases	GTPases protein, subunit Rag
rpm	Revolutions per minute
REDD1	Protein regulated in development and DNA damage Response 1
ROS	Reactive oxygen species
S	Singlet
S14	Ribosomal protein S14
SDS-PAGE	Sodium dodecyl polyacrylamide gel electrophoresis
SREBP	Sterol regulatory element binding protein
SIRT1	Sirtuin 1
S. cerevisiae	Saccharomyces cerevisiae
SHP	Small heterodimer partner
SMP	Submithocondrial particle
t	Triplet
T2D	Type 2 diabetes

TBSCl	Tert-butyldimethylsilyl chloride
TEA	Triethylamine
TLC	Thin layer chromatography
TILs	Tumor-infiltrating lymphocytes
TNFa	Tumour necrosis factor a
TSC1	Tuberous sclerosis 1
TMSCl	Trimethylsilyl chloride
TORC2	Transcriptional co-activator

Chapter 1

Introduction

1.1. Metformin

Metformin (*N*,*N*-dimethyl biguanide hydrochloride) (Figure 1.1) is known under the commercial name Glucophage and has a half-life of six hours in the body.[1] Metformin is representative of the general class of biguanides and is widely used to reduce high blood sugar levels in type 2 diabetic (T2D) patients.[1]

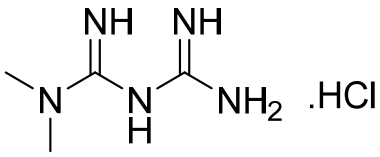

Figure 1.1. Chemical structure of Metformin

The history of Metformin dates to the use of *Galega officinalis Linn* (*G. officinalis*, Figure 1.2) as an herbal medicine in medieval Europe. *G. officinalis* was used as a medication for the treatment of different diseases such as Plague, Miasma, Dysuria and even to relieve snake bites.[2] Metformin was also used to stimulate lactation in cows to increase milk production.[3]

Figure 1.2. *G. officinalis Linn*

In 1917, guanidine extracted from *G. officinalis* had shown hypoglycaemic activity in animals, but was too toxic for clinical use.[4] Research in this area provided additional observations on the antidiabetic actions of *G. officinalis* extracts. In 1929, a few synthetic biguanides were prepared, but despite their non-toxic properties in animals, they were not further tested in humans.[5]

Later in 1957, metformin started to be clinically developed and used in Paris, France and was shown to possess antidiabetic activity in patients with T2D.[6] At the same time, an American team reported similar results for phenformin (phenylethyl biguanide).[7] One year later, Meherent *et al.* report the same antidiabetic properties of buformin (butyl biguanide)[8], which opened the door for the usage of phenformin and buformin as antidiabetic drugs. However, despite their interesting antidiabetic properties and potency, many reports showed their association with lactic acidosis, causing their withdrawal from the market in 1970. At that moment, researchers have started to look back at metformin, because it lacked toxicity related to lactic acidosis.[9]

In 1995, a report from the UK Prospective Diabetes Study demonstrated that metformin controlled the level of glycaemia, reduced cardiovascular-related mortality and increased survival in overweight diabetic type 2 patients.[10] In the recent strategies of both the American Diabetes Association (ADA) and the European Association of Study of Diabetes (EASD), metformin was approved as a first choice therapy for T2D.[11] In Canada, metformin became available in 1972 and is currently the most prescribed antidiabetic drug.[12]

1.2. Antidiabetic effect of metformin

Different mechanisms are involved in the reduction of serum glucose levels induced by metformin, but the most obvious result of metformin use is a decrease in hepatic glucose production without hypoglycemia.[13,14] Production of glucose requires energy in the form of adenosine triphosphate (ATP). By decreasing the production of ATP in liver cells, metformin

reduces hepatic glucose production. In addition to this action on the liver, metformin increases insulin sensitivity, which increases glucose uptake from hepatocytes.[15] Other antidiabetic drugs, like sulfonylureas, also reduce blood glucose levels, but they also contribute to elevated levels of insulin, increasing neoplastic growth through the activation of insulin receptors.[16] In muscles, metformin increases the tyrosine kinase activity of the insulin receptors and promotes the translocation of glucose transport leading to glucose uptake from muscles.[17]

Cellular uptake of metformin in the hepatic cells is promoted by the organic cationic transporter (OCT 1). Inhibition of complex I of the mitochondrial respiratory chain has been hypothesized to be the result of metformin action.[18] Whether complex I is the main target of metformin or not will be discussed in chapter 3. Complex I may reduce both the gradient of protons across mitochondrial membrane, and ATP synthesis. Inhibition of complex I leads to an increase in the ratios of adenosine mono-phosphates and tri-phosphates (AMP/ATP) or adenosine di-phosphates and tri-phosphates (ADP/ATP), which activate the 5-activated protein kinase (AMPK).[13a] AMPK is a multi-subunit enzyme that is known as a major manager of cell energy and lipid biosynthesis (Figure 1.3).[13a]

On the other hand, the decrease of ATP itself inhibits fructose-1,6-bisphosphatase, a vital enzyme for gluconeogenesis.[19] Metformin activates liver kinase B1 (LKB1)/AMPK signaling which leads to the inhibition of genes coding proteins involved in fatty acid synthesis (FAS), such as ribosomal protein S14 (S14) and acetyl-CoA carboxylase (ACC), by phosphorylation of the transcription factors of carbohydrate responsive element binding protein (ChREBP), hepatocyte nuclear factor 4 (HNF4) and co-activators (Figure 1.3).[20]

Metformin decreases hepatic lipid synthesis by increasing the fatty acid oxidation and inhibition of lipogenesis through the phosphorylation and consequent inactivation of pivotal

enzymes. Metformin blocks translocation of transcriptional co-activator (TorC2) and suppresses the expression of its target genes in hepatocytes. These functions lead to the overall inhibition of glucose production (Figure 1.3).[13a]

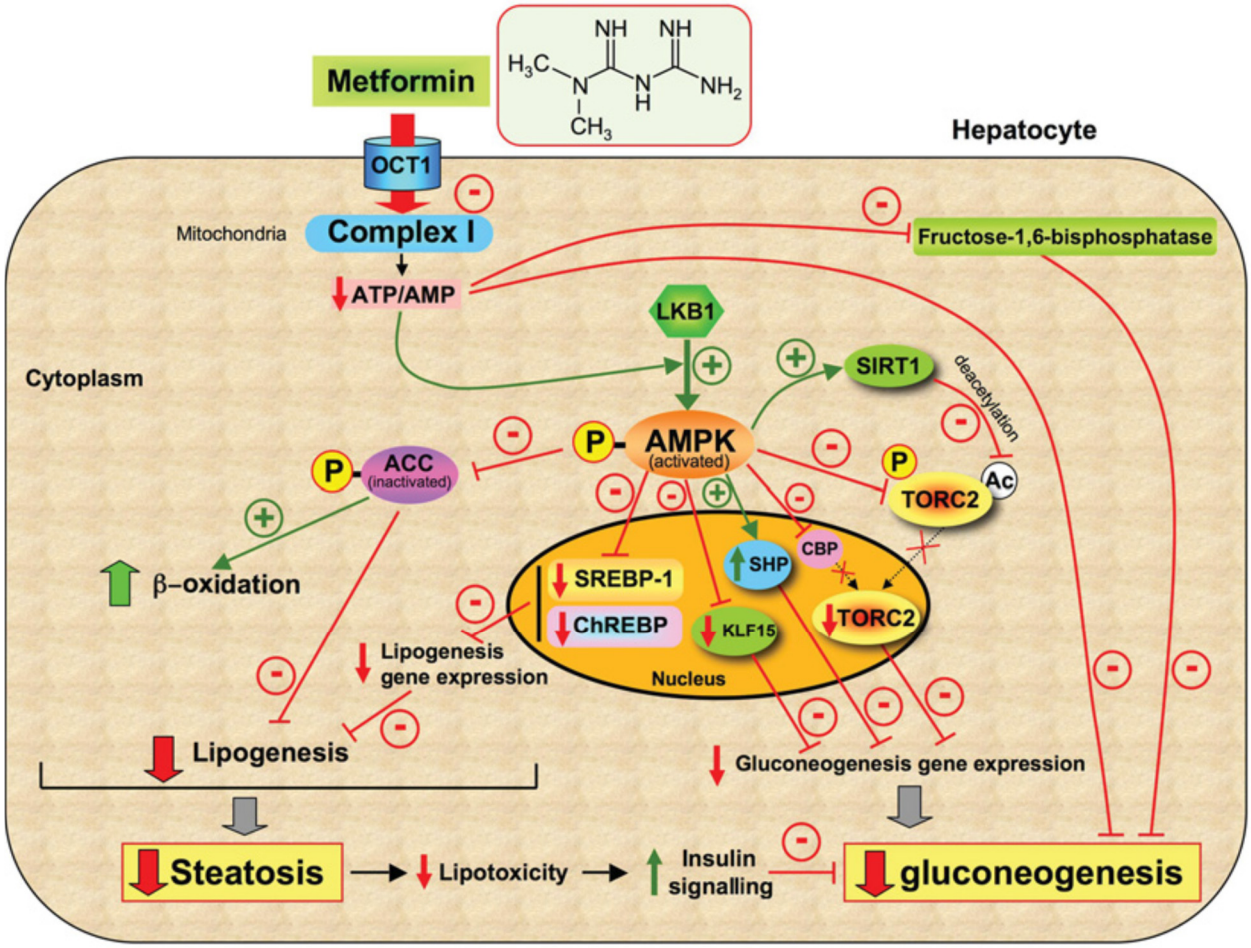

Figure1.3. Molecular mechanisms of the effect of metformin on hepatic gluconeogenesis[21]

Another mechanism of gluconeogenesis inhibition occurs in the nucleus of the cell, through the suppression of TORC2 and the increase of the activity of hepatic Sirtuin 1 (SIRT1), a NAD^+-dependent protein deacetylase.[22,23] The increase of the small heterodimer partner (SHP)-mediated AMPK inhibits hepatic gluconeogenesis through the interaction with cAMP response element-binding protein (CREB).[24] In addition, metformin quenches the activity of Kruppel Like Factor 15

(KLF15) which has an important role in genes coding for gluconeogenesis and amino acid catabolic enzymes (Figure 1.3).[25] It is believed that metformin regulates lipogenesis gene expression by decreasing the level of the transcription factor ChREBP and the sterol regulatory element binding protein (SREBP) *via* AMPK phosphorylation (Figure 1.3).[13a, 20b]

Recently, it was proven that in addition to glucose metabolism, metformin has other areas of potential therapeutic applications, including cardiovascular diseases and cancer therapy.[26]

1.3. Metformin and the inhibition of cancer cell growth

The association between cancer and diabetes has been widely investigated from a number of research fields included epidemiological, metabolic, preclinical and clinical.[27] T2D generally increases the risk of different types of cancer such as liver, colorectal, pancreas, bladder, kidney, endometrial and breast cancers and non-Hodgkin's lymphoma,[28] but T2D patients treated with metformin showed decreased cancer incidence and mortality.[29]

In 2005, the Evans's laboratory recognized the reduced risk of cancer in diabetic patients receiving metformin with dose-response association.[30] In 2009, the same research group confirmed a 63% reduction in the risk of cancer for diabetic patients using metformin.[31] In 2009, Li *et al.* reported a 62% reduction in the risk of pancreatic cancer in diabetic patients taking metformin.[32] These results support the use of metformin in cancer treatment. Later *in vitro* and *in vivo* studies confirmed the antitumor activity of metformin on different types of cancer cell lines in animal models (Table 1.1).[25]

Table 1.1. Protective effect of metformin in animal models of cancer[25]

Cancer model	Tumour type	Treatment	Administration
Xenograft	Pancreas	250 mg/kg	Intraperitoneal (IP)
	Lung	50 mg/kg	Oral
	Colon	250 mg/kg	IP
	Prostate	200 µg/ml; 1 mg/day	Oral; IP
	Breast	2 mg/ml	Oral
	Leukaemia	250 mg/kg	IP
	Cancer stem	100 µg/ml	IP
Chemically induced	Breast	50-500 mg/kg	Oral
	Lung	250 mg/kg	IP
	Colon	250 mg/kg	IP
	Pancreas	320 mg/kg	Oral
HER2/neu mice	Breast	100 mg/kg	Oral
$PTEN^{+/-}$ mice	All	300 mg/kg	Oral
$PTEN^{Min/-}$ mice	Gastrointestinal polyps	250 mg/kg	Oral

HER2/neu: a type of receptor tyrosine kinase, $PTEN^{+/-}$ mice: lung tumor resistance

Metformin can inhibit cancer cell proliferation by acting both at the macroscopic and cellular state. In the macroscopic state, there are numerous probable explanations for how metformin reduces the risk of cancer in metformin-treated T2D patients. Notably, T2D and cancer show similar risk factors including age, obesity, physical inactivity, diet, alcohol and smoking.[28] For example, obesity is consistently associated with the increase of cancer risk.[33] Several factors mediate the effects of obesity on cancer, such as sex hormones and inflammatory cytokines.[34] Several studies have shown that the higher level of sex hormones, including estrogen and estradiol, in the serum of obese women correlate with cancer growth and metastasis.[35] Moreover, *in vitro* and *in vivo* studies have shown that obesity raises the cancer risk by increasing inflammatory cytokine levels, including those of interleukin-6 (IL-6) and tumour necrosis factor a (TNFa).[36] The increase of cytokine levels leads to chronic inflammation directly associated with cancer growth, through various mechanisms.

Hyperinsulinaemia is another important factor that increases the risk of cancer in T2D patients.[37] A condition in which there is an excess of insulin circulating in the blood, hyperinsulinemia that may induce the growth of neoplastic tissues, through several mechanisms, including the activation of insulin-like growth factor 1 receptors (IGF1-Rs), and the disturbance of the level of free circulating hormones and growth factors level in the blood.[38] Metformin can inhibit hyperinsulinaemia and consequently may lower the risk of cancer by reducing the hepatic glucose output.[39]

Metformin may also decrease the risk of cancer in T2D patients by decreasing the production of inflammatory cytokines.[40] In the cellular state, the antitumor effect of metformin could be divided in two main categories of AMPK-dependent and AMPK-independent activity.

1.4. The AMPK-depended mechanism

Multiple pathways are considered to be involved in the anti-tumor activities of metformin in the cell. Metformin has a direct preventive action on tumour growth through a mechanism involving the activation of the LKB1/AMPK signalling (Figure 1.4).[41] It can suppress tumor cell growth and proliferation through the inhibition of transcriptional co-activator (mTORC1) signalling. mTORC1 signaling may control cancer cell growth and proliferation in multiple ways, including phosphorylation of tuberous sclerosis 1 (TSC1), tuberous sclerosis 2 (TSC2), and the regulatory protein of mTOR (Raptor).[42]

Metformin may inhibit tumor cell proliferation by mediating protein p53 expression and phosphorylation by AMPK.[43] However, the role of p53 in the activity of metformin as an inhibitor of cancer cell growth is debatable, because studies have confirmed that metformin blocks tumor cell cycle without changes in p53 status.[44] Other studies have shown that the inhibitory effect of metformin on cancer cell growth is associated with p53 activity (Figure 1.4).[45]

Tumor cell growth can also be controlled by modulation of specific small non coding RNAs (miRNAs).[46] The activation of miRNAs can act to promote or suppress tumor growth. In addition, metformin can induce the insulin like growth factor (IGF)/insulin signaling through the AMPK-depended phosphorylation of protein insulin receptor substrate 1 (IRSI) (Figure 1.4).[47]

1.5. The AMPK-independed mechanism

Metformin can inhibit cancer cell proliferation without AMPK activation (Figure 1.4). For example, the Rag subunit guanosine triphosphate hydrolases (Rag GTPases) are specific enzymes regulating mTOR signaling in the cell. Blockage of the Rag GTPases/mTORC1 signaling by metformin leads to the inhibition of cancer cell proliferation (Figure 1.4).[48]

Tumor cells use glucose as a source of energy for fast growth and proliferation. Production of glucose-6-phosphate (G6P), catalysed by hexokinases (HK) I and II, has an important role in glucose metabolism. Metformin inhibits cancer cell proliferation by inhibiting the enzymatic function of HKI and II.[49] Metformin could inhibit cancer cell proliferation *via* the decrease of the cyclin D1 level and through the activation of the proteins regulated in the development and DNA damage Response 1 (REDD1).[50] It can also reduce the production of reactive oxygen species (ROS) that leads to a lower oxidative stress and consequently lowers the risk of DNA damage and mutagenesis in normal cells.[51] In addition, metformin induces cell apoptosis and autophagy by down regulation of the transcription 3 (Stat3) activity and B-cell lymphoma 2 (Bcl-2) expression (Figure 1.4).[52]

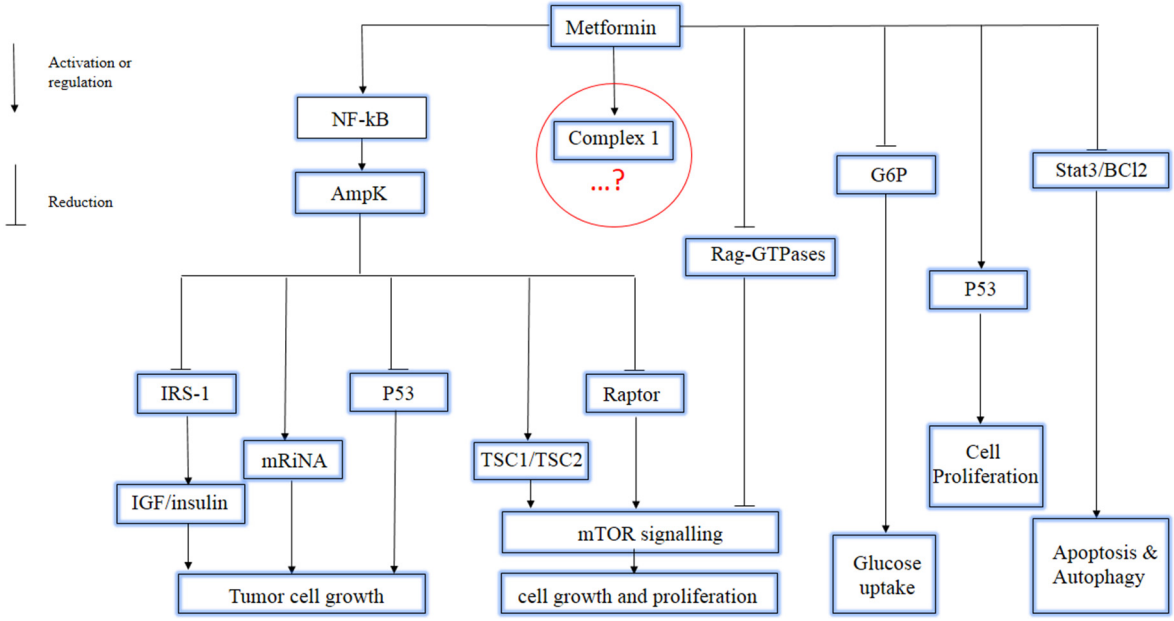

Figure1.4. Effect of metformin on cancer cells[53]

1.6. Cellular target of metformin in cancer cells

As previously mentioned, the principal target of metformin in the cell have been thought to be the complex I of the mitochondrial electron transport respiratory chain.[54] Complex I (NADH:

ubiquinone oxidoreductase) is one of the five complexes present in the inner membrane of mitochondria and has a vital role for respiration and oxidative phosphorylation in mitochondria. Complex I uses electrons from the oxidization of NADH to NAD^+ to reduce ubiquinone to ubiquinol. The NADH ubiquinone redox reaction releases energy that is used to create an electrochemical gradient across the mitochondrial inner membrane. This leads to the synthesis of ATP by complex V (ATP synthase). In addition, complex I is the main source of ROS in mitochondria.[55]

In 2000, two independent groups, El-mir and Owen, both mentioned complex I as the possible target of metformin in the cell.[18, 56] El-mir *et al.* examined the effect of metformin on isolated rat hepatocytes, permeabilized hepatocytes and isolated liver mitochondria,[56] and showed that at high concentrations (10±1 mM), metformin decreased oxygen consumption and mitochondrial membrane potential in intact cells (Figure 1.5).

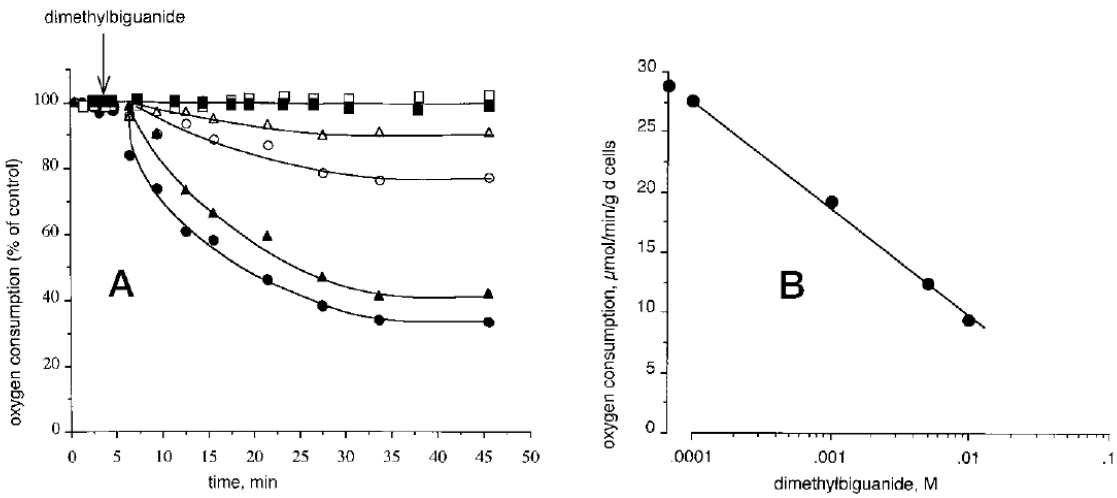

Figure 1.5. Effect of metformin on oxygen uptake in intact isolated hepatocytes, permeabilized hepatocytes and isolated liver mitochondria.[56]

Panel A: filled circles, 10 mM; filled triangles, 5 mM; open circles, 1 mM; open triangles, 0.1 mM; permeabilized hepatocytes (open squares) or isolated mitochondria (filled squares), 2 mg of protein/ml. Panel B shows dose dependence of hepatocyte oxygen consumption rate after 30 min of incubation.

Inhibition of complex I by metformin was claimed not to occur through a direct interaction with the respiratory chain, because no effect was observed on isolated mitochondria. An indirect effect of metformin on the respiratory chain complex I was proposed an undefined signaling pathway. On the other hand, Owen *et al.* provided evidence that metformin affected directly complex I,[18] by showing that reduced oxidation of glutamate and malate inhibited hepatoma cell growth by 13 and 30% after 24 and 60 h, respectively (Figure 1.6).

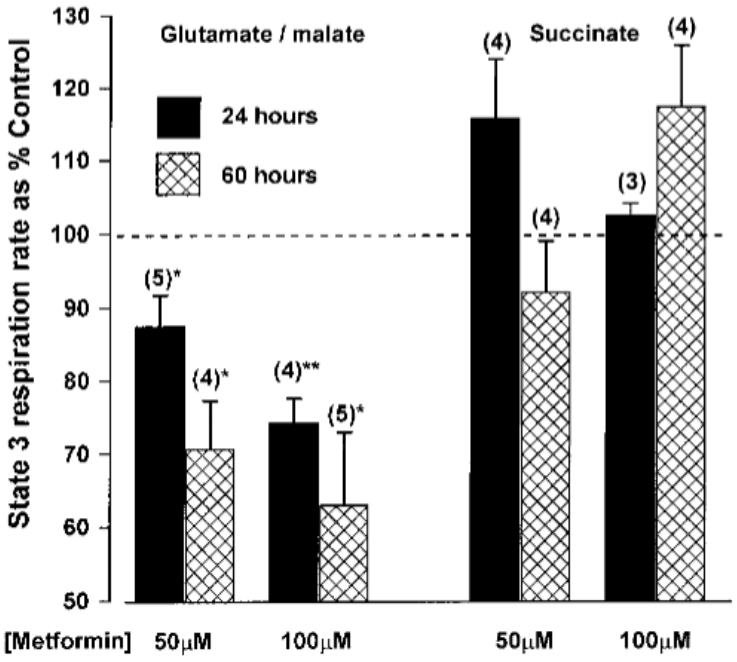

Figure 1.6. Inhibition of mitochondrial respiration by metformin in permeabilized rat hepatoma cells.[18]

Recently, the effect of different biguanides on purified complex I has been investigated by Bridges *et al.*[57] They demonstrated that high concentrations (in the millimolar range) of metformin can indirectly inhibit complex I activity by inhibiting ubiquinone reduction and independently, reactive oxygen species production. They also showed that metformin inhibited the mitochondrial ATP synthase activity.

1.6.1. Effect of metformin and other biguanides on isolated complex I

Bridge *et al.* studied the effect of five pharmacologically relevant biguanides on the oxidative phosphorylation in mammalian mitochondria. All five biguanides inhibited complex I and the more hydrophobic biguanides were more effective inhibitors (Figure 1.7 A and B).[57] However, a high concentration of metformin (19.4 ± 1.4 mM) was required to inhibit the NADH:

decylubiquinone oxidoreduction, showing that metformin is a weak inhibitor of isolated complex I.

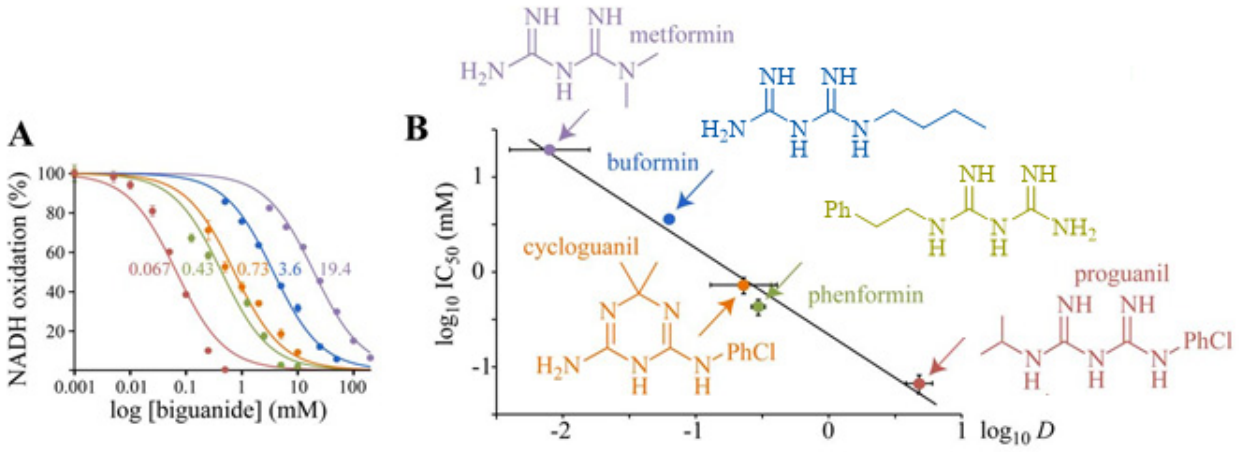

Figure 1.7. Effects of biguanides on isolated bovine complex I.[57]

(A) Dependence of NADH oxidation on biguanide concentration, relative to a biguanide-free control. Colours are as in (B), and the half maximal inhibitory concentration (IC50) values (in mM) are noted. (B) Relationship between the inhibition (IC50) and octanol:PBS partition coefficient (D) of the biguanides.

In order to understand how biguanides can bind to the complex I, the effect of biguanides at different stages of NADH oxidoreduction were studied: NADH oxidation through the flavin mononucleotide, ubiquinone reduction and intramolecular electron transfer across the inner membrane.[55] By several experiments, the authors demonstrated that biguanides do not inhibit complex I by inhibiting NADH oxidation nor by blocking intramolecular electron transfer chain. Instead, metformin's rate-determining inhibition step was mechanistically related to ubiquinone reduction.

1.6.2. Effect of metformin and other biguanides on complex V

The effects of biguanides on complex V (F_1F_0-ATPase) were monitored following ATP hydrolysis and ATP synthesis. Formation of ADP (obtained from ATP hydrolysis) in submitocondrial particles (SMPs) was affected by metformin. All five biguanides inhibited ATP hydrolysis with similar efficiency correlating with hydrophobicity (Figure 1.8).[57]

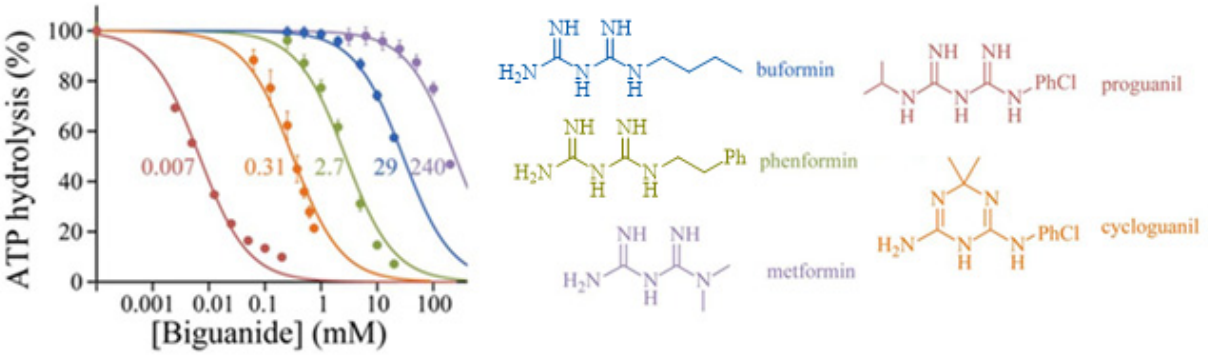

Figure 1.8. Effect on biguanides on the inhibition of ATP hydrolysis[57]

The inhibition of NADH-driven ATP synthesis induced by metformin has also been compared with that of piericidin, a strong complex I inhibitor (Figure 1.9).[57] The results were almost the same, indicating that the inhibition of ATP synthesis is a consequence of the inhibition of complex I. Biguanides were proposed to inhibit complex I at two different sites: one disturbing the reactivity of the flavin and the other inhibiting the catalytic site.

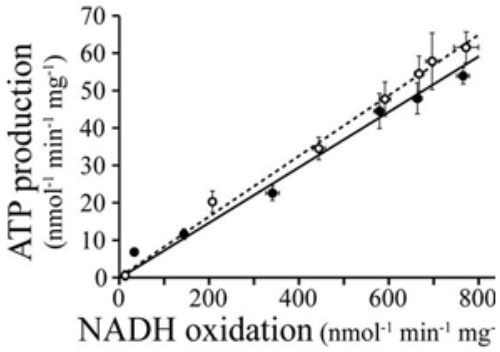

Figure 1.9. Relative inhibition of ATP production in SMPs in the presence of piericidin (open circles) and metformin (filled circles).[57]

Although the target of metformin has been claimed to be complex I, the activity of complex I has only been studied indirectly in the presence of metformin. Taking together the results presented above, we decided to identify the putative target of metformin.

1.7. Our objectives

We hypothesized that metformin could have interact directly with one or several proteins in the mitochondria leading to inhibition of the cancer cell proliferation. Therefore, we conjugated metformin to biotin to probe for potential mitochondrial proteins that bound metformin. The biotin-(strept)avidin system has been well exploited for protein and nucleic acid detection and purification. Biotin may be conjugated to metformin and the resulting conjugate used for affinity chromatography to isolate proteins for identifying by mass spectrometry (MS). Iidentification of the exact protein or proteins responsible for binding to metformin should help to better understand its mechanism of action and may open the door for structural changes that would provide more potent inhibitor.

1.8. References

1. Shaw, R. J.; Lamia, K. A.; Vasquez, D.; Koo, S.-H.; Bardeesy, N.; DePinho, R. A.; Montminy, M.; Cantley, L. C., *Science.* **2005**, 310, 1642-1646.

2. Bailey, C. J.; Day, C., *Practical Diabetes* **2004**, 21, 115-117.

3. Mori, A.; Cohen, B. D.; Lowenthal, A. Japan Guanidino Compounds Research Association Meeting. *Guanidines: Historical, biological, biochemical, and clinical aspects of the naturally occurring guanidino compounds*; Plenum Press; New York, **1985**.

4. Watanabe, C., *J. Biol. Chem.* **1918**, 33, 253.

5. Hesse, E.; Taubmann, G., *Naunyn Schmiedebergs Arch. Exp. Pathol. Pharmakol.* **1929**, 142, 290-308.

6. Sterne, J., *Maroc Med.* **1957**, 36, 1295-1296.

7. Ungar, G.; Freedman, L.; Shapiro, S. L., *Exp. Biol. Med.* **1957**, 95, 190-192.

8. Mehnert, H.; Seitz, W., *Munch Med Wschr.* **1958**, 100, 1851-1856.

9. Schäfer, G., *Diabetes Metab.* **1982,** *9*, 148-163.

10. Group, U. P. D. S., *Lancet.* **1998**, 352, 854-865.

11. (a)Adler, A. I.; Shaw, E. J.; Stokes, T.; Ruiz, F., *Brith. Med. J.* **2009**, 338; (b)Nathan, D. M.; Buse, J. B.; Davidson, M. B.; Ferrannini, E.; Holman, R. R.; Sherwin, R.; Zinman, B., *Clin Diabetes.* **2009**, 27, 4-16.

12. Campbell, I., *Brith. Med. J. (Clinical research ed.)* **1984,** 289, 289-297.

13. (a)Zhou, G.; Myers, R.; Li, Y.; Chen, Y.; Shen, X.; Fenyk-Melody, J.; Wu, M.; Ventre, J.; Doebber, T.; Fujii, N., *J. Clin. Invest.* **2001**, 108, 1167-1174; (b)Krentz, A. J.; Bailey, C. J., *Drugs*. **2010**, 65, 385-411.

14. Kirpichnikov, D.; McFarlane, S. I.; Sowers, J. R., *Ann. Intern. Med.* **2002**, 137, 25-33.

15. Gunton, J. E.; Delhanty, P. J.; Takahashi, S.-I.; Baxter, R. C., *J. Clin. Endocrinol. Metab.* **2003**, 88, 1323-1332.

16. Pollak, M., *Nat. Rev. Cancer*. **2008**, 8, 915-928.

17. Fischer, Y.; Thomas, J.; Rösen, P.; Kammermeier, H., *Endocrinology*. **1995**, 136, 412-420.

18. DORAN, E.; HALESTRAP, A. P., *Biochem. J.* **2000**, 348, 607-614.

19. Miller, R. A.; Birnbaum, M. J., *J. Clin. Invest.* **2010**, 120, 2267-2270.

20. (a)Foretz, M.; Ancellin, N.; Andreelli, F.; Saintillan, Y.; Grondin, P.; Kahn, A.; Thorens, B.; Vaulont, S.; Viollet, B., *Diabetes.* **2005**, 54, 1331-1339; (b)Kawaguchi, T.; Osatomi, K.; Yamashita, H.; Kabashima, T.; Uyeda, K., *J. Biol. Chem*. **2002**, 277, 3829-3835; (c)Leclerc, I.; Lenzner, C.; Gourdon, L.; Vaulont, S.; Kahn, A.; Viollet, B., *Diabetes*. **2001**, 50, 1515-1521.

21. Buler, M.; Aatsinki, S.-M.; Izzi, V.; Hakkola, J., *PLoS One.* **2012**, 7, e49863.

22. Caton, P. W.; Nayuni, N. K.; Kieswich, J.; Khan, N. Q.; Yaqoob, M. M.; Corder, R., *J. Endocrinol.* **2010**, 205, 97-106.

23. Koob, G. F.; Bloom, F. E., *Sci.* **1988**, 715-723.

24. He, L.; Sabet, A.; Djedjos, S.; Miller, R.; Sun, X.; Hussain, M. A.; Radovick, S.; Wondisford, F. E., *Cell.* **2009**, 137, 635-646.

25. Viollet, B.; Guigas, B.; Garcia, N. S.; Leclerc, J.; Foretz, M.; Andreelli, F., *Clin. Sci.* **2012**, 122, 253-270.

26. Malek, M.; Aghili, R.; Emami, Z.; Khamseh, M. E., *ISRN Endocrinol.* **2013**, 636927.

27. Arcidiacono, B.; Iiritano, S.; Nocera, A.; Possidente, K.; Nevolo, M. T.; Ventura, V.; Foti, D.; Chiefari, E.; Brunetti, A., *Experimental Diabetes Research.* **2012**, 789174.

28. Vigneri, P.; Frasca, F.; Sciacca, L.; Pandini, G.; Vigneri, R., *Endocr. Relat. Cancer.* **2009**, 16, 1103-1123.

29. Rizos, C. V.; Elisaf, M. S., *Eur. J. Pharmacol.* **2013**, 705, 96-108.

30. Evans, J. M.; Donnelly, L. A.; Emslie-Smith, A. M.; Alessi, D. R.; Morris, A. D., *Brith. Med. J.* **2005**, 330, 1304-1305.

31. Libby, G.; Donnelly, L. A.; Donnan, P. T.; Alessi, D. R.; Morris, A. D.; Evans, J. M., *Diabetes Care.* **2009**, 32, 1620-1625.

32. Li, D.; Yeung, S. C. J.; Hassan, M. M.; Konopleva, M.; Abbruzzese, J. L., *Gastroenterology.* **2009**, 137, 482-488.

33. Calle, E. E.; Rodriguez, C.; Walker-Thurmond, K.; Thun, M. J., *N. Engl. J. Med.* **2003**, *348*, 1625-1638.

34. Davoodi, S. H.; Malek-Shahabi, T.; Malekshahi-Moghadam, A.; Shahbazi, R.; Esmaeili, S., *Iran. J. Cancer. Prev.* **2013**, 6, 186-190.

35. Bracci, P. M., *Mol. Carcinog.* **2012**, 51, 53-63.

36. Fain, J. N., *Vitam. Horm.* **2006**, 74, 443-477.

37. Giovannucci, E.; Harlan, D. M.; Archer, M. C.; Bergenstal, R. M.; Gapstur, S. M.; Habel, L. A.; Pollak, M.; Regensteiner, J. G.; Yee, D., *CA: Cancer. J. Clin.* **2010**, 60, 207-221.

38. Wilcox, G., *Clin. Biochem. Rev.* **2005**, 26, 19-39.

39. Pernicova, I.; Korbonits, M., *Nat. Rev. Endocrinol.* **2014**, 10, 143-156.

40. Moiseeva, O.; Deschênes-Simard, X.; St-Germain, E.; Igelmann, S.; Huot, G.; Cadar, A. E.; Bourdeau, V.; Pollak, M. N.; Ferbeyre, G., *Aging Cell.* **2013**, 12, 489-498.

41. Shackelford, D. B.; Shaw, R. J., *Nat. Rev. Cancer.* **2009**, 9, 563-575.

42. (a)Gwinn, D. M.; Shackelford, D. B.; Egan, D. F.; Mihaylova, M. M.; Mery, A.; Vasquez, D. S.; Turk, B. E.; Shaw, R. J., *Mol. Cell.* **2008**, 30, 214-226; (b)Inoki, K.; Zhu, T.; Guan, K.-L., *Cell.* **2003**, 115, 577-590.

43. Jones, R. G.; Plas, D. R.; Kubek, S.; Buzzai, M.; Mu, J.; Xu, Y.; Birnbaum, M. J.; Thompson, C. B., *Mol. Cell.* **2005**, 18, 283-293.

44. (a)Sahra, I. B.; Laurent, K.; Giuliano, S.; Larbret, F.; Ponzio, G.; Gounon, P.; Le Marchand-Brustel, Y.; Giorgetti-Peraldi, S.; Cormont, M.; Bertolotto, C., *Cancer. Res.* **2010**, 70, 2465-2475; (b)Hadad, S.; Hardie, D.; Appleyard, V.; Thompson, A., *Clin. Transl. Oncol.* **2014**, 16, 746-752.

45. (a)Nelson, L. E.; Valentine, R. J.; Cacicedo, J. M.; Gauthier, M.-S.; Ido, Y.; Ruderman, N. B., *Am. J. Physiol. Cell. Physiol.* **2012**, 303, C4-C13; (b) Malki, A.; Youssef, A., *Oncol. Res.* **2011**, 19, 275-285.

46. Pulito, C.; Donzelli, S.; Muti, P.; Puzzo, L.; Strano, S.; Blandino, G., *Ann. Transl. Med.* **2014**, 2, 18-34.

47. Ning, J.; Clemmons, D. R., *Mol. Endocrinol.* **2010**, 24, 1218-1229.

48. Kalender, A.; Selvaraj, A.; Kim, S. Y.; Gulati, P.; Brûlé, S.; Viollet, B.; Kemp, B. E.; Bardeesy, N.; Dennis, P.; Schlager, J. J., *Cell Metab.* **2010**, 11, 390-401.

49. Salani, B.; Marini, C.; Rio, A. D.; Ravera, S.; Massollo, M.; Orengo, A. M.; Amaro, A.; Passalacqua, M.; Maffioli, S.; Pfeffer, U., *Sci. Rep.* **2013**, 3, 2070-2087.

50. Sahra, I. B.; Laurent, K.; Loubat, A.; Giorgetti-Peraldi, S.; Colosetti, P.; Auberger, P.; Tanti, J.-F.; Le Marchand-Brustel, Y.; Bost, F., *Oncogene.* **2008**, 27, 3576-3586.

51. Algire, C.; Moiseeva, O.; Deschênes-Simard, X.; Amrein, L.; Petruccelli, L.; Birman, E.; Viollet, B.; Ferbeyre, G.; Pollak, M. N., *Cancer Prev. Res.* **2012**, 5, 536-543.

52. Feng, Y.; Ke, C.; Tang, Q.; Dong, H.; Zheng, X.; Lin, W.; Ke, J.; Huang, J.; Yeung, S.-C.; Zhang, H., *Cell Death Dis.* **2014**, 5, e1088.

53. Christodoulou, M. I.; Scorilas, A, *Curr. Med. Chem.* **2017**, 24, 14-56.

54. Detaille, D.; Guigas, B.; Leverve, X.; Wiernsperger, N.; Devos, P., *Biochem. Pharmacol.* **2002**, 63, 1259-1272.

55. Hirst, J., *Annu. Rev. Biochem.* **2013**, 82, 551-575.

56. El-Mir, M.-Y.; Nogueira, V.; Fontaine, E.; Avéret, N.; Rigoulet, M.; Leverve, X., *J. Biol. Chem.* **2000**, 275, 223-228.

57. Bridges, H. R.; Jones, A. J.; Pollak, M. N.; Hirst, J., *Biochem. J.* **2014**, 462, 475-487.

Chapter 2

Synthesis of the biotin-conjugated biguanide

2.1. Introduction

There are several strategies that have been used to identify proteins targets of small molecules.[1] The most well-known and widely used method employs biochemical isolation by affinity chromatography, in which an analogue of the small molecule is covalently attached to biotin. The biotinylated version of the compound may bind to strept(avidin)-agarose beads.[2] As outlined in chapter 1**,** we hypothesized that a biotinylated biguanide (BFB), a metformin analog, can be used to identify proteins exhibiting binding affinity for metformin in a mitochondrial lysate.

In this chapter, we present different strategies envisioned for the synthesis of a biotin-conjugated biguanide and an ammonium salt control (Scheme 2.1) for the evaluation of non-specific binding in the affinity chromatography assays.

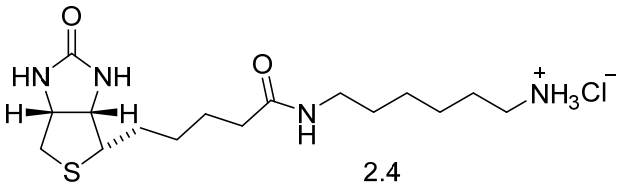

2.4

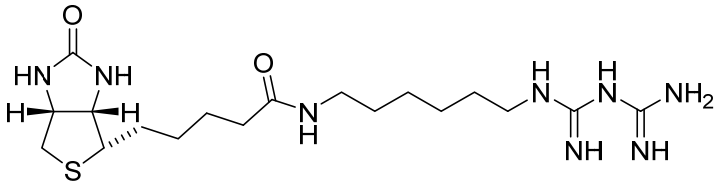

2.5

Scheme 2.1. Structures of the designed biotin-functionalized ammonium salt and biotinylated biguanide

2.2. Results and discussion

The designed biotin-conjugated biguanide contains three major parts: the biotin unit that strongly binds to the (strept)avidin,[3] the biguanide group to be recognized by proteins with binding affinity for metformin and an appropriate linker.

2.2.1. Synthetic protocol A

The first strategy that we envisioned for the synthesis of a biotin conjugated biguanide was based on the most common way to synthesize substituted biguanides, the reaction of dicyandiamide (DCD) with a primary ammonium salt. This method (Scheme 2.2) starts with the acylation of amine **2.1** with biotin-NHS **2.2.** After removal of the Boc group, the biguanide was proposed in the last synthetic step by reaction of ammonium chloride salt **2.4** with dicyandiamide (DCD)**.**

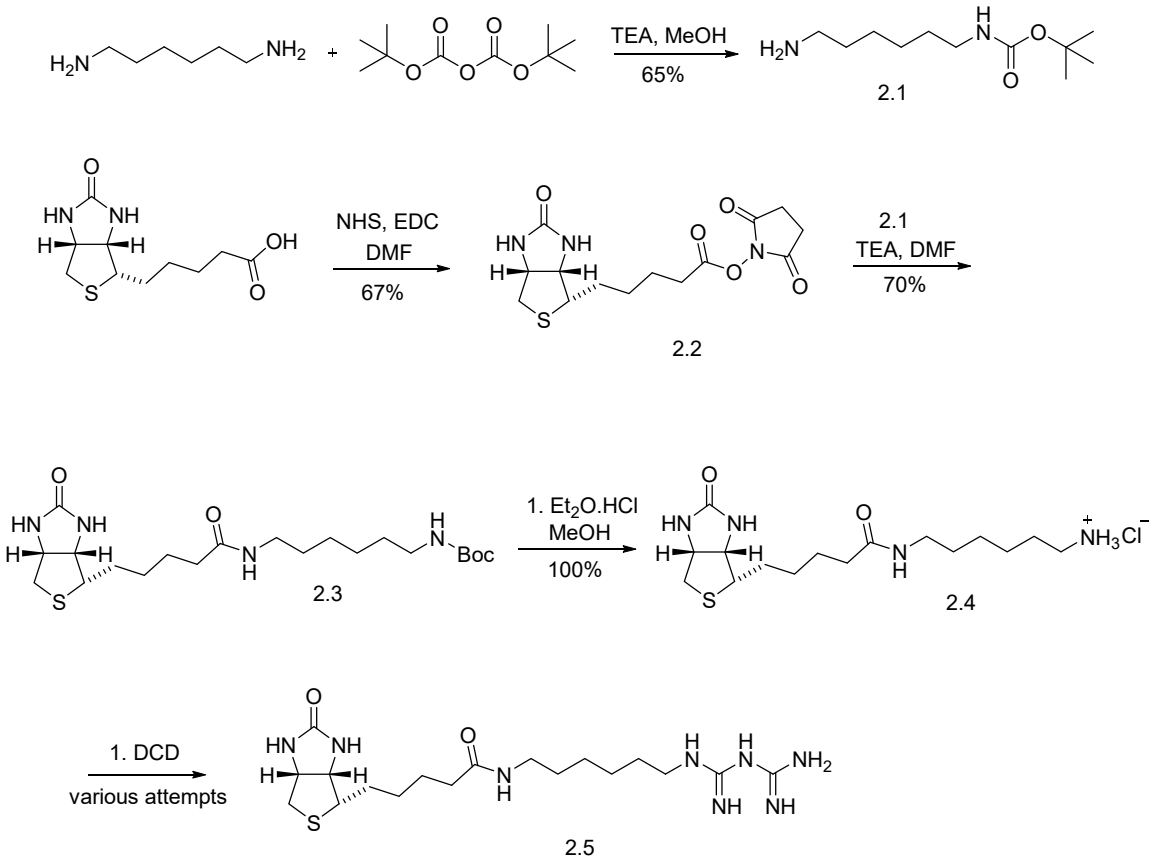

Scheme 2.2. Proposed synthetic protocol A

First, we have successfully synthesised amine **2.1** by the reaction of the di-*tert*-butyl dicarbonate with an excess of the 1,6-diaminohexane in 10% TEA:MeOH.[4] In the next step, we employed NHS and EDC to activate biotin.[5] Biotin-NHS reacted with the primary amine group of **2.1** to form amide **2.3**. Hydrochloride salt **2.4** was obtained by deprotection of the Boc group from **2.3**. The final step entailed reaction of DCD and **2.4**. Unfortunately, various conditions (presented Table 2.1) were tried, but they did not provide **2.5**. Under fusion conditions, a trace of biotinylated biguanide **2.5** was observed, along with many by-products.

Table 2.1. Attempts to synthesize BFB 2.5 using method type A

entry	*Reaction*	*Conditions*	*MS result*
1	Reflux in water	Heating at reflux an equimolar solution of **2.4** and DCD in H_2O for 3h	No mass of **2.5**
2	Reflux in xylene	Heating an equimolar solution of **2.4** and DCD in xylene at 140 °C for 48 h	No mass of **2.5**
3	Microwave (MW) reaction *via* protic acid catalysis	Irradiation of (1.1 eq) of **2.4** and (1.1 eq) DCD with 1.02 eq HCl in CH_3CN at 150°C for 15 min	No mass of **2.5**
4	Fusion method	Heating an equimolar solution of **2.4** and DCD at 160 °C for 60 min without solvent	Mass of **2.5** observed

The fusion method for the synthesis of biguanide was reported in 1892 by Bamberger and Dieckmann.[6] Commonly, the reaction is conducted between equimolar amounts of the primary amine hydrochloride salt and dicyandiamide at a very high temperature (160-180 °C) without solvent. The mixture of the dicyandiamide (42 mg, 0.5 mmoles) and hydrochloride salt **2.4** (188 mg, 0.5 mmoles) was heated up to 160 °C for 60 min. The melted reaction mixture solidified and cooling to room temperature. The desired mass of compound **2.5** was observed in a complex mixture of by-products. Different chromatography methods and preparative LC-MS methods were tried, but compound **2.5** was never obtained in sufficient purity.

The LC-MS analysis of the crude product indicated a low yield of **2.5** contaminated with starting material **2.4** which had a similar retention time. Therefore, we decided to optimize the

yield of this step by increasing the reaction time (Table 2.2), as well as by varying the ratio of the starting materials (Table 2.3).

Table 2.2. Effect of the reaction time on the formation of 2.5

	DCD (number of eq.)	**2.4** (number of eq.)	Reaction time	Yield
1	1	1	90 min	27%
2	1	1	2 h	24%
3	1	1	3 h	28%

Table 2.3. Effect of the ratio of the DCD on the yield of 2.5

	DCD (number of eq.)	**2.4** (number of eq.)	Reaction time	Yield of **2.5** based on LCMS analysis
1	3	1	90 min	34%
2	6	1	90 min	36%
3	8	1	90 min	50%

Increasing the reaction time did not change the yield of the reaction. Increasing the number of equivalents of DCD increased the yield of **2.5** with less by-products (Figure 2.1). Starting molecule **2.4** was not completely consumed in the reaction, even when 8 equivalents of DCD were used. The content of **2.5** was estimated in the crude reaction mixture by LCMS (Acq method, LC_20_95_15min_ACN, column, polar RP 30X2.00mm, $t_{r2.5}$ = 6 min, $t_{r2.4}$ = 5.4 min).

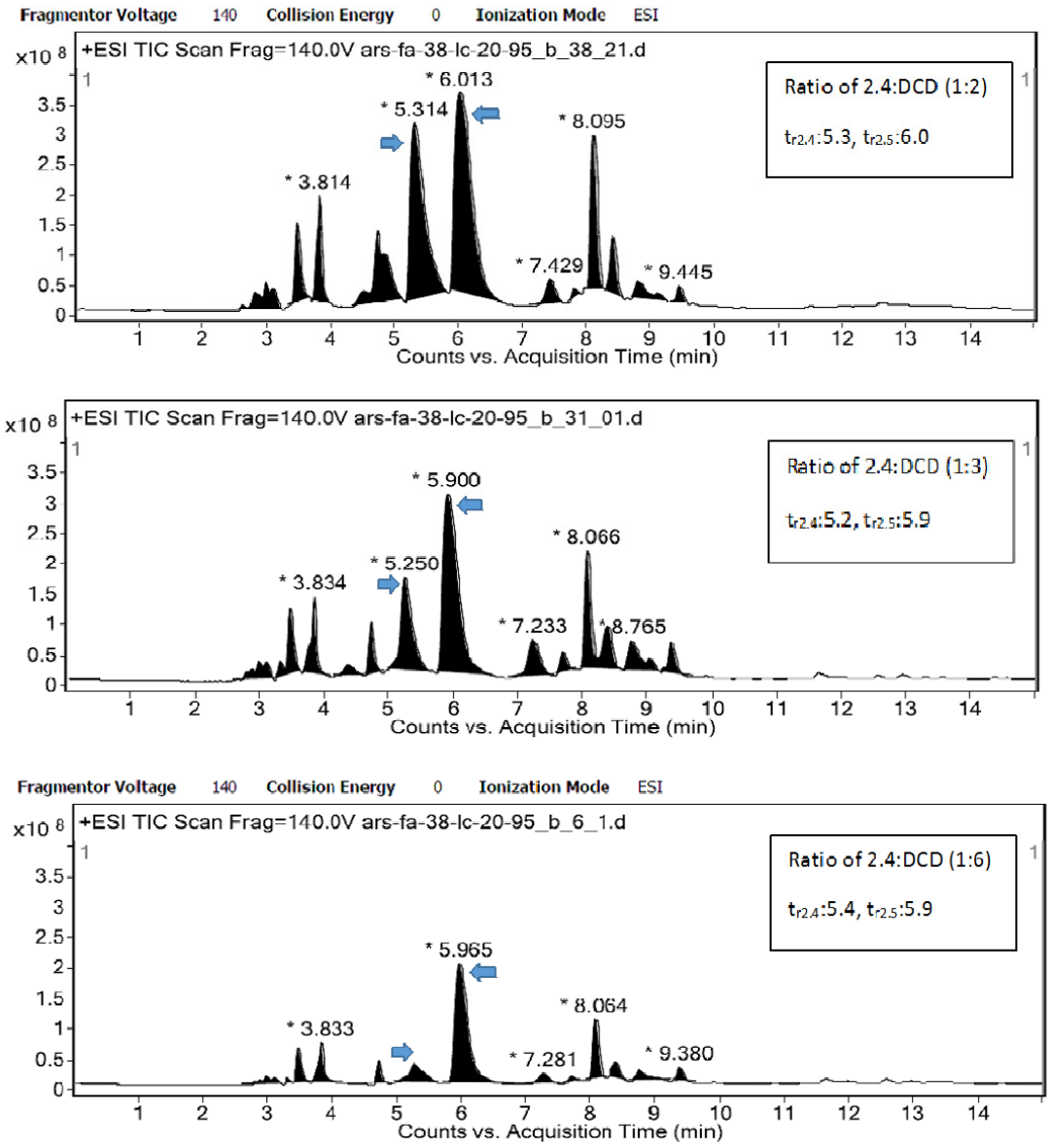

Figure 2.1. Screening the LCMS of the crude sample, obtained from the fusion method by increasing the ratio of DCD

Different separation methods were employed to purify **2.5** (Table 2.4), however, none gave **2.5** with an acceptable purity. Instead of spending additional time trying to improve the purification, we decided to modify our synthetic strategy.

Table 2.4. Attempts to purify the BFB 2.5 obtained from the fusion method

	Purification method	Condition
1	Extraction	EtOAc/H_2O (1:1)
2	Silica column	From 2 % to 20% of MeOH in DCM
3	Silica preparative plate	20%MeOH, 79%DCM, and 1% NH_4OH
4	Reverse column (C18)(cartridge)	From 100% to 20 % of H_2O in ACN

2.2.2. Synthetic protocol B

Following our fruitless results with the previous method, a new synthetic strategy was envisaged for the synthesis of **2.5** (Scheme 2.3). The method starts with the synthesis of a biguanide-functionalized linker **2.8**, for conjugated with biotin-NHS in an esterification reaction. One advantage of this method compared to the previous one is its lower cost, because biotin, the most expensive material, is used in the last step of the procedure. In addition, this route has one step less than the previous one. Unfortunately, this procedure was also abandoned because we were not able to properly purify biguanide **2.8**.

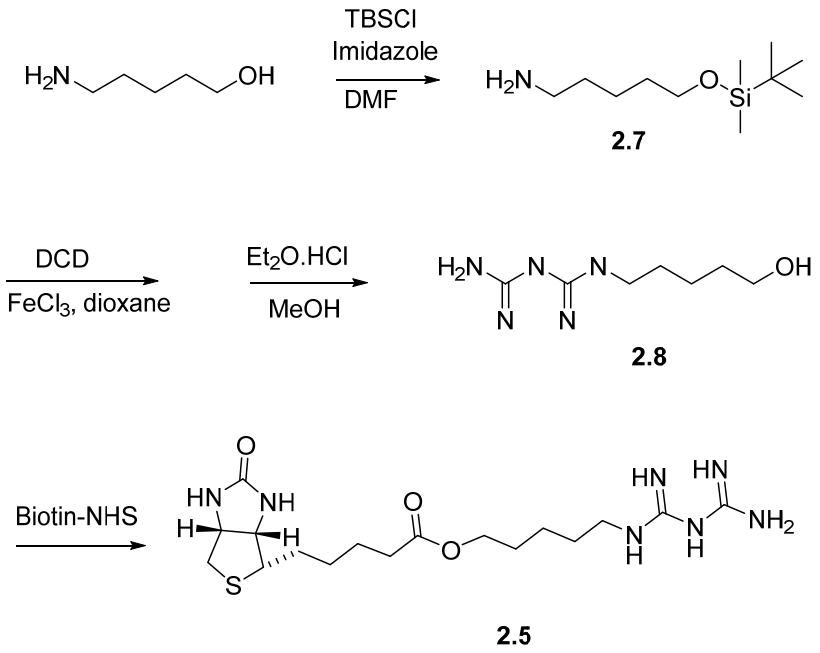

Scheme 2.3. Proposed synthetic method B

In the first step of this synthesis, commercial aminohexanol and *tert*-butyldimethylsilyl chloride were reacted in equimolar amounts using imidazole in DMF.[7] For the formation of the biguanide, several methods were tried (Table 2.5). Based on LC-MS analysis, too many by-products and very low yields were obtained.

Table 2.5. Attempts to synthesize biguanide 2.8

	Reaction method	Conditions	Results
1	Fusion method	Heating an equimolar (1 eq) of **2.7** and DCD at 160 °C for 60 min without solvent	Not successful
2	MW Irradiation *via* HCl catalysis	MW irradiation of an equimolar (1.1 eq) of **2.7** and DCD with 1.02 eq of HCl in CH_3CN at 150 °C for 15 min	Not successful
3	MW Irradiation *via* TMSCl catalysis	MW irradiation of an equimolar (1.1 eq) of **2.7** and DCD with 1.02 eq of TMSCl in CH_3CN at 150 °C for 15 min	Not successful
4	Reflux, with $FeCl_3$ catalyst	Heating at reflux an equimolar (1 eq) of **2.7**, DCD (1 eq) and $FeCl_3$ (1 eq) in dioxane for 90 min Followed by adding 3 eq. of HCl conc.	Expected mass of the **2.8** observed

In 1898, Suyama reported an effective method for the preparation of substituted biguanides in the presence of $FeCl_3$ or $ZnCl_2$ under mild conditions (Scheme 2.4).[8]

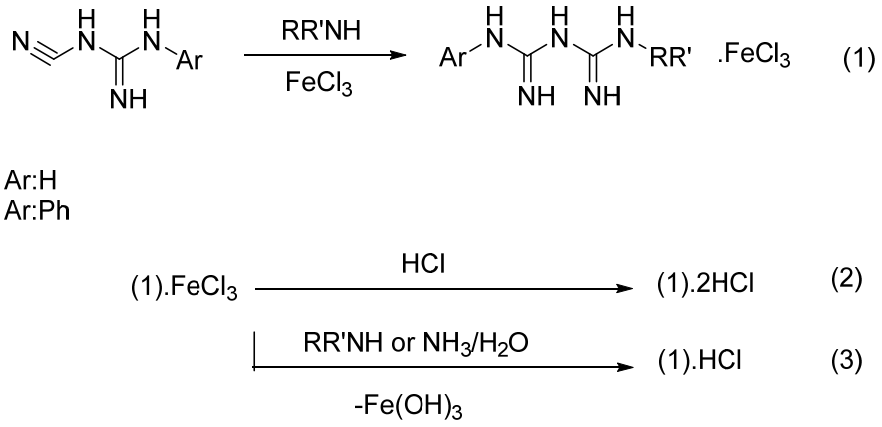

Scheme 2.4. Synthesis of biguanide compounds using $FeCl_3$ as catalysis[8]

A 1:1:1 mixture of **2.7** (217 mg, 1mmol): DCD (84 mg, 1mmol) and $FeCl_3$ (162 mg, 1mmol) in dioxane was maintained under reflux for 90 min. Then the reaction was cooled to room temperature and 3 eq. of concentrated HCl were added to precipitate the biguanide salt. Addition of HCl resulted in the formation of an oily suspension of **2.8** containing many other by-products. A different molar ratio (1:1:3) was examined in DCM and THF, but also failed to give product **2.8**. At this point, we decided, one more time to change the synthetic strategy.

2.2.3. Synthetic protocol C

The successful synthesis of **2.5** was accomplished in five steps using the synthetic route presented in Scheme 2.5, featuring a combination of the two methods presented before.

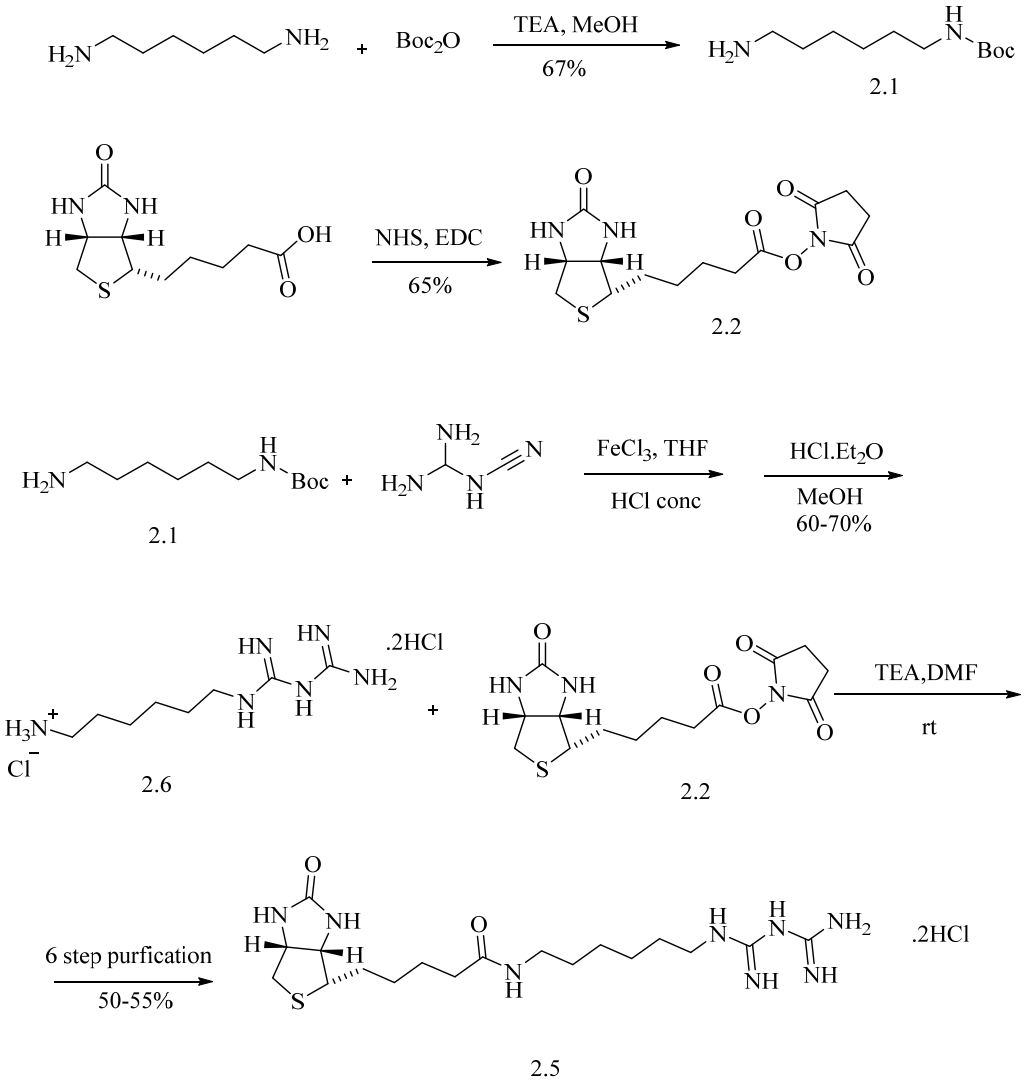

Scheme 2.5. Synthetic of biotin conjugated biguanide **2.5**

Synthesis of **2.1** and biotin-NHS **2.2** have been previously described.[4-5] The functionalization of the linker **2.1** with DCD was realized using $FeCl_3$ as catalyst. A semisolid precipitate was obtained using an equimolar reaction mixture of amine **2.1** (109 mg, 0.5 mmol), dicyandiamide (42 mg, 0.5 mmol) and $FeCl_3$ (81 mg, 0.5mmol) in THF. The quench of the reaction was done through the addition of 3 equiv. of HCl conc., followed by the addition of a dry solution of $HCl{\cdot}Et_2O$ (2 M).

In the last step, functionalized biguanide **2.6** and biotin-NHS **2.2** are coupled via an amide bond. The reaction was conducted by adding the base (TEA) to the solution of the reactants in DMF. This reaction was best performed on a 0.5 mmol scale. We investigated the potential application of this method in a larger scale, but the product was cleaner on the smaller scale.

2.3. Purification of 2.5 by preparative HPLC

Conjugate **2.5** from the latter synthetic procedure was purified by preparative HPLC. The pairs of large and small Luna 5 PFP(2) 100Å analytical columns, water pumps model 2998 and 3100 mass detector were employed. First, a method was developed using an analytical column (LC_0_95_15min_ACN, column Luna 5 PFP(2) 100A, 160x3.0 mm, t_{rBFB} = 13.08 min). Then a preparative LC-MS protocol was used to purify 50 mg of **2.5,** which was dissolved in 2 ml of MeOH and passed through the filter to obtain an homogeneous solution. In each injection, 100 µl are eluted through the column (LC_0_95_15min_ACN, column Luna 5 PFP(2) 100Å, 150x21.20 mm). Biotin-conjugated biguanide **2.5** was detected and collected between 17 and 19 min. After 20 injections, the collected fractions were combined and concentrated to give the pure final product as a white solid.

2.4. Experimental

All organic compounds were purchased from Aldrich Chemicals and Oakwood Chemical in their highest available purity and were used without further purification. Analytical and HPLC-grade solvents for workup and purification procedures, and HPLC analysis were purchased from commercial suppliers and used as received. Anhydrous solvents were obtained by filtration through drying columns with a Glass Contour system (Irvine, CA). Silica gel chromatography was performed by using 230–400 mesh silica gel (Silicycle). The particle size of the aluminum oxide was between 70-290 mesh. ^{1}H NMR and ^{13}C NMR spectra were recorded with a Bruker spectrometer at 400 or 500 MHz. Coupling constant *J* values were measured in Hertz (Hz) and chemical shift values in parts per million (ppm).^{1}H NMR spectra were recorded in MeOD (3.31, 4.78 ppm) or DMSO-d_6 (2.50 ppm). ^{13}C NMR spectra were recorded in MeOD (49.15 ppm) or DMSO-d_6 (39.52 ppm). Centrifugation was performed with an Eppendorf 5804 instrument. Exact mass measurements were performed on a LC-MSD instrument in electrospray ionization (ESI-pos) mode at the Centre régional de spectrométrie de masse de l'Université de Montréal.

2.4.1. 6-(*tert*-Butoxycarbonylamino)hexylamine (2.1)

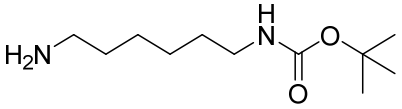

A solution of di-*tert*-butyl dicarbonate (7.27 g, 0.033 moles) in MeOH (20ml) was added to a solution of 1, 6-diaminohexane (11.6 g, 0.1 moles) in 10% TEA:MeOH (100 mL). The mixture was heated at reflux for 2 h and stirred at room temperature overnight. The reaction was monitored by TLC (4% NH_4OH/MeOH). The volatiles were removed *in vacuo*. The residue was dissolved in CH_2Cl_2 and washed with a solution of 10% aqueous Na_2CO_3, dried over anhydrous sodium sulfate, filtered and concentrated under reduced pressure. The oily residue was purified by column

chromatography on silica gel (1:10:89 NH_4OH:MeOH:$CHCl_3$) to give 6-(tert-butoxycarbonylamino)hexylamine **2.1** as light yellow oil.

MS (ESI-pos) m/z: Calcd for $C_{11}H_{25}N_2O_2^+$ $[M+H]^+$: 217.1871, Found. 217.1940; LC-MS purity >99.5(Acq method, LC_20_95_15min_MeOH, column, Atlantis C18 3.9x100mm, 3µm, t_r= 6.54min).

^{1}H NMR (500 MHz, MeOD) δ: 3.04 (t, 2H, *J* = 8.7 Hz), 2.66 (t, 2H, *J* = 9 Hz), 1.49 (m, 4H), 1.45 (s, 9H), 1.36 (m, 4H).

^{13}C NMR (500 MHz, MeOD) δ 157.1, 78.3, 40.9, 39.8, 31.96, 29.50, 27.37, 26.23, 26.20.

2.4.2. (2,5-Dioxopyrrolidin-1-yl-5-((3a*S*,4*S*,6a*R*)-2-oxohexahydro-1*H*-thieno[3,4-*d*]imidazol-4-yl)pentanoate (2.2)

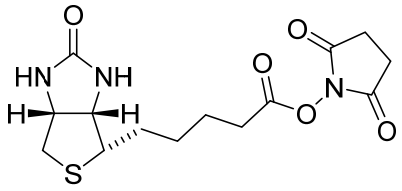

Biotin (244 mg, 1 mmoles), EDC (228 mg, 1.195 mmoles) and NHS (137 mg, 1.195 mmoles) were dissolved in DMF (50 mL) in a 100 mL round-bottomed flask equipped with a magnetic stirrer. The reaction mixture was stirred overnight at room temperature. The volatiles were removed *in vacuo* and the residue were triturated with EtOH:AcOH:H_2O (95:1:4). The biotin-NHS **2.2** (230 mg, 67% yield) was obtained as a white solid that was used in the next step without further purification.

MS (ESI+) m/z: Calcd for $C_{14}H_{20}N_3O_5S^+$ $[M+H]^+$: 342.1045, Found 342.1126.

^{1}H NMR (400 MHz, DMSO) δ: 6.41 (s, 1H), 6.36 (s, 1H), 4.33-4.29 (m, 1H), 4.14-4.17 (m, 1H), 3.09-3.12 (m, 1H), 2.83-2.86 (m, 3H), 2.67 (t, 2H, *J* = 7.2 Hz), 2.58 (d, 1H, *J* = 12.4), 1.55-1.67 (m, 4H), 1.42-1.46 (m, 4H).

^{13}C NMR (400 MHz, DMSO) δ 170.7, 169.3, 163.1, 61.4, 59.6, 55.6, 36.24, 30.4, 28.2, 28.0, 25.8, 24.7.

2.4.3. 6-((((Amino(iminio)methyl)amino)(iminio)methyl)amino)hexan-1-aminium (2.6)

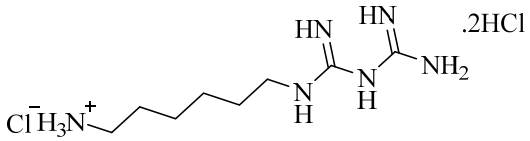

A mixture of amine **2.1** (109 mg, 0.5 mmoles), dicyandiamide (42 mg, 0.5 mmoles) and $FeCl_3$ (81 mg, 0.5 mmoles) was heated at reflux in THF (5ml) for 90 min, The reaction was cooled to room temperature and treated with 3 equivalents of concentrated HCl to form a precipitate that was filtered and washed 3 times with THF. The solid was dissolved in 2 ml of MeOH, treated with 6 ml of a dry solution of 2 mM HCl in Et_2O, and stirred at room temperature for 2 h. The volatiles were removed *in vacuo.* The residue was partitioned between EtOAc and H_2O (1:1). The aqueous phase was separated and freeze-dried to give yellow solid.

MS (ESI+) m/z: Calcd for $C_8H_{21}N_6^+$ $[M+H]^+$: 201.18, Found 201.21.

^{1}H NMR (500 MHz, MeOD) δ 3.37 (s, 2H), 2.96 (s, 2H), 1.73 (s, 4H), 1.49 (s, 4H).

^{13}C NMR (125 MHz, MeOD) δ 155.1, 152.5, 42.7, 39.2, 27.0, 25.8, 25.7, 25.6.

2.4.4. Amino((iminio((6-(5-((3aS,4S,6aR)-2-oxohexahydro-1H-thieno[3,4-d]imidazol-4-yl) pentanamido)hexyl)amino)methyl)amino)methaniminium (2.5)

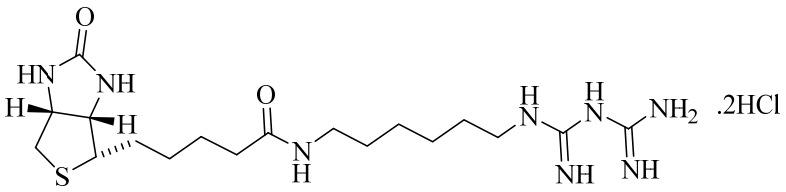

A solution containing **2.4** (378 mg, 1 mmole) and DCD (84 mg, 1mmole) were dissolved in DMF (10 ml), and treated with triethyl amine (0.14 ml, 1.4 mmoles). The resulting mixture was stirred overnight under N_2. After removal of the volatiles *in vacuo*, the solid was washed three times with 3x5 ml acetone. The solid was purified by flash column chromatography on neutral aluminum oxide (DCM:MeOH, from 2% to 15% MeOH, followed by H_2O wash). The total volume of H_2O was reduced to 1-2 ml. Precipitation from the aqueous phase with an excess of acetone gave **2.5** white needles (245 mg, 0.5 mmol, 50 %). The needles were isolated by centrifugation (10 min, speed 4230 rpm or 1000 rcf) and freeze-dried.

MS (ESI+) m/z: Calcd for $C_{18}H_{35}N_8O_2S^+$ $[M+H]^+$: 427.26, Found 427.2.

LC-MS purity >99.5(Acq method, LC_0_95_22min_ACN, column Luna 5µ PFP(2) 150x3.00mm, 100 Å, t_r = 11.14 min).

^{1}H NMR (500 MHz, MeOD) δ 4.53-4.50 (m, 1H), 4.34-4.31 (m, 1H), 3.23-3.18 (m, 5H), 2.95 (dd, 1H, *J* = 13 Hz, *J* = 5 Hz), 2.73 (d, 1H, *J* = 13 Hz), 2.22 (t, 2H, *J* = 7.2 Hz), 1.46-1.79 (m, 14H); ^{13}C NMR (500 MHz, MeOD) δ 174.7, 164.7, 159.5, 62.0, 60.2, 55.6, 41.1, 39.7, 38.7, 35.4, 28.9, 28.4, 28.1, 26.1, 26.0, 25.6.

2.4.5. *tert*-Butyl(6-(5-((3aS,4S,6aR)-2-oxohexahydro-1H-thieno[3,4-d]imidazol-4-yl)pentan amido)hexyl)carbamate (2.3)

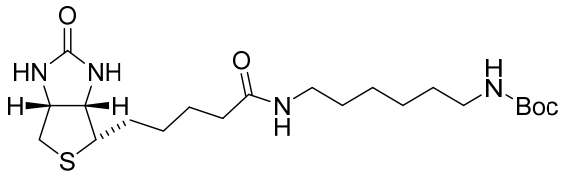

Biotin-NHS (**2.2**, 341 mg, 1 mmoles) and 6-(*tert*-butoxycarbonylamino)hexylamine (**2.1**, 218 mg, 1 mmol) were dissolved in DMF (50 mL) and stirred for 24 h at room temperature. After disappearance of the starting materials and appearance of a new product on the TLC plate was observed. The volatiles were removed under reduced pressure and the residue was purified by silica gel column chromatography (0 to 8% MeOH in CH_2Cl_2) to give **2.3** as a white solid (310 mg, 0.7 mmol, 70%).

MS (ESI+) m/z: Calcd for $C_{21}H_{39}N_4O_4S^+$ $[M+H]^+$: 443.2614; Found 443.2714.

LC-MS purity >99.5(Acq method, LC_40_95_10min_MeOH, column, XSelect C18 4.6x100mm, t_r = 10.087min).

^{1}H NMR (500 MHz, MeOD) δ 4.52-4.50 (m, 1H), 4.33-4.31 (m, 1H), 3.20-3.24 (m, 1H), 3.16-3.19 (m, 2H), 3.04 (t, 2H, *J* = 7 Hz), 2.95 (dd, 1H, *J* = 12.5 Hz, *J* = 5 Hz), 2.72 (d, 1H, *J* = 13 Hz), 2.21 (t, 2H, *J* = 7.3 Hz), 1.75-1.78 (m, 4H), 1.55-1.67 (m, 6H), 1.47 (s, 9H), 1.36 (m, 4H); ^{13}C NMR (500 MHz, MeOD) δ 174.5, 164.7, 157.1, 78.3, 61.9, 60.2, 55.6, 39.8, 39.6, 38.8, 35.4, 29.5, 28.9, 28.3, 28.1, 27.4, 26.2, 26.1, 25.5.

2.4.6. 6-(5-((3aS,4S,6aR)-2-Oxohexahydro-1H-thieno[3,4-d]imidazol-4yl)pentanamido)hexan-1-ammonium chloride (2.4)

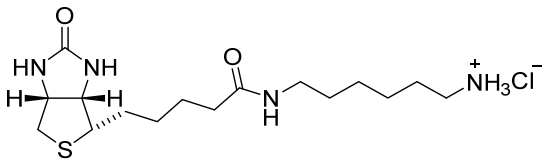

Carbamate **2.3** (365 mg, 1 mmol) in MeOH (40 mL) was treated with a solution of HCl gas in dry Et_2O (5 ml of a 2 mM solution) and stirred at room temperature for 3 h. The volatiles were removed *in vacuo* to give an oily residue that was freeze-dried to give N–(6-aminohexyl)-5-((3aS,4S,6aR)-2-oxohexahydro-1H-thieno[3,4-d]imidazol-4-yl)pentanamide (378 mg, 1 mmole, 100 %) as a white solid without further purification.

HRMS (ESI+) m/z: Calcd for $C_{16}H_{31}N_4O_2S^+$ $[M+H]^+$: 343.2162, Found 343.2230.

LC-MS purity >99.5(Acq method, LC_0_95_15min_MeOH, column, XSelect C18 4.6x100mm, 5µm, t_r = 8.05min).

^{1}H NMR (500 MHz, MeOD) δ 4.62-4.65 (m, 1H), 4.43-4.45 (m, 1H), 3.27-3.31 (m, 1H), 3.23 (t, 2H, *J* = 7 Hz), 3.00 (dd, 1H, *J* =13 Hz, *J* = 5 Hz), 2.94 (t, 2H, *J* = 7.8 Hz), 2.78 (d, 2H, *J* = 13 Hz), 2.28 (t, 2H, *J* = 7.2 Hz), 1.69-1.79 (m, 8H), 1.47-1.57 (m, 6H).

^{13}C NMR (500 MHz, MeOD) δ 175.0, 164.4, 62.7, 61.1, 55.4, 39.3, 39.2, 39.0, 35.0, 28.6, 28.3, 28.2, 27.0, 25.9, 25.6, 25.5.

2.5. Conclusion

After having tried different procedures, we were finally able to develop a synthetic method and a purification step to synthesize pure biotin-conjugated biguanide. Biotin conjugated biguanide and its quaternary ammonium analog were used to identify mitochondrial proteins having binding affinity to metformin. These results are presented in the next chapter.

2.6. References

1. Schenone, M.; Dančík, V.; Wagner, B. K.; Clemons, P. A., *Nat. Chem. Biol.* **2013**, 9, 232-240.

2. Nguyen, C.; Teo, J.-L.; Matsuda, A.; Eguchi, M.; Chi, E. Y.; Henderson, W. R.; Kahn, M., *Proc. Natl. Acad. Sci.* **2003**, 100, 1169-1173.

3. Low, W. K.; Dang, Y.; Schneider-Poetsch, T.; Shi, Z.; Choi, N. S.; Rzasa, R. M.; Shea, H. A.; Li, S.; Park, K.; Ma, G., *Methods enzymol.* **2007**, 431, 303-324.

4. Gardner, R. A.; Ghobrial, G.; Naser, S. A.; Phanstiel IV, O., *J. Med. Chem.* **2004**, 47, 4933-4940.

5. Kimura, Y.; Ito, S.; Shimizu, Y.; Kanai, M., *Org. Lett.* **2013**, 15, 4130-4133.

6. Bamberger, E.; Dieckmann, W., *Eur. J. Inorg. Chem.* **1892**, 25, 543-546.

7. Nederberg, F.; Appel, E.; Tan, J. P.; Kim, S. H.; Fukushima, K.; Sly, J.; Miller, R. D.; Waymouth, R. M.; Yang, Y. Y.; Hedrick, J. L., *Biomacromolecules.* **2009**, 10, 1460-1472.

8. Suyama, T.; Soga, T.; Miyauchi, K., *ChemInform.* **1989**, 20, 20-42.

Chapter 3

Identification of the metformin's target by affinity chromatography

3.1. Introduction

As outlined previously, mitochondrial Complex I has been proposed to be the target of metformin, responsible for cancer inhibition in T2D patients. However, there is no proof of direct interaction between metformin and any specific subunit from the Complex I or other proteins involved in the mitochondrial respiratory chain.

Here, after having validated that the biotinylated biguanide **2.5** was active at the same level as metformin, we performed a pull-down experiment with this biotinylated biguanide **2.5** using amine **2.4** as control in cancerous KP4 cells, with streptavidin *Dynabeads*, in order to identify the proteins that show specific interactions with metformin. The results presented in this chapter have significant implications in the understanding of the mechanism of action of metformin and the inhibition of cancer cell proliferation.

Experiments and results presented below were performed in collaboration with Marie-Camille Rowell from Professor Ferbeyre's group (Department of Biochemistry and Molecular Medicine, University of Montreal).

3.1.1. Biotin-Strept(avidin) System

D-Biotin, vitamin H, is present in all living cells and is important in several biological processes (Figure 3.1).[1] It is abundant in certain plant and animal tissues, such as egg yolk, brain, liver and blood. Moreover, biotin can be conjugated with many proteins and small molecules without changing its binding properties.[1] The natural proteins that bind biotin are avidin and streptavidin.

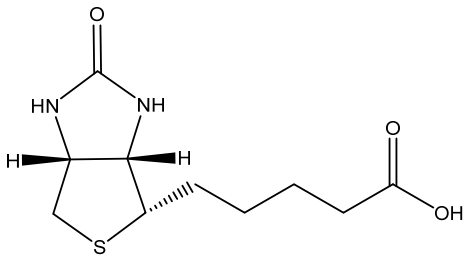

Figure 3.1. Structure of biotin

Avidin is a 67 KDa glycoprotein that contains four equal subunits of 128 amino acids. Streptavidin has four subunits.[2] The affinity constant of biotin-strept(avidin) couple is 10^{15} M^{-1} which represents the strongest non covalent interaction known to date in nature.[2] Moreover, biotin-avidin and biotin-streptavidin systems are extremely stable even under harsh reaction conditions.[3] The biotin–streptavidin complex is more often employed than the biotin-avidin system because of its lower nonspecific binding.[3] Biotin fits tightly inside of the streptavidin active site (Figure 3.2).[4] However, the biotin terminal carboxylate is located at the exterior of the protein, which makes functionalization possible, without affecting binding affinity between streptavidin and the biotinylated molecules or proteins.[3] The biotinylation of small molecules and proteins has found application in the identification of different protein targets and the immobilization of proteins at surfaces.[3]

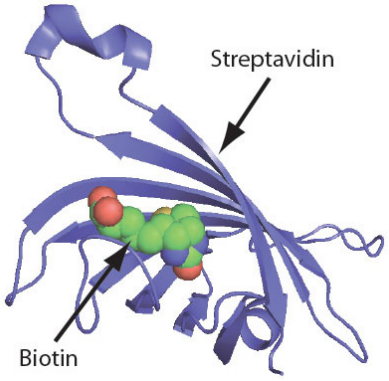

Figure 3.2. Biotin-streptavidin interaction[4]

3.1.2. Affinity chromatography method for the identification of proteins interacting with metformin

Among the large number of methods that can be used for the identification of proteins that specifically bind a bioactive molecule[5], affinity chromatography followed by mass spectrometry is widely used.[6] As shown in Figure 3.3, a biotinylated ligand is first incubated with proteins form cell lysate to capture those that interact with the ligand. These proteins are then isolated from the lysate using an avidin or streptavidin-immobilized column, eluted by disruption of their interaction with the biotinylated ligand and separated by sodium dodecyl polyacrylamide gel electrophoresis (SDS-PAGE). Finally the isolated proteins are identified by mass spectrometry.[7]

In principle, this method is applicable to any small molecule, assuming biological activity is not disrupted by biotinylation. Ligands have been identified for many proteins, such as receptors, enzymes and ion channels.[8] The experimental details of this method are influenced by the binding properties of the biotinylated ligand and its mode of interaction with the proteins.[8] In many cases, nothing may be known about the interaction mode, such that different experimental procedures must be tried to optimize the proteins affinity and elution. The elution methods may be summarized as the following (shown in Figure 3.3):

(I) Elution from the column with a SDS buffer. The purified sample contains in this case specific and nonspecific proteins

(II) Competition with excess amounts of free ligand

(III) Classify with an inactive molecule A

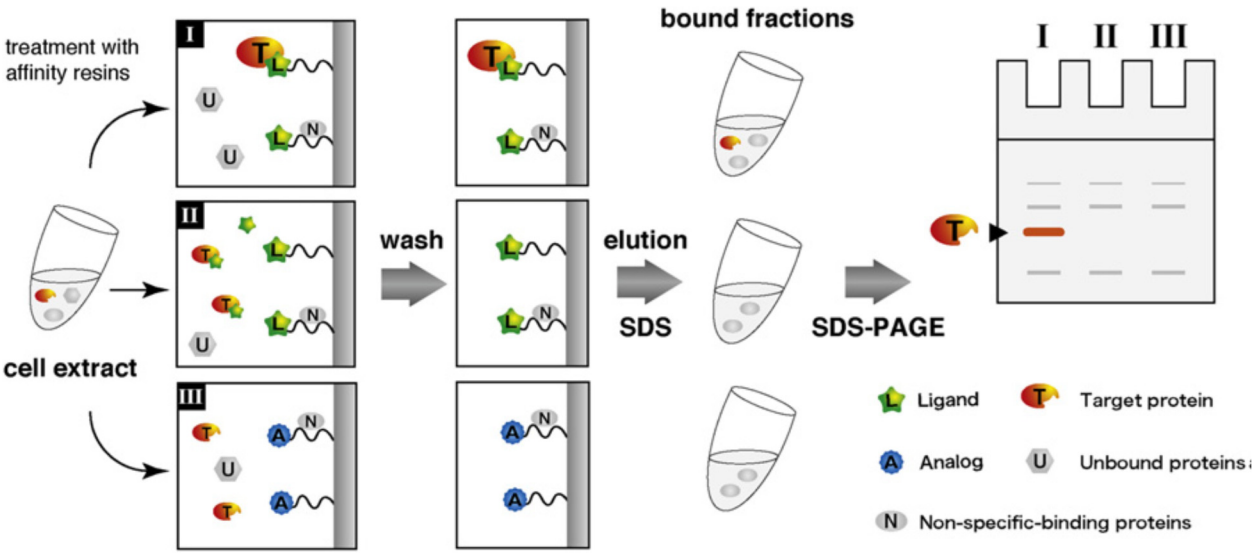

Figure 3.3. Identification of the protein target of a bioactive small molecule using affinity chromatography .[6]

The order of elution from the column depends on the strength of interaction between the ligand and the protein. High binding affinity ligands exhibit dissociation constants (K_D) usually ranging from 10^{-7} to 10^{-15} M.[6] Another important factor is the quantity of the target protein in the lysate. A high concentration of target protein accelerates the formation of the ligand-target protein complex and results consequently in higher yields of isolation by affinity chromatography.[5a] A high concentration of free ligand has generally a negative effect on separation by affinity chromatography. In the presence of an excess amount of ligand, the target proteins cannot bind to the resin and are not isolated, even if they possess a specific interaction with the ligand (Figure 3.3 (II)).

A particular problem often observed with affinity chromatography is false positives which are nonspecific binding proteins. In fact, nonspecific binding is the major problem of this method. Non-specific proteins are hard to remove from the column, even after several washes with different

kinds of buffers.[6] To overcome this problem, well-designed control molecules that lack biological activity are useful. Protein targets can be distinguished from nonspecific binders by comparison of the binding patterns of ligand and control pull-downs on SDS-PAGE gels (Figure 3.3 (I), (III)). [5b]

3.1.3. Structure of the ATP synthases enzyme

ATP synthase (adenosine triphosphate synthase, F_1F_0-ATPase) is a multisubunit protein and an important enzyme for cellular metabolism (Figure 3.4),[9] Present in the plasma membrane of bacteria, in the thylakoid membranes of chloroplasts and in mammalian cells,[10] ATP synthase performs the synthesis of ATP (adenosine triphosphate) from ADP (adenosine diphosphate) and phosphate (Pi) by using the potential energy from the transmembrane electrochemical proton gradient. ATP synthase can also produce energy by hydrolysing ATP and act as a proton pump.[11]

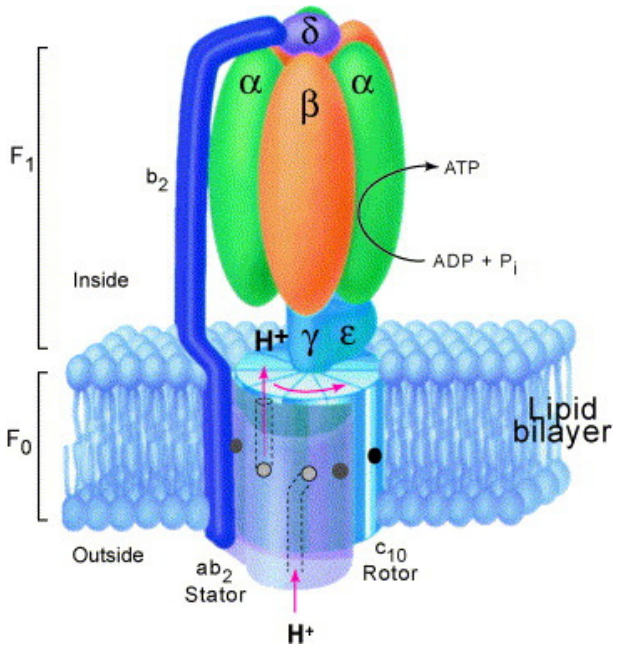

Figure 3.4. ATP synthase in the inner membrane of mitochondria.[9]

ATP synthases, from bacteria to humans, are composed of an assembly of two rotary motors F_1 and F_0 that mechanical rotate around a central stalk (Figure 3.4).[9] Different organisms show variation in the subunit composition and the structure of the F_0 and F_1 (Table 3.1).

Table 3.1. The subunit composition of ATP synthase of different species; *Escherichia coli* (*E. coli*), *Saccharomyces cerevisiae* (*S. cerevisiae*) and *Homo sapiens* (*H. sapiens*).[12a, 12b, 12c]

		Bacteria		**Mitchondria**			
		E. coli		*S. cerevisiae*		*H. sapiens*	
		Subunit	**Gene**	**Subunit**	**Gene**	**Subunit**	**Gene**
F_1		α_3	*uncA*	α_3 (1)	*ATP1*	α_3	*ATP5A1*
		β_3	*uncD*	β_3 (2)	*ATP2*	β_3	*ATP5B*
		γ	*uncG*	γ (3)	*ATP3*	γ	*ATP5C1-2*
		ε	*uncC*	δ	*ATP16*	δ	*ATP5D*
		-		ε	*ATP15*	ε	*ATP5E*
	Regulatory proteins			Inh1p	*INH1*	IF_1	*ATPIF1*
				Stf1p	*STF1*		
				Stf2p	*STF2*		
F_0		a	*uncB*	6	*ATP6(mt)*	a	*ATP6(mt)*
		-		8	*ATP8(mt)*	A6L	*ATP8(mt)*
		c_{10-12}	*uncE*	9_{10}	*ATP9*	c_8	*ATPG1-3*
		δ	*uncH*	OSCP	*ATP5*	OSCP	*ATP5O*
		b_2	*uncF*	b (4)	*ATP4*	b	*ATP5F1*
				d	*ATP7*	d	*ATP5H*
				h	*ATP14*	F_6	*ATP5J*
				f	*ATP17*	f	*ATP5J2*
				e	*ATP21*	e	*ATP5I*
				g	*ATP20*	g	*ATP5L, ATP5L2*
				J	*ATP18*	-	
				k	*ATP19*	-	

A large protein with a molecular weight of 550-650 KDa, ATP synthase has 16-18 subunits in mammals.[11] In mammalian ATP synthase, the F_1 motor is a water soluble protein possessing the subunits α, β , γ, δ, ε, and the inhibitor factor 1 (IF1) (Figure 3.5).[13] The F_0 motor is bound to the inner mitochondrial membrane and built of subunits a, b, c, d, F_6, the oligomycin sensitivity

conferring protein (OSCP), the accessory subunits e, f, g and a protein that is encoded by mitochondria DNA (A6L) (Figure 3.5).

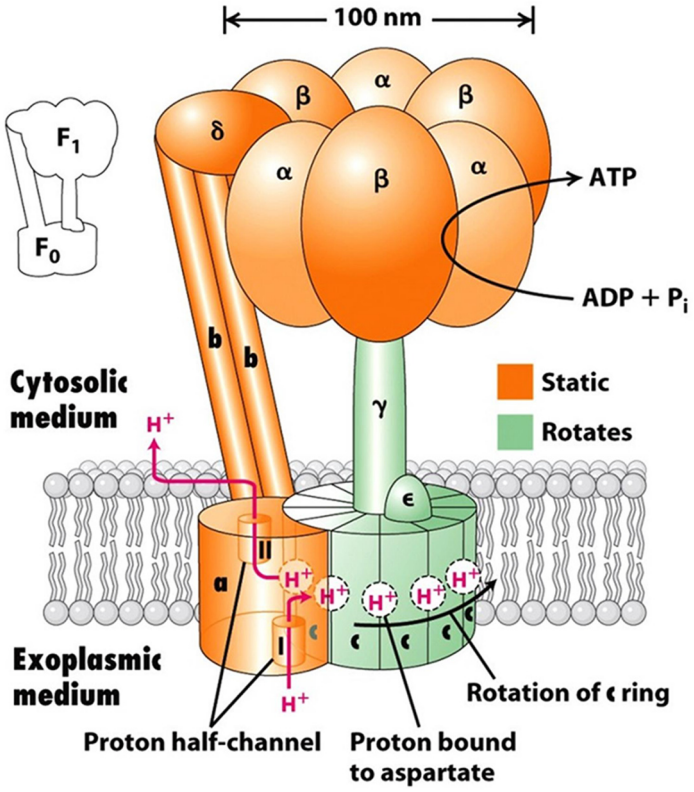

Figure 3.5. Schematic representation of mammalian ATP synthase.[14]

In mammalians, the subunits α and β possess molecular masses of 55.3 and 51.7 KDa respectively, and bind nucleotides in their catalytic domains.[15] The subunit γ has a molecular mass of 30.3 KDa.[16] The subunit γ binds to the ε-δ complex forming the foot part of the central stalk.[15,17] The mammalian subunit ε is the smallest subunit of F_1 with a molecular mass of 5.8 KDa and has no homologue in chloroplasts and bacteria.[17] This subunit is localized between the two domains of the δ subunits and has an important role in stabilizing the central stalk.[17] Different studies including fluorescent tagging, fluorescent anisotropy measurements and cross linking, have provided evidence for the rotational movement of the subunit ε in the ATP synthase.[18a,18b]

The two parts of the F_1 and F_0 motors are connected by two stalks, one central and one peripheral.[13] The subunits γ, δ and ε constitute the central stalk. The peripheral stalk is formed by the subunits b, d, F_6 and OSCP.[13] The subunit b provides a link between the F_1 and F_0 parts and acts as a scaffold for the peripheral stalk subunits.[19] The subunits d and F_6 have also an important role in the assembly and the catalytic function of ATP synthase.[20] Subunits c, a and the small hydrophobic subunits form a proton channel in the membrane.[21] It is notable that the exact function of these small subunits is not clear yet, especially because of the lack of high resolution structural information for these proteins.[22]

The function of the central stalk is to change the conformation of the stalk proteins and to convert the energy between the two parts F_1 and F_0. The peripheral stalk provides a rigid link and acts as a peripheral stalk containing the two mentioned parts.[23] The c ring is connected to the central stalk *via* the δ-ε subunits.[24] The central stalk and c ring form the rotor part of the ATP synthase.[25]

The F_0 looks like a rotary electrochemical generator and forms a proton channel towards the F_1. The F_0 motor transforms the electrochemical energy of protons into torque that enables the F_1 to work as an ATP synthesizer. In hydrolysis mode, F_1 converts the energy of ATP hydrolysis into torque, causing F_0 to act as an ion pump.[26] The basic residues Arg-210/Arg-159, which are localized close together in the transmembrane helix of the subunit a, have been known to have a critical role for proton transportation.[27] A high resolution structure of F_0 has not been resolved, but different studies, including analysis by nuclear magnetic resonance-spectroscopy, X-ray diffraction and atomic force microscopy, support the model shown in the Figure 3.5. According to this model, protons flow from the F_0 subunit leading to the rotation of the c ring and consequently inducing the rotation of the central stalk. This rotation changes the conformation of the catalytic

part, priming the synthesis of ATP.[30] The ATP synthase activity can be switched to ATP hydrolysis activity by the inhibitor protein IF1, which is located at the bottom of the catalytic part of the α/β subunites.[13,29]

3.1.4. The ATP synthases subunit e (ATP5I)

The ATP synthase subunit e is a small basic hydrophilic protein with an isoelectric point of 9.78.[30] It is localized in the inner mitochondria membrane with a specific N_{in}-C_{out} orientation.[31] Its hydrophobic N-terminal region is anchored to the inner mitochondrial membrane and its hydrophilic C-terminal contains a conserved coiled-coil motif that exists in the intermembrane space.[32]

The F_0-ATPase subunit e was first identified in the bovine heart by Walker *et al.*[33] The amino acid sequence of the precursor of protein rat subunit e is composed of 289 amino acids and its mature polypeptide chain is composed of 70 amino acid residues, and has a molecular weight of 8123 Da (~8 KDa).[30] The rat subunit e is highly homologue with the bovine heart subunit e, but it has no homology with the bacterial and chloroplast enzymes. Similar subunits exist in bacteria γ chloroplasts (Table 3.1),[34] and have been identified in the F_0-secteur of mammalian and yeast *S.cerevisiae* mitochondria.[31,35] Experimental studies suggested that the subunit e has an important role in supporting the dimerization and oligomerisation of the ATP synthase.[38] Immunoblot analysis of *S.cerevisiae* showed that two moles of purified ATP synthase contains two mole of subunit e.[30] Two models (Figure 3.6) have been proposed to explain the role of subunit e in the assembly of ATP synthase dimer and oligomers in the mitochondrial membrane.[32]

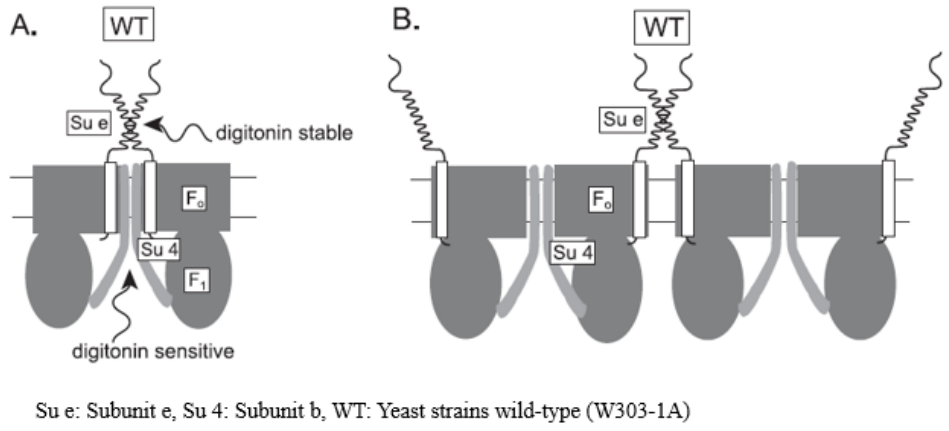

Su e: Subunit e, Su 4: Subunit b, WT: Yeast strains wild-type (W303-1A)

Figure 3.6. The role of subunit e in stabilizing the ATP synthase dimer (A) and oligomers (B).[32]

The precise function of F_0-ATP synthase subunit e is unknown. Studies have shown that the mitochondrial ATP synthase activity of *S. cerevisiae* decreases when the subunit e is removed. This decrease does not affect cell growth, but reduces the amount of ATP synthase per mg of mitochondrial protein (e.g. ATP synthase specific activity).[31] The subunit e is involved in the formation of the supramolecular structure of the mithochondrial ATP synthase and plays a key role in energy metabolism of the ATP within the putative proton dependent regulatory region.[36, 37a, 37b]

3.2. Materials and methods

3.2.1. Cell culture and treatments

Human pancreatic ductal carcinoma cell line KP-4 was a gift from Dr. Nabeel Bardeesy (Massachusetts General Hospital). Cells were grown in Dulbecco's modified eagle media (DMEM) 1x (Wisent) supplemented with 10% fetal bovine serum (FBS, Wisent) and 1% penicillin/streptomycin (Wisent). Metformin hydrochloride for treatment of cells was purchased from Sigma-Aldrich (PHR1084).

3.2.2. Mitochondrial protein isolation

KP-4 cells (~4 x 10^7, RIKEN) were grown in 15 cm tissue culture dishes using DMEM, then washed with ice-cold phosphate buffer saline (PBS), (137 mM NaCl, 2.7mM KCl, 10 mM Na_2HPO_4 x $7H_2O$, 2mM KH_2PO_4). Mitochondrial crude extract was obtained using the mitochondria isolation kit for cultured cells (Abcam, ab110170) according to manufacturer's instructions. Briefly, cells were scraped in ice-cold PBS, frozen and thawed to weaken membranes, then disrupted using a Dounce homogeneizer (2 mL, pestle B). After centrifugation, crude mitochondrial pellets were obtained and resuspended in LM buffer pH 7.8 (1% lauryl maltoside, 1x Phostop, PBS 1x pH 7.8). Mitochondrial lysates were incubated on ice for 30 min, then cleared by centrifugation for 10 min at 16 000 g at 4°C. The concentration of the supernatant was measured using the bicinchoninic acid (BCA) assay (Pierce 23225).

3.2.3. Immunoblotting

KP-4 cells ($2.5x10^5$) were seeded in 6 cm plates. The day after, the media was changed for new media containing either 10 mM metformin hydrochloride, 10 mM **2.5** or **2.4** for 24 h. Adherent KP-4 cells were rinsed twice with cold PBS 1x and scraped in Laemmli lysis buffer (4% SDS, 20% glycerol, 120 mM Tris-HCl pH 6.8). Lysates were boiled for 5 min at 95°C. The protein concentration was measured using a Nanodrop2000c spectrophotometer (ThermoScientific). Proteins samples (20 µg) were treated with 0.02% of bromophenol blue and 10% B-mercaptoethanol, separated on SDS-PAGE then transferred on a nitrocellulose membrane (0.45µm, Bio-Rad). The latter was blocked 1 h with PBS 0.05%, then incubated overnight at 4°C for 1 h at room temprature with primary antibodies diluted in PBS containing 0.1% bovine serum albumin (BSA) and 0.02% NaN_3. The membrane was washed three times for 10 min using PBS containing 0.05% Tween 20, incubated for 1h at room temperature with secondary antibodies, and

diluted in PBS containing 1% milk. The membrane was washed again three times using the above protocol. The signal was revealed using enhanced chemiluminescence reagent (ECL), (GE Healthcare Life Sciences, #RPN2106). The following primary antibodies were used for this work were: anti-phospho-ACC S79 (Rabbit, 1:1000, Cell signaling 3661S), anti-AMPK (Rabbit, 1:1000, Cell signaling 2532), anti-phospho-AMPK T172 (Rabbit, 1:1000, Cell signaling 2531S), and anti-Beta-Actin (Mouse, 1:20000, Cell signaling 3700). Secondary antibodies used for this work are: anti-rabbit IgG conjugated to HRP (Goat, 1:3000, Bio-Rad 170-6515), anti-mouse IgG conjugated to HRP (Goat, 1:3000, Bio-Rad 170-6516).

3.2.4. Indirect capture of biotinylated metformin

Mitochondrial proteins (0.5 mg) were incubated with either 1 mM of biotinylated metformin **2.5** or 1 mM **2.4** for 3h at room temperature with agitation. Dynabeads MyOne streptavidin C1 (ThermoFisher Scientific, 65001) were washed three times by vortexing using LM buffer at pH 7.8. To the lysates 0.5 mg of beads were added, and the mixture was incubated for 30 min at 4°C with agitation. The beads from both conditions were respectively recovered and washed three times for 30 min at 4°C with LM buffer pH 7.8. Elution of proteins bound to **2.5** was performed using LM buffer at pH 7.8 containing 50 mM of metformin hydrochloride (PHR1084, Sigma) during for 30 min at room temperature. The supernatant was recovered, treated with an appropriate volume of 6X loading buffer (0.5 M Tris-HCl pH 6.8, 30% glycerol, 10% SDS, 1% bromophenol blue and 15% β-mercaptoethanol) and boiled 3 times for 5 min followed by vortexing for 10 s. The recovery of proteins bound to biotin-linker-NH_3^+ **2.4** Bio-Met **2.5** after elution was achieved by boiling and vortexing 3X 5 min the beads in LM buffer containing appropriate quantity of 6X loading buffer. Three samples were prepared in two replicates per

sample and analyzed by the Mass spectrometry platform at IRIC (Institute for Research on Immunology and Cancer) for protein identification.

3.2.5. Mass spectrometry

Samples were separated in two, Proteins were separated by SDS-PAGE. The gel was dyed with Coomassie Colloidal Blue to detect proteins. For each condition, bands were cut and underwent tryptic digestion followed by LC-MS/MS. The following table shows the identifications of each sample loaded on the gel.

Table 3.2. Conditions for mass spectrometry

	Name	Explantation of compound
1	Control – B1	Pull-down with **2.4**, elution by boiling, replicate 1
2	Control – B2	Pull-down with **2.4**, elution by boiling, replicate 2
3	Bio-Met – M1	Pull-down with **2.5**, elution by metformin, replicate 1
4	Bio-Met – B1	Pull-down with **2.5**, elution by boiling, replicate 1
5	Bio-Met – M2	Pull-down with **2.5**, elution by metformin, replicate 2
6	Bio-Met – B2	Pull-down with **2.5**, elution by boiling, replicate 2

3.3. Results and discussion

3.3.1. *In vivo* activity of 2.5

The biological activity of **2.5** was verified to insure ability to activate AMPK signaling like metformin. A SDS-PAGE and a Western Blot (immunoblotting) analysis (page 54) were performed on 2.5 and metformin.

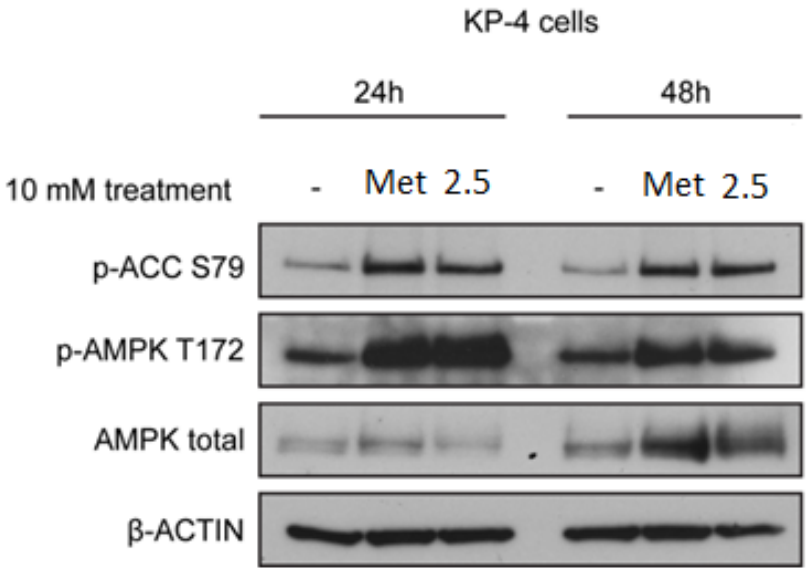

Figure 3.7. Western blot analysis of KP-4 cells by metformin or **2.5.**

As shown in Figure 3.7, the Western blot analysis showed similar levels of AMPK activation when KP-4 cells were treated with metformin or **2.5** after 24 h and 48 h.

3.3.2. Identification of metformin-AMP5I interaction

The isolation of the target proteins using the streptavidin pull down method, followed by mass spectrometer's analysis were performed using the inner mitochondrial membrane from cell lysate. One binding protein that was detected in the lysate, had an apparent molecular weight of 8 KDa. By mass spectrometry, the protein was identified as the ATP5I. The identity of the 8 kDa protein was confirmed by western blot analysis using specific antibodies after the pull down assay (Figure 3.8).

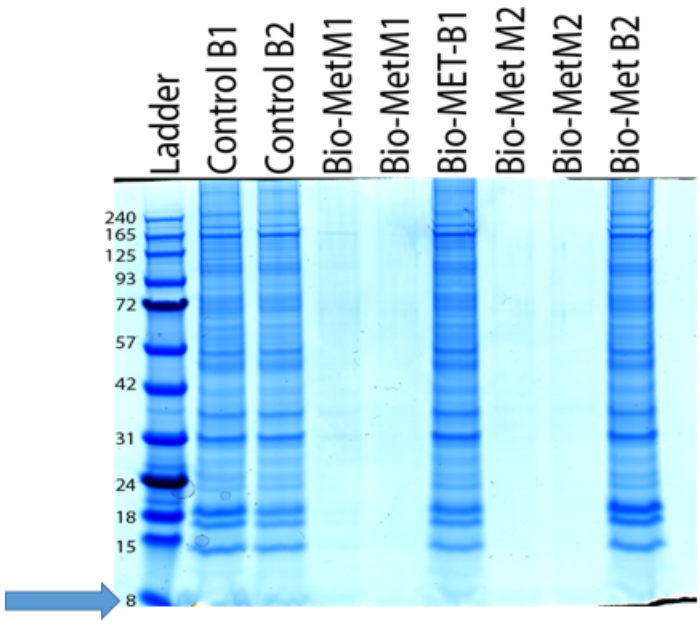

Figure 3.8. Coomassie staining of the SDS-PAGE showing proteins recovered after pull-down for the identified samples.

The 8 KDa band was not observed in the SDS-PAGE, because the gel was cut exactly at this position. The specificity of ATP5I binding was confirmed by an additional experiment performed in the Professor Febeyre's laboratory, using specific antibodies to identify ATP5I in the Western-blot analysis (results not shown).

3.3.3. Association of ATP5I with the anticancer properties of metformin

Our present work suggests that metformin has a direct interaction with the ATP synthase subunit e (ATP5I). ATP synthase, which is essential for cell growth, catalyzes the synthesis of ATP from ADP and phosphate, using electrochemical energy. ATP5I seems to have an important role to regulate the function of ATPase but unfortunately, little is known about the structure and the function of this elusive protein. The interaction of the subunit e with metformin might prevent

the peripheral stalk from changing the conformations between extended and curve modes and consequently inhibiting the ATP synthase function.

Previously, metformin was retorted to block cancer cell proliferation by inhibition of the complex I.[38] Moreover, metformin has been shown to act as an inhibitor of the ATP synthase, but it does not affect the intracellular AMP/ATP ratio. Inhibition of ATP synthase has been thought to be a consequence of the effect of metformin on complex I; however, the mechanism by which complex I can affect ATP synthase is not completely clear. Activation of AMPK by metformin leads to the inhibition of the nuclear factor kB (NF-kB), which is a protein complex that controls transcription of DNA through inhibition of complex I. In addition, metformin prevents translocation of NF-kB to the nucleuse in an AMPK independent manner.[39]

3.4. Conclusion

Putting together all this information and recent results, we believe that metformin directly binds the ATP5I and inhibits its activity, leading to the inhibition of mitochondrial respiration which stops cell proliferation. This interaction changes likely the electrochemical gradient across the inner mitochondrial membrane that activates the AMPK signaling, leading to the inhibition of the complex I activity. The change of the electrochemical gradient through the inner mitochondrial membrane may be reasonably implicated in other mitochondrial actions including reduced ROS production, and reduced oxidative stress, reduced DNA damage.[40]

3.5. References

1. Laitinen, O. H.; Nordlund, H. R.; Hytönen, V. P.; Kulomaa, M. S. *Trends Biotechnol.* **2007,** 25, 269-277.

2. Weber, P. C.; Ohlendorf, D.; Wendoloski, J.; Salemme, F. *Science.* **1989,** 243, 85-88.

3. Diamandis, E. P.; Christopoulos, T. K. *Clin. Chem.* **1991,** 37, 625-636.

4. DeChancie, J.; Houk, K. *J. Am. Chem. Soc.* **2007,** 129, 5419.

5. a. Terstappen, G. C.; Schlüpen, C.; Raggiaschi, R.; Gaviraghi, G. *Nat. Rev. Drug Discov.* **2007,** 6, 891-903; b. Lomenick, B.; Olsen, R. W.; Huang, J.*ACS Chem. Biol.* **2010,** 6, 34-46; c. Kawatani, M.; Osada, H. *Med. Chem. Commun.* **2014,** 5, 277-287.

6. Sato, S.-i.; Murata, A.; Shirakawa, T.; Uesugi, M. *Chem. Biol.* **2010,** 17, 616-623.

7. Aebersold, R.; Mann, M. *Nature.* **2003,** 422, 198-207.

8. Shuker, S. B.; Hajduk, P. J.; Meadows, R. P.; Fesik, S. W. *Science.* **1996,** 274, 1531-1534.

9. Fillingame, R. H.; Angevine, C. M.; Dmitriev, O. Y. *Biochim. Biophys. Acta.* **2002,** 1555, 29-36.

10. Boyer, P. D. *Angew. Chem. Int. Ed.* **1998,** 37, 2296-2307.

11. Capaldi, R. A.; Aggeler, R. *Trends Biochem Sci.* **2002,** 27, 154-160.

12. a. Boyer, P. D. *Annu. Rev. Biochem.* **1997,** 66, 717-749; b. Kucharczyk, R.; Zick, M.; Bietenhader, M.; Rak, M.; Couplan, E.; Blondel, M.; Caubet, S.-D.; di Rago, J.-P.*BBA-MOL CELL RES.* **2009,** 1793, 186-199; c. Watt, I. N.; Montgomery, M. G.; Runswick, M. J.; Leslie, A. G.; Walker, J. E. *Proc. Natl. Acad. Sci.* **2010,** 107, 16823-16827.

13. Jonckheere, A. I.; Smeitink, J. A.; Rodenburg, R. J. *J. Inherit. Metab. Dis.* **2012,** 35, 211-225.

14. Lodish, H. **2008**. *Molecular Cell Biology*, 6th ed. W. H. Freeman and company. https://biochemist01.wordpress.com/tag/atp/

15. Wittig, I.; Schägger, H. *BBA-Bioenergetics.* **2008,** 1777, 592-598.

16. Matsuda, C.; Endo, H.; Hirata, H.; Morosawa, H.; Nakanishi, M.; Kagawa, Y. *FEBS Lett.* **1993,** 325, 281-284.

17. Gibbons, C.; Montgomery, M. G.; Leslie, A. G.; Walker, J. E. *Nat. Struct. Mol. Biol.* **2000,** 7, 1055-1061.

18. a. Aggeler, R.; Ogilvie, I.; Capaldi, R. A. *J. Biol. Chem.* **1997,** 272, 19621-19624; b. Duncan, T. M.; Bulygin, V. V.; Zhou, Y.; Hutcheon, M. L.; Cross, R. L. *Proc. Natl. Acad. Sci.* **1995,** 92, 10964-10968.

19. Velours, J.; Durrens, P.; Aigle, M.; Guérin, B. *FEBS J.* **1988,** 170, 637-642.

20. Velours, J.; Vaillier, J.; Paumard, P.; Soubannier, V.; Lai-Zhang, J.; Mueller, D. M. *J. Biol. Chem.* **2001,** 276, 8602-8607.

21. Devenish, R. J.; Prescott, M.; Rodgers, A. J. *Int. Rev. Cell. Mol. Biol.* **2008,** 267, 1-58.

22. Rak, M.; Zeng, X.; Brière, J.-J.; Tzagoloff, A. *BBA-Mol. Cell. Res.* **2009,** 1793, 108-116.

23. Wilkens, S.; Dunn, S. D.; Chandler, J.; Dahlquist, F. W.; Capaldi, R. A. *Nat. Struct. Biol.* **1997,** 4, 198-201.

24. Stock, D.; Leslie, A. G.; Walker, J. E. *Science.* **1999,** 286, 1700-1705.

25. Schulenberg, B.; Aggeler, R.; Murray, J.; Capaldi, R. A. *J. Biol. Chem.* **1999,** 274, 34233-34237.

26. Dimroth, P.; von Ballmoos, C.; Meier, T. *EMBO Reports.* **2006,** 7, 276-282.

27. Junge, W.; Lill, H.; Engelbrecht, S. *Trends Biochem Sci.* **1997,** 22, 420-423.

28. Stock, D.; Gibbons, C.; Arechaga, I.; Leslie, A. G.; Walker, J. E. *Curr Opin Struct Biol.* **2000,** 10, 672-679.

29. Minauro-Sanmiguel, F.; Wilkens, S.; García, J. J. *Proc. Natl. Acad. Sci. U.S.A.* **2005,** 102, 12356-12358.

30. Higuti, T.; Kuroiwa, K.; Kawamura, Y.; Yoshihara, Y. *Biochemistry.* **1992,** 31, 12451-12454.

31. Arselin, G.; Vaillier, J.; Salin, B.; Schaeffer, J.; Giraud, M.-F.; Dautant, A.; Brèthes, D.; Velours, J. *J. Biol. Chem.* **2004,** 279, 40392-40399.

32. Everard-Gigot, V.; Dunn, C. D.; Dolan, B. M.; Brunner, S.; Jensen, R. E.; Stuart, R. A. *Eukaryot Cell.* **2005,** 4, 346-355.

33. Walker, J. E.; Lutter, R.; Dupuis, A.; Runswick, M. J. *Biochemistry.* **1991,** 30, 5369-5378.

34. Walker, J. E.; Saraste, M.; Gay, N. J. *Nature.* **1982,** 298, 867-869.

35. Arnold, I.; Bauer, M. F.; Brunner, M.; Neupert, W.; Stuart, R. A. *FEBS Lett.* **1997,** 411, 195-200.

36. Arselin, G.; Giraud, M. F.; Dautant, A.; Vaillier, J.; Brethes, D.; Coulary-Salin, B.; Schaeffer, J.; Velours, J. *FEBS J.* **2003,** 270, 1875-1884.

37. a. Swartz, D. A.; Park, E. I.; Visek, W. J.; Kaput, J. *J. Biol. Chem.* **1996,** 271, 20942-20948; b. Levy, F. H.; Kelly, D. *Am. J. Physiol. Cell Physiol.* **1997,** 272, C457-C465.

38. Bridges, H. R.; Jones, A. J.; Pollak, M. N.; Hirst, J. *Biochem. J.* **2014,** 462, 475-487.

39. Moiseeva, O.; Deschênes-Simard, X.; St-Germain, E.; Igelmann, S.; Huot, G.; Cadar, A. E.; Bourdeau, V.; Pollak, M. N.; Ferbeyre, G. *Aging cell.* **2013,** 12, 489-498.

40. Pollak, M. N. *Cancer Discov.* **2012,** 2, 778-790.

Chapter 4

Conclusion

In this thesis we addressed the challenges brought by previous knowledge that metformin acts as a cancer inhibitor, without knowing the nature of the targeted protein. First, we described the experimental protocol for the synthesis of a biotinylated biguanide **2.5** and a control **2.4**. These two biotinylated compounds were then used in affinity chromatography to detect, isolate and identify proteins that can bind metformin. One specific interaction has been identified between the ATP synthases-subunit e (ATP5I) and metformin.

The ATP5I belongs to the complex V family proteins that play an important role in cellular signaling. How the binding of metformin to the ATP synthases-subunit results in changing the signaling through the inner mitochondrial membrane and specifically inhibiting the activity of complex I needs further studies especially to determinate the structure and function of this elusive protein (ATP5I). The movement of subunit e within the ATP synthase may provide means of regulation and information transfer between distant parts of the rotary ATPase and complex I. Thereby, inhibition of these molecular machines may block cancer cell proliferation, because cancerous cells need more energy as they divide faster. Further investigations should provide new insights into energy coupling relationship between ATP synthases and complex I and their interaction with metformin.

Appendix

Spectral data related to chapter 2

6-(tert-Butoxycarbonylamino)hexylamine (2.1)

^{1}HNMR

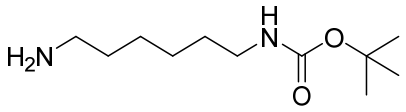

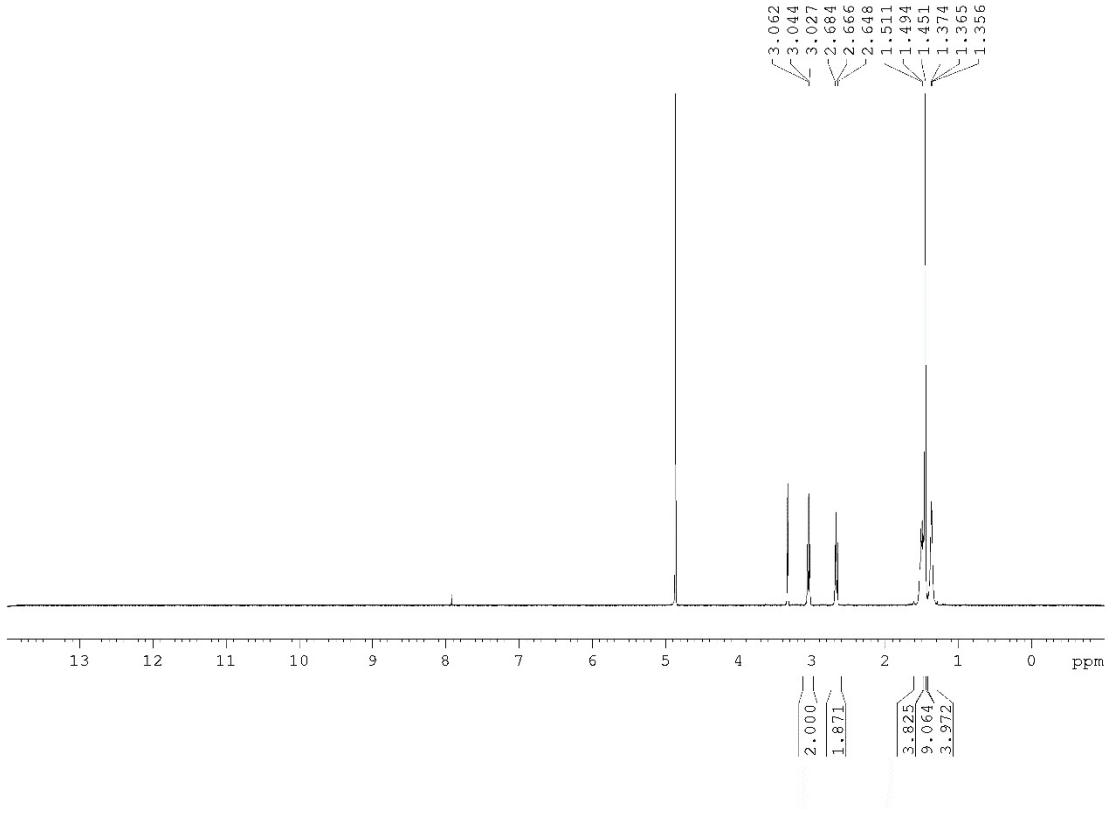

^{13}CNMR

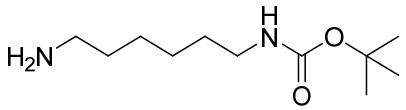
H
N
O
O
H2N

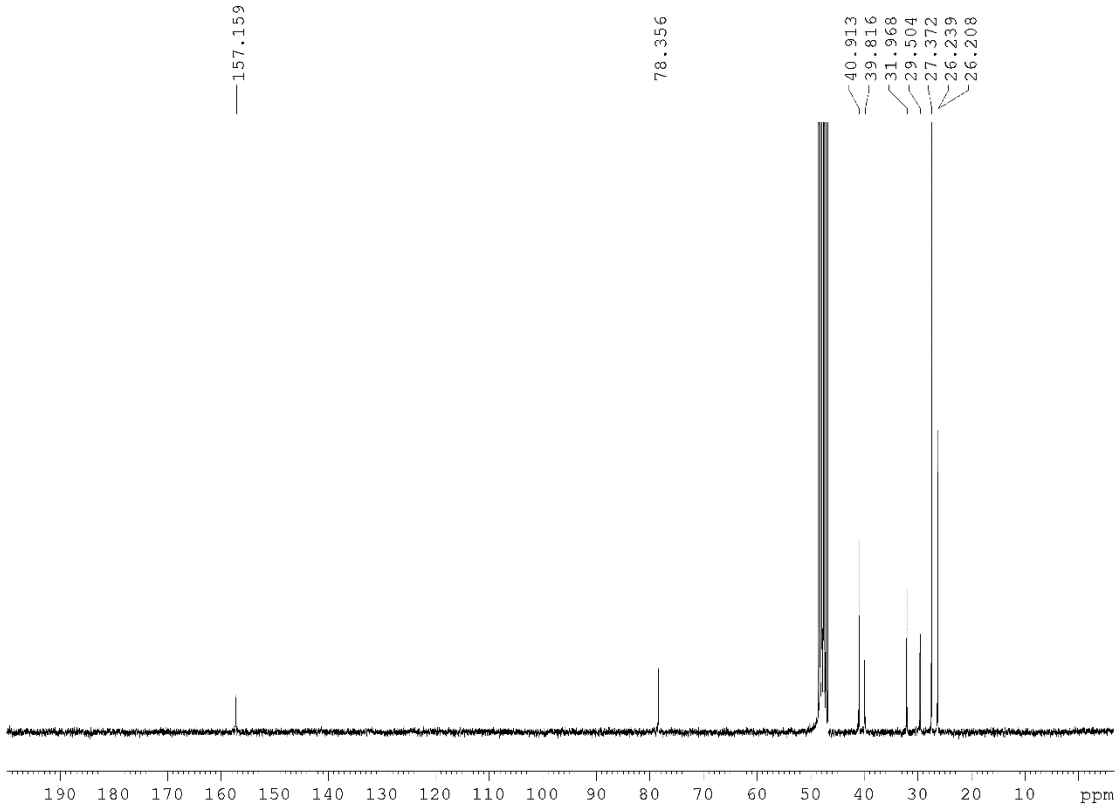
157.159
78.356
40.913
39.816
31.968
29.504
27.372
26.239
26.208
190 180 170 160 150 140 130 120 110 100 90 80 70 60 50 40 30 20 10 ppm

LCMS

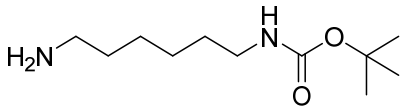
H
N
O
O
H_2N

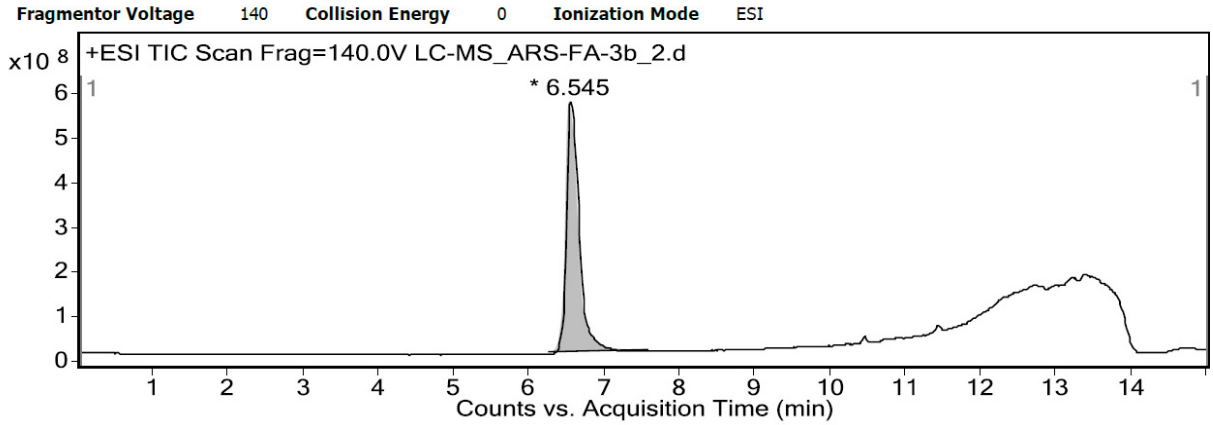
Fragmentor Voltage 140 Collision Energy 0 Ionization Mode ESI
+ESI TIC Scan Frag=140.0V LC-MS_ARS-FA-3b_2.d
x10 8
* 6.545
Counts vs. Acquisition Time (min)

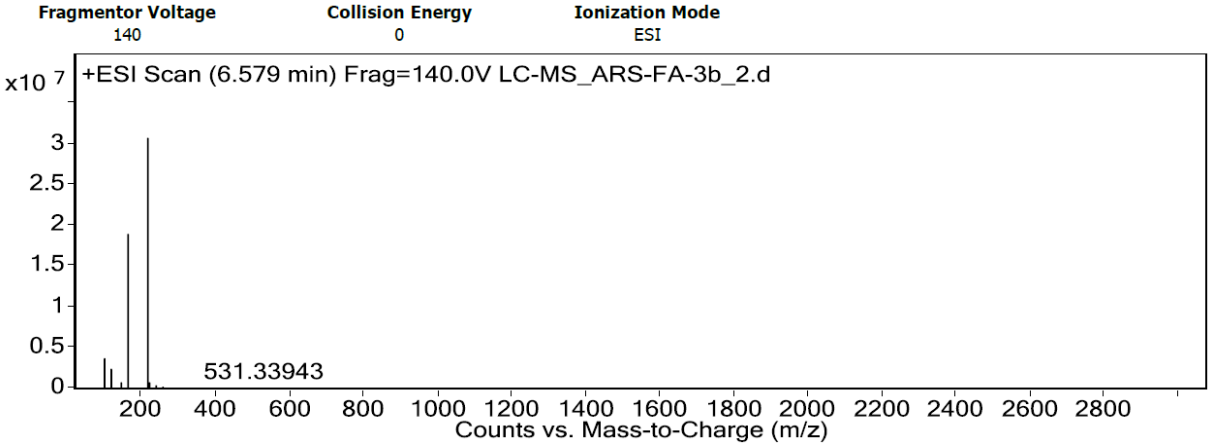
Fragmentor Voltage 140 Collision Energy 0 Ionization Mode ESI
+ESI Scan (6.579 min) Frag=140.0V LC-MS_ARS-FA-3b_2.d
x10 7
531.33943
Counts vs. Mass-to-Charge (m/z)

(2,5-dioxopyrrolidin-1-yl5-((3a*S*,4*S*,6a*R*)-2-oxohexahydro-1*H*-thieno[3,4-*d*]imidazol-4-yl)pentanoate (2.2)

[1]HNMR

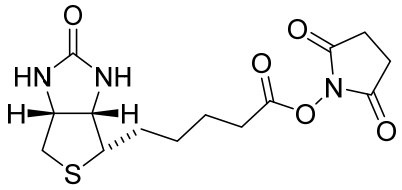

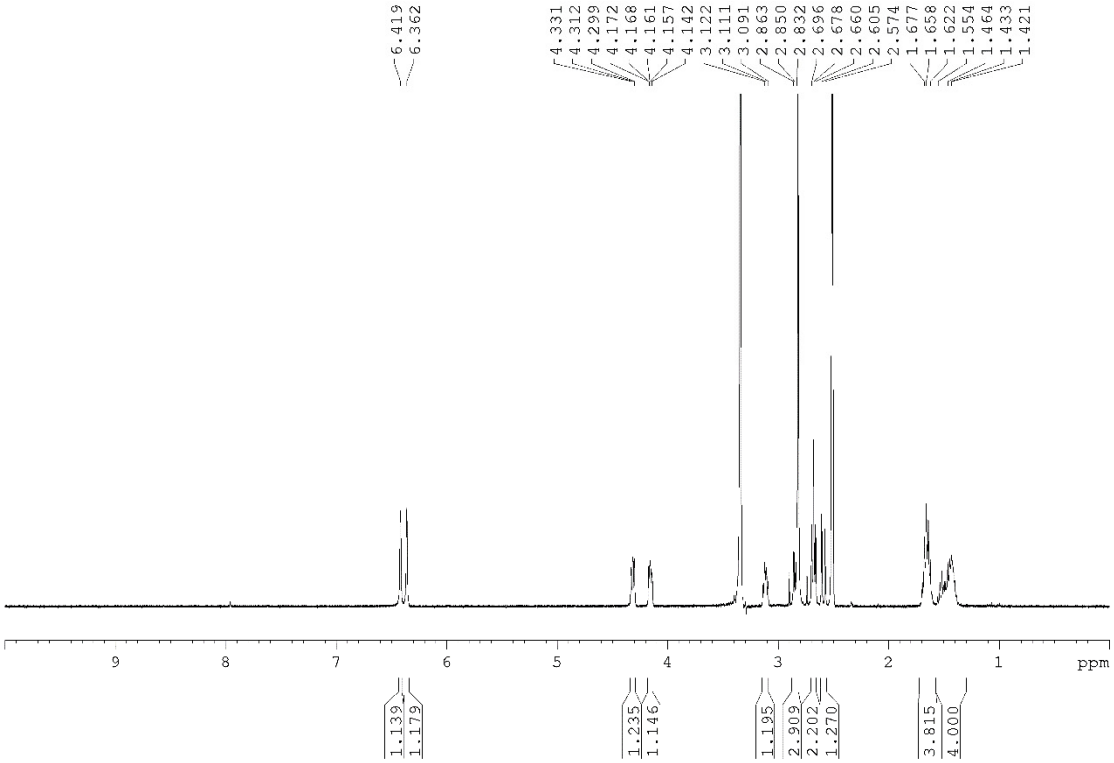

^{13}CNMR

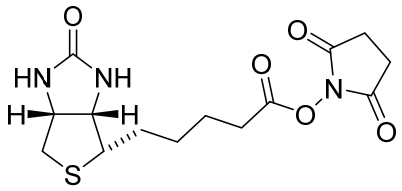
O
HN
NH
H
H
S
O
O
N
O
O

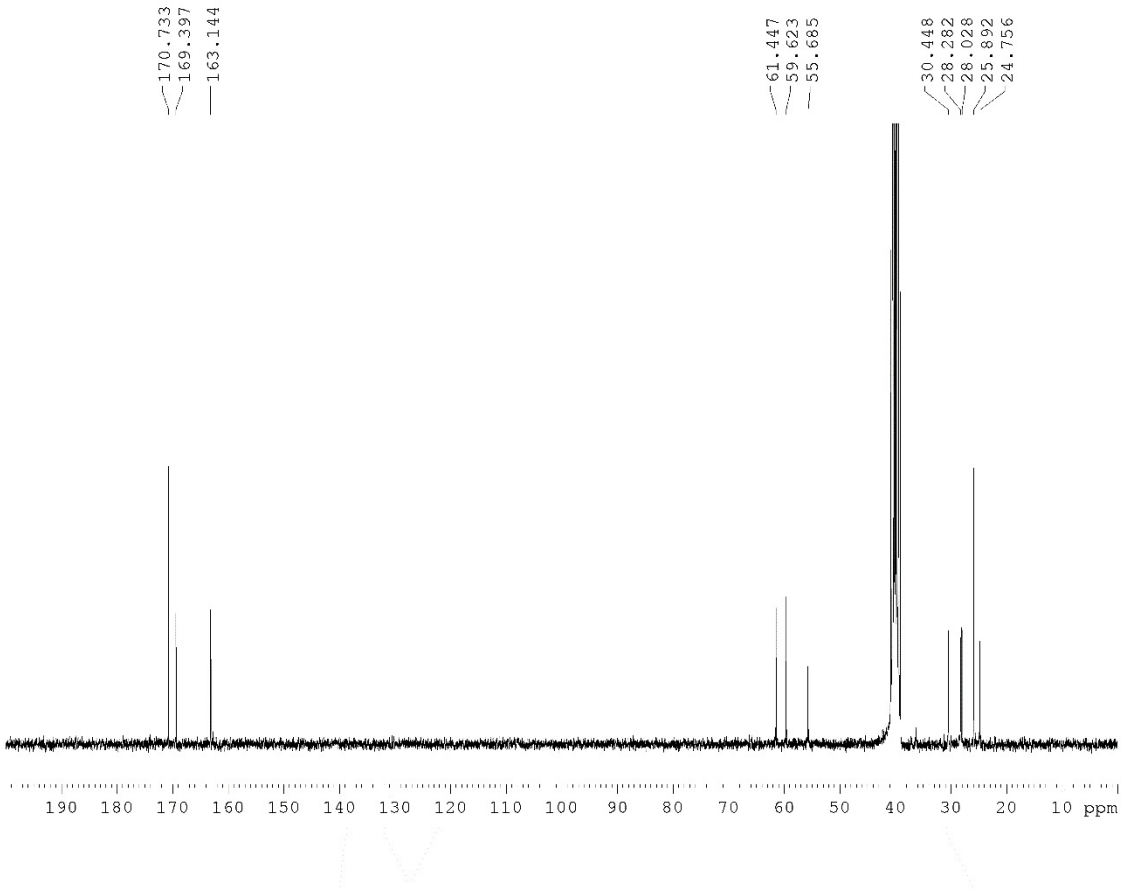
170.733
169.397
163.144
61.447
59.623
55.685
30.448
28.282
28.028
25.892
24.756
190 180 170 160 150 140 130 120 110 100 90 80 70 60 50 40 30 20 10 ppm

tert-butyl(6-(5-((3aS,4S,6aR)-2-oxohexahydro-1H-thieno[3,4-d]imidazol-4-yl) pentanamido) hexyl)carbamate (2.3)

^{1}HNMR

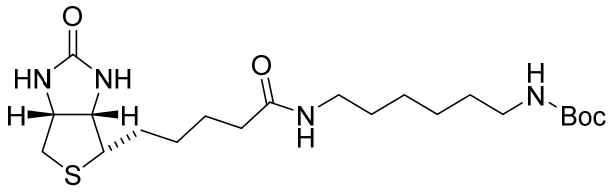

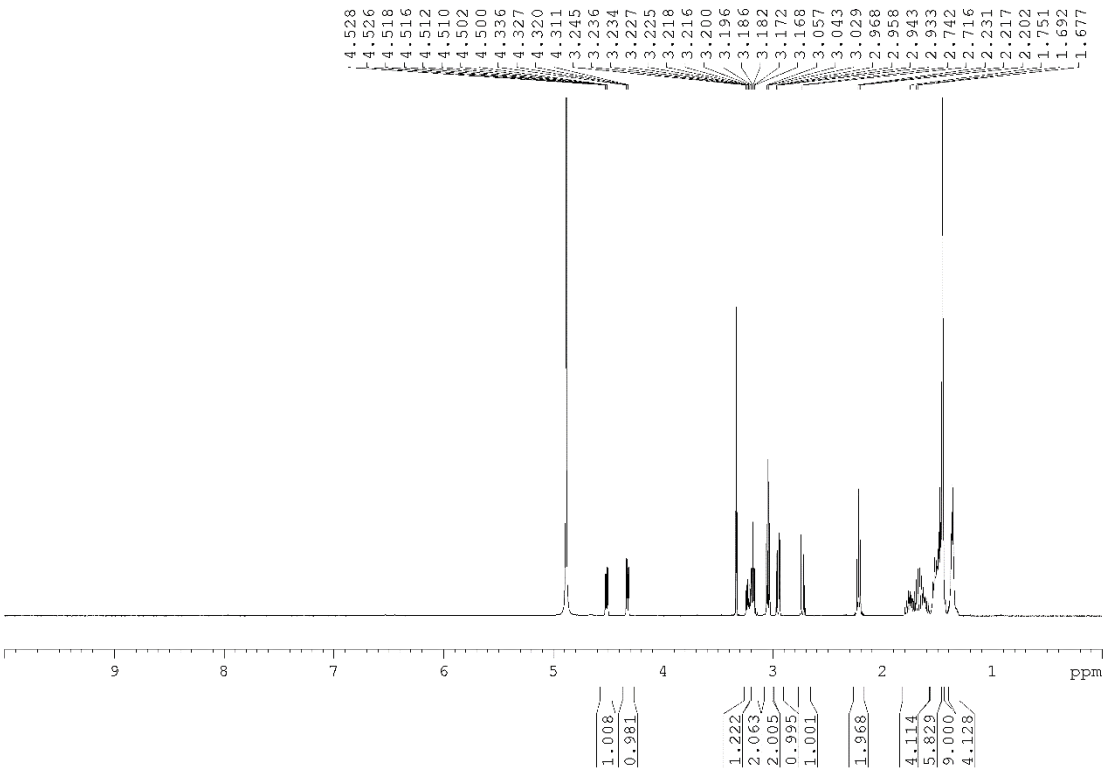

^{13}CNMR

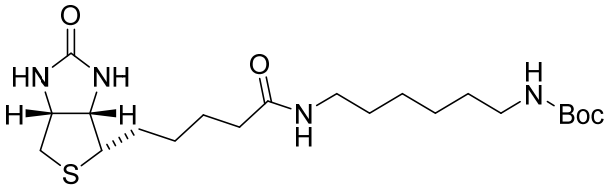
O
HN
NH
H
H
S
O
N
H
H
N
Boc

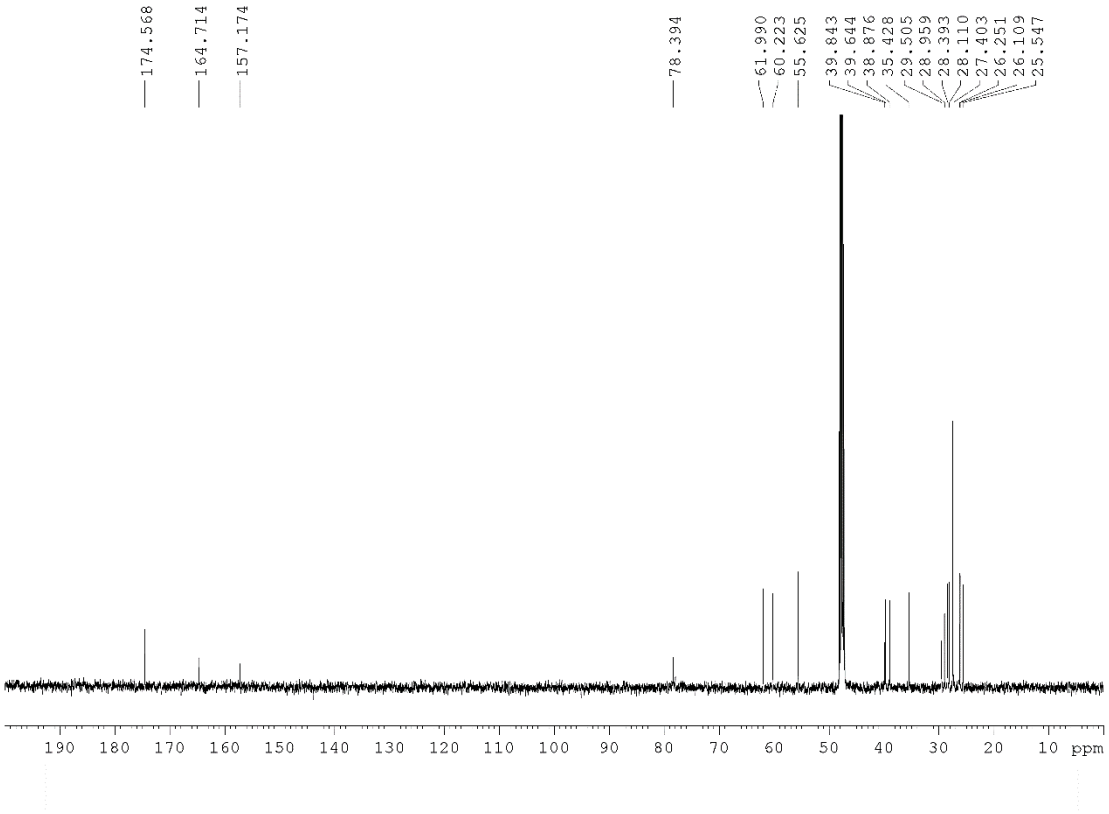
174.568
164.714
157.174
78.394
61.990
60.223
55.625
39.843
39.644
38.876
35.428
29.505
28.959
28.393
28.110
27.403
26.251
26.109
25.547
190 180 170 160 150 140 130 120 110 100 90 80 70 60 50 40 30 20 10 ppm

LCMS

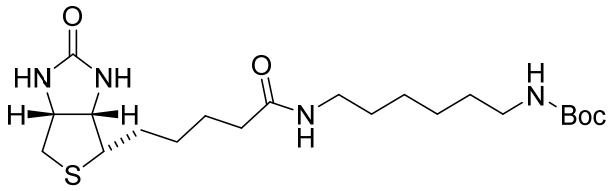
O
HN
NH
H
H
S
O
N
H
H
N
Boc

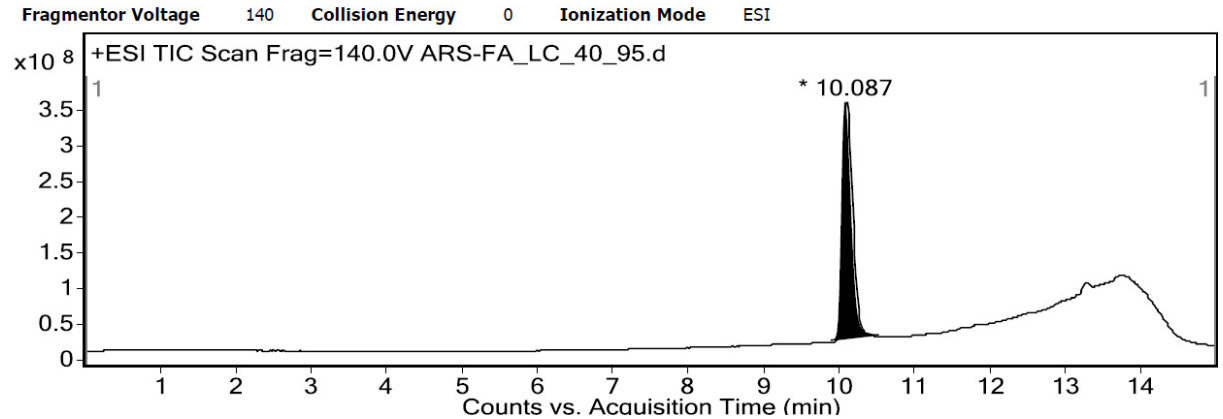
Fragmentor Voltage 140 Collision Energy 0 Ionization Mode ESI
+ESI TIC Scan Frag=140.0V ARS-FA_LC_40_95.d
x10 8
* 10.087
Counts vs. Acquisition Time (min)

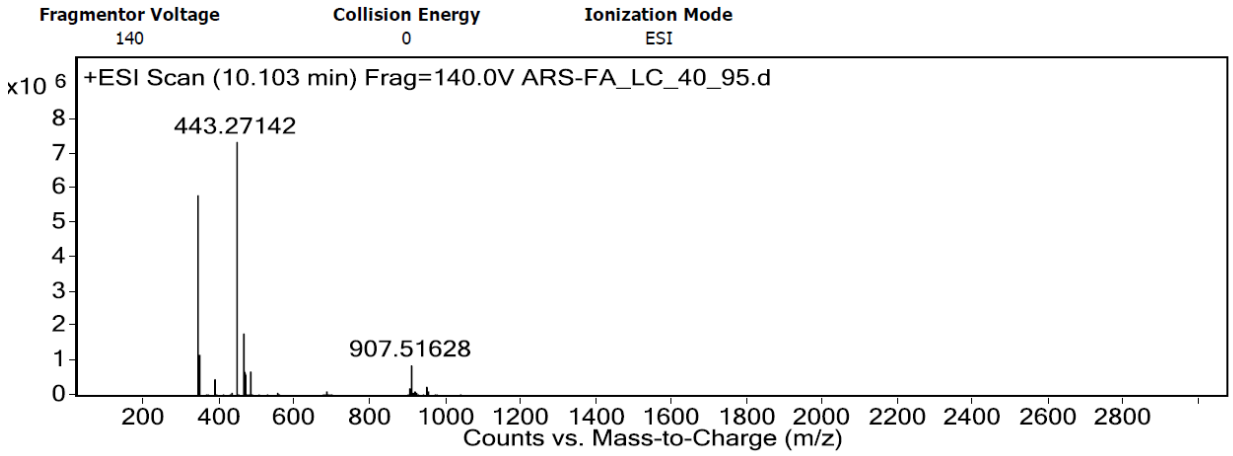
Fragmentor Voltage 140
Collision Energy 0
Ionization Mode ESI
+ESI Scan (10.103 min) Frag=140.0V ARS-FA_LC_40_95.d
x10 6
443.27142
907.51628
Counts vs. Mass-to-Charge (m/z)

6-(5-((3aS,4S,6aR)-2-oxohexahydro-1H-thieno[3,4-d]imidazol-4-yl)pentanamido)hexan-1-aminium (2.4) (Control molecule)

^{1}HNMR

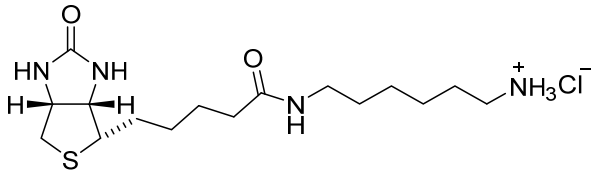

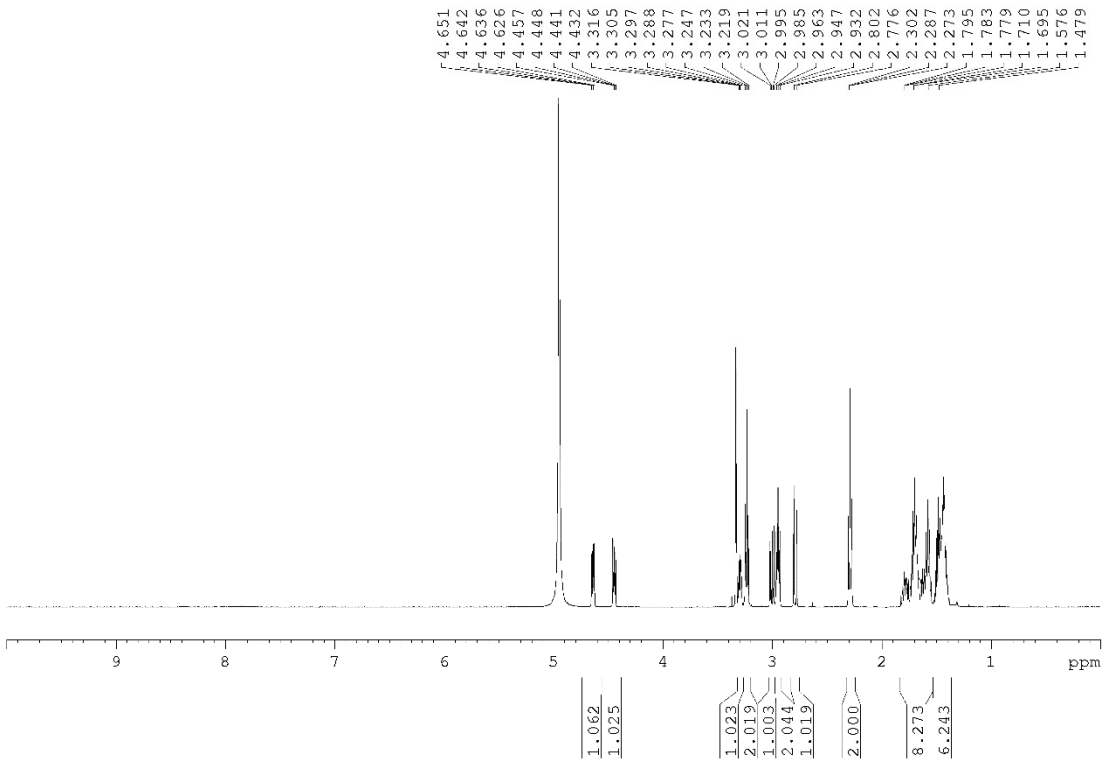

^{13}CNMR

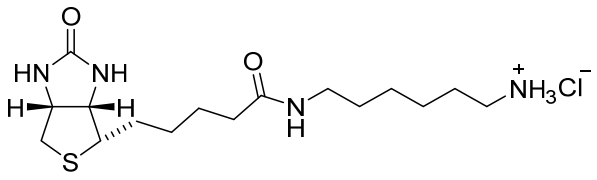
O
HN
NH
H
H
S
O
N
H
+
NH3Cl−

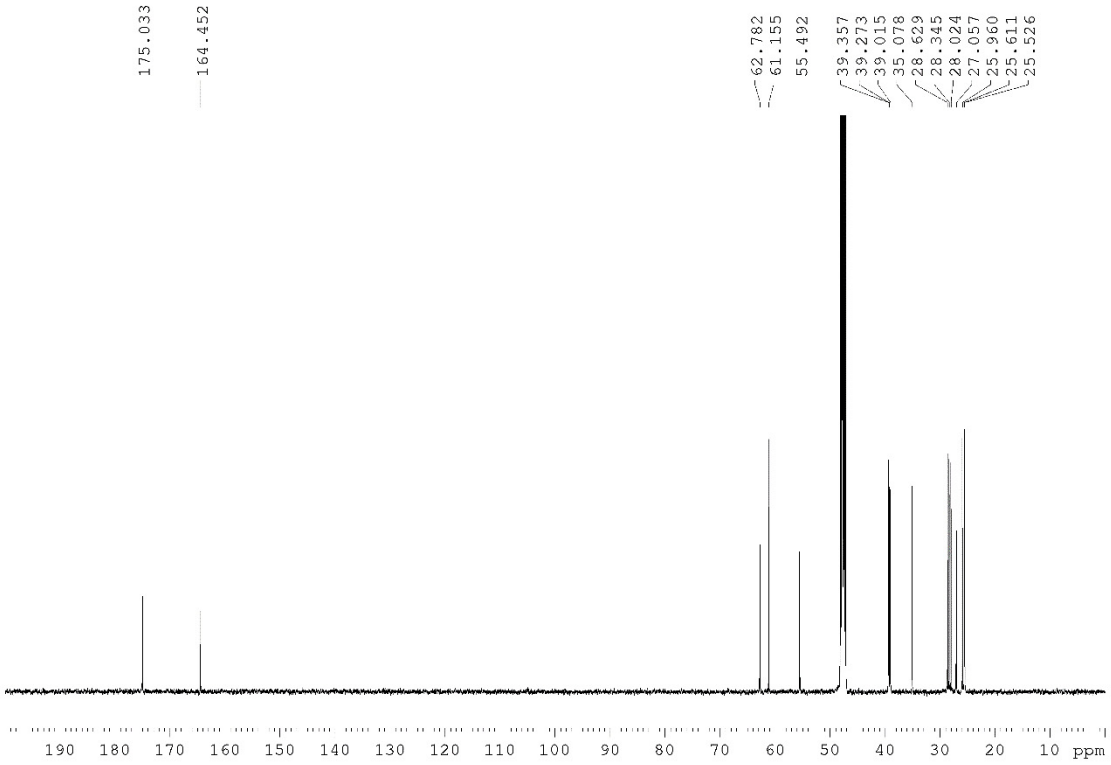
175.033
164.452
62.782
61.155
55.492
39.357
39.273
39.015
35.078
28.629
28.345
28.024
27.057
25.960
25.611
25.526
190 180 170 160 150 140 130 120 110 100 90 80 70 60 50 40 30 20 10 ppm

HSQC

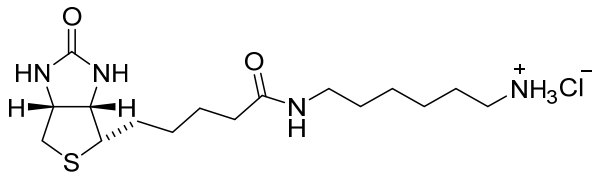
O
HN
NH
H
H
S
O
N
H
+
NH3Cl−

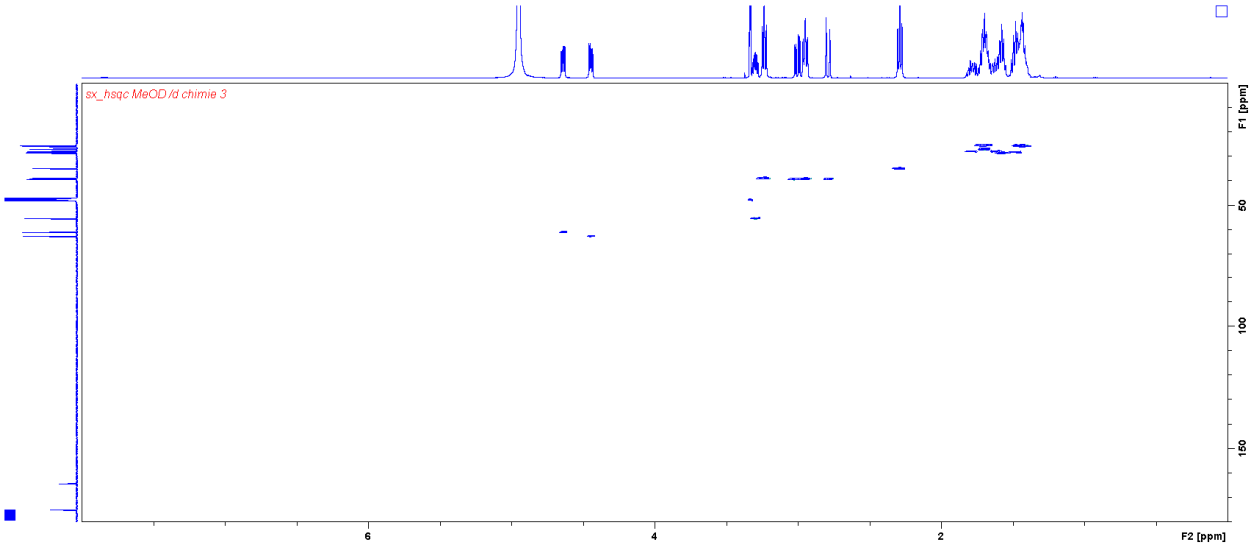
sx_hsqc MeOD /d chimie 3
F1 [ppm]
50
100
150
6
4
2
F2 [ppm]

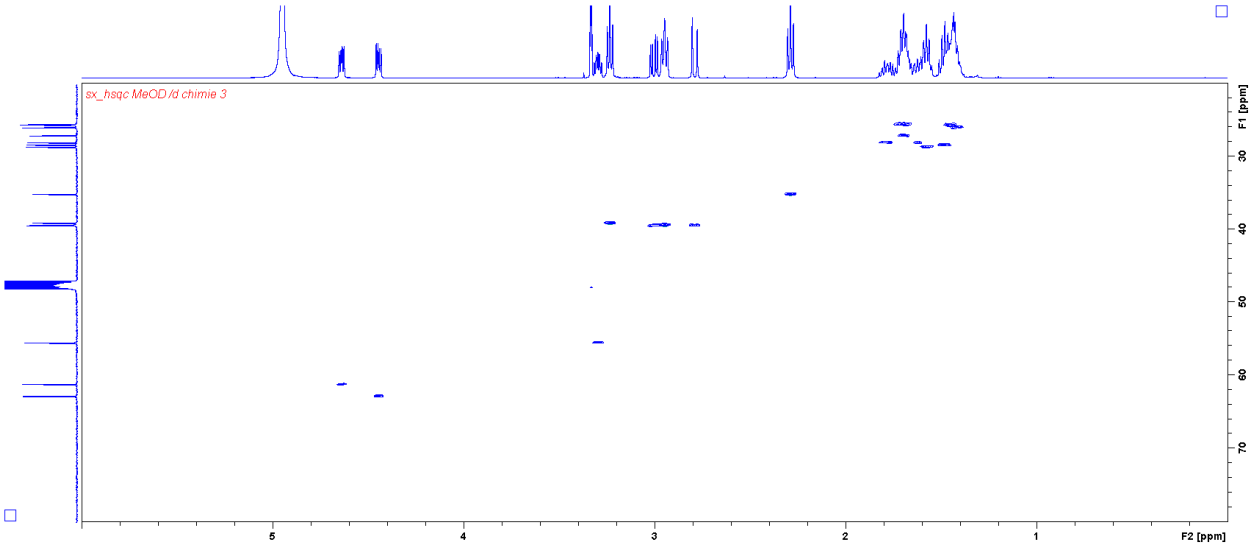
sx_hsqc MeOD /d chimie 3
F1 [ppm]
30
40
50
60
70
5
4
3
2
1
F2 [ppm]

Cosy

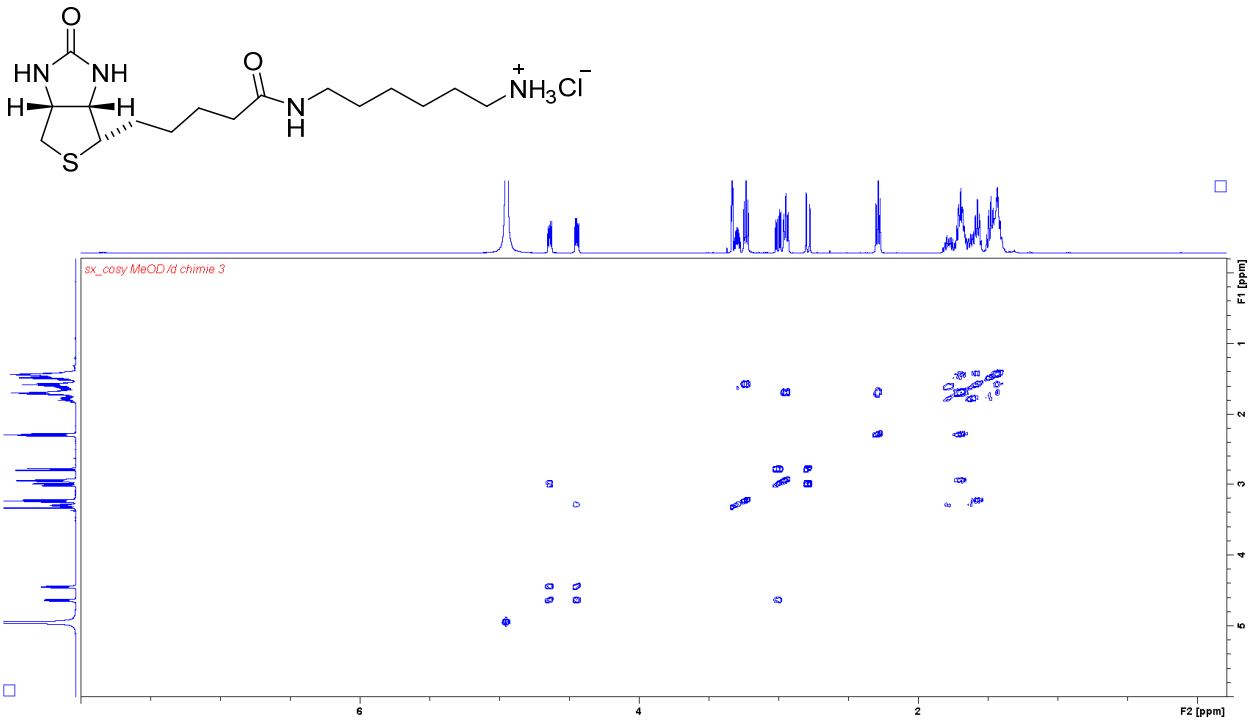

LCMS

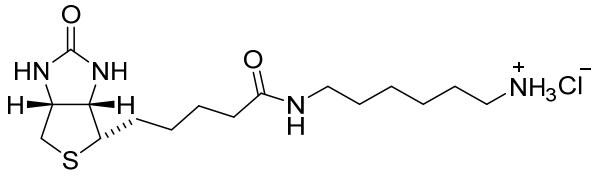
O
HN
NH
H
H
S
O
N
H
NH3Cl

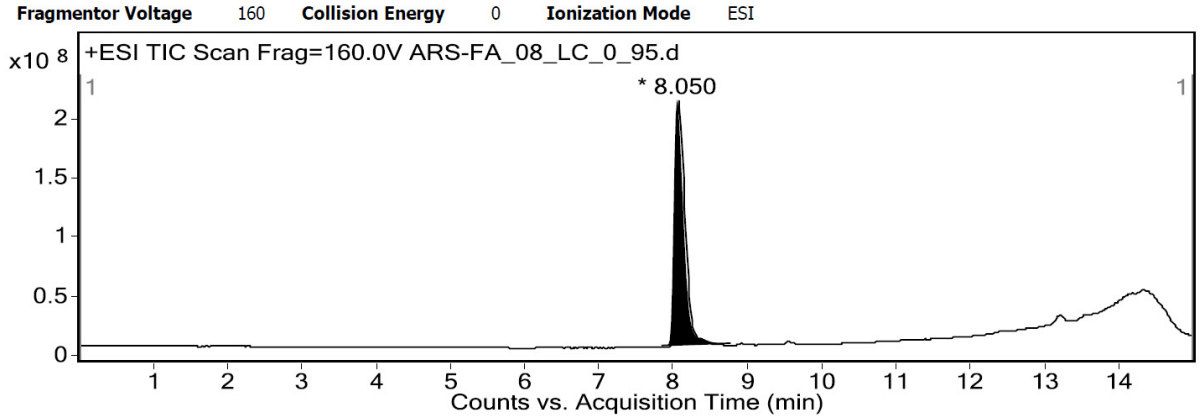
Fragmentor Voltage 160 Collision Energy 0 Ionization Mode ESI
x10 8
+ESI TIC Scan Frag=160.0V ARS-FA_08_LC_0_95.d
* 8.050
Counts vs. Acquisition Time (min)

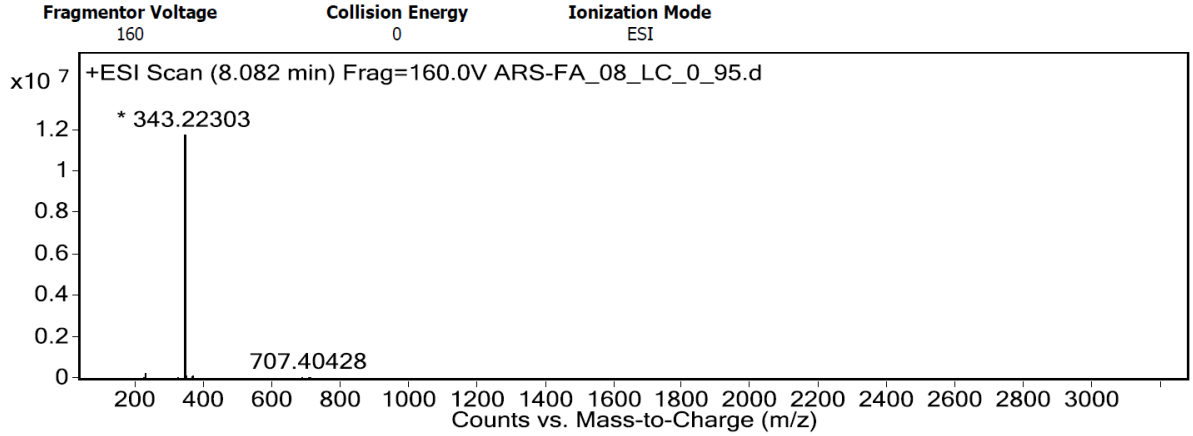
Fragmentor Voltage 160 Collision Energy 0 Ionization Mode ESI
x10 7
+ESI Scan (8.082 min) Frag=160.0V ARS-FA_08_LC_0_95.d
* 343.22303
707.40428
Counts vs. Mass-to-Charge (m/z)

amino((iminio((6-(5-((3aS,4S,6aR)-2-oxohexahydro-1H-thieno[3,4-d]imidazol-4-yl) pentanamido)hexyl)amino)methyl)amino)methaniminium (2.5) (BFB molecule)

^{1}HNMR

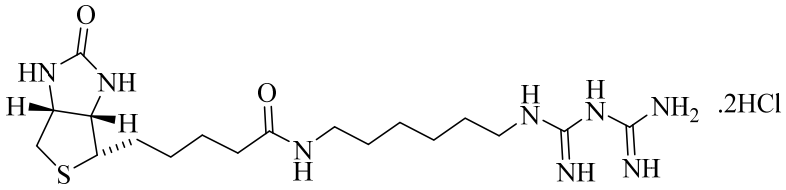

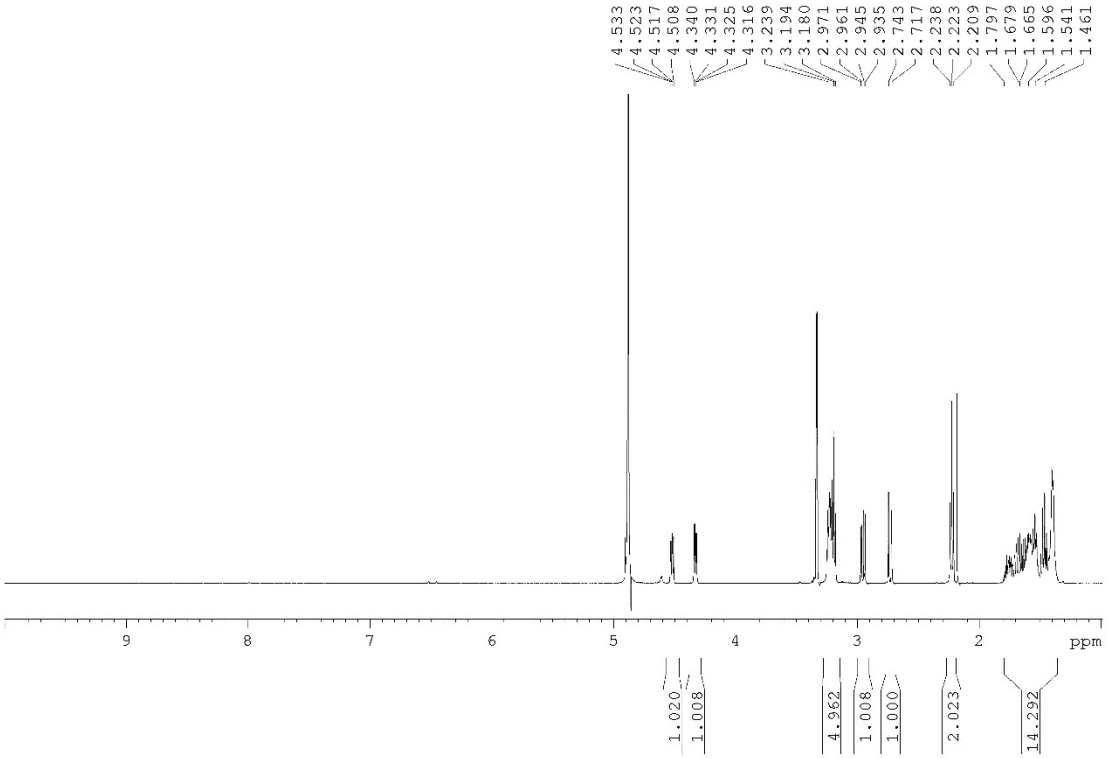

^{13}CNMR

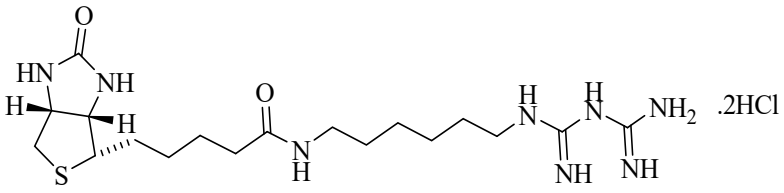
O
HN
NH
H
H
S
O
N
H
H
N
H
N
NH
NH2
.2HCl

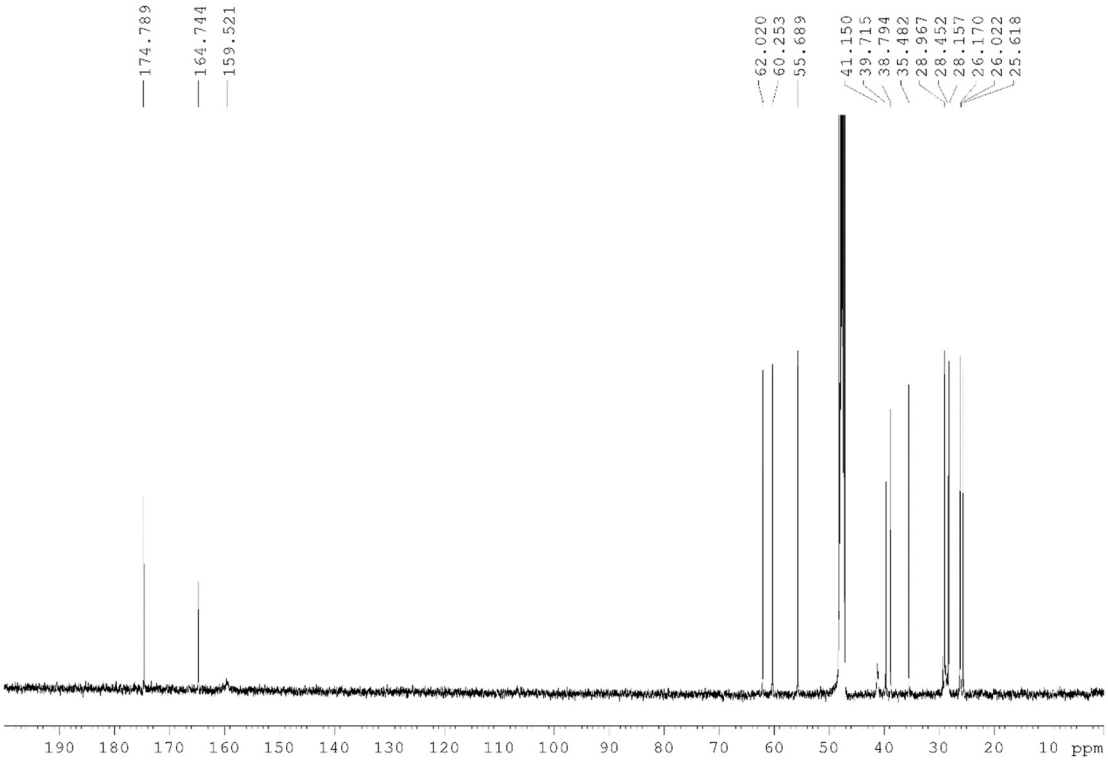
174.789
164.744
159.521
62.020
60.253
55.689
41.150
39.715
38.794
35.482
28.967
28.452
28.157
26.170
26.022
25.618
190 180 170 160 150 140 130 120 110 100 90 80 70 60 50 40 30 20 10 ppm

HSQC

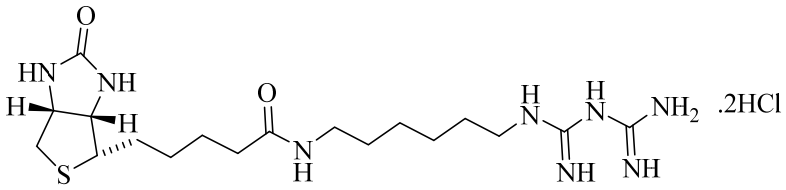
O
HN
NH
H
H
S
O
N
H
H
N
H
N
NH
NH
NH2
.2HCl

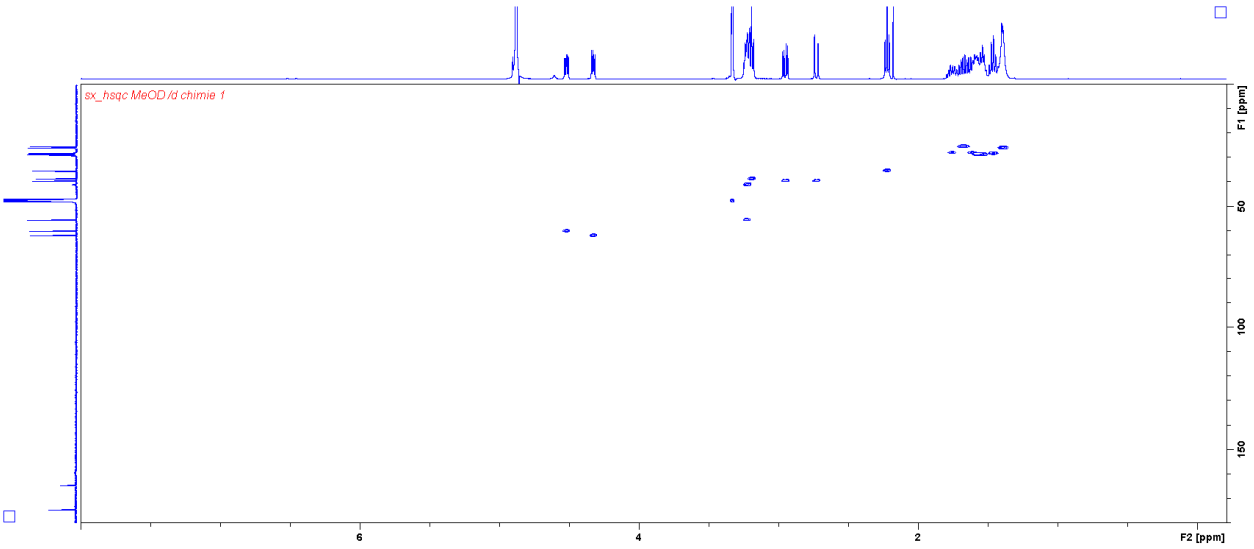
sx_hsqc MeOD /d chimie 1
F1 [ppm]
50
100
150
6
4
2
F2 [ppm]

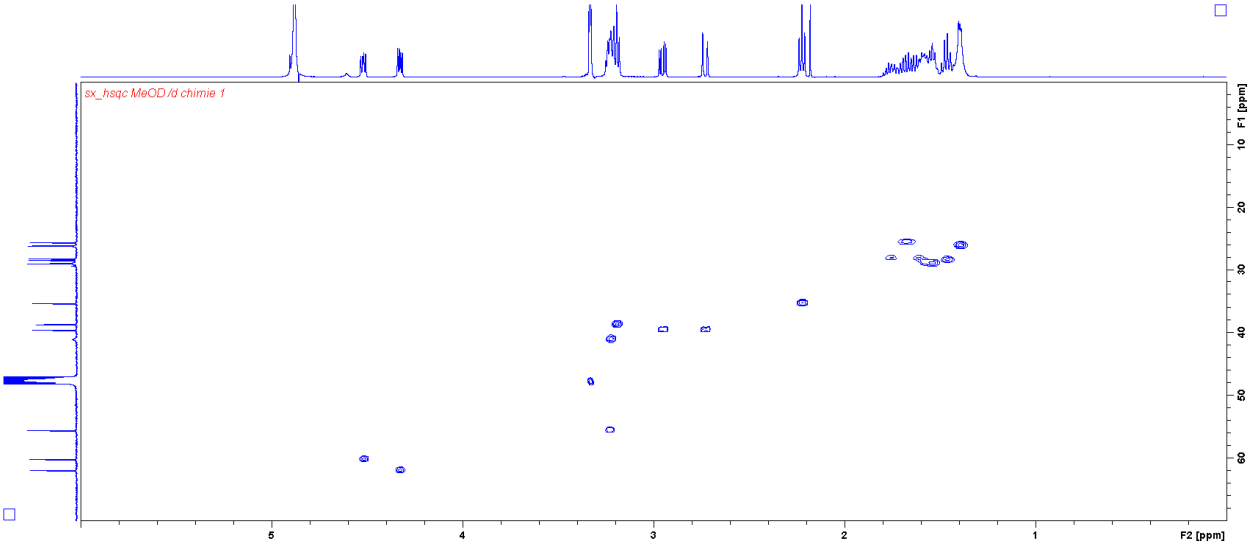
sx_hsqc MeOD /d chimie 1
F1 [ppm]
10
20
30
40
50
60
5
4
3
2
1
F2 [ppm]

Cosy

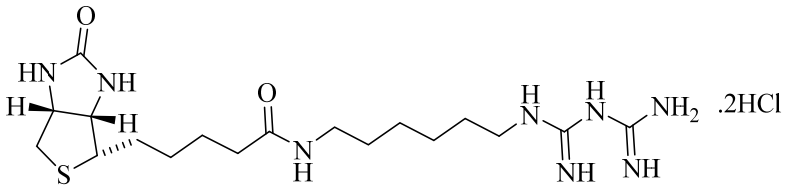
O
HN
NH
H
H
S
O
N
H
H
N
H
N
NH
NH
NH2
.2HCl

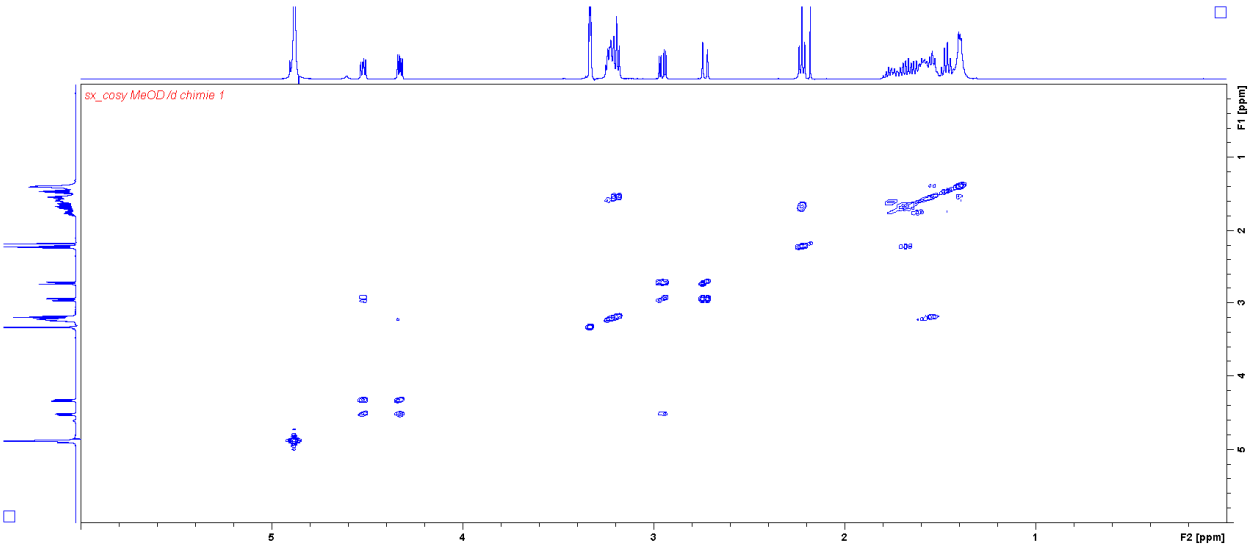
sx_cosy MeOD /d chimie 1
F1 [ppm]
F2 [ppm]
1
2
3
4
5

LCMS

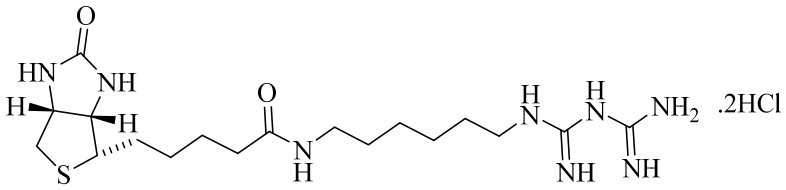
O
HN
NH
H
H
O
N
H
H
N
H
N
NH2
.2HCl
S
NH
NH

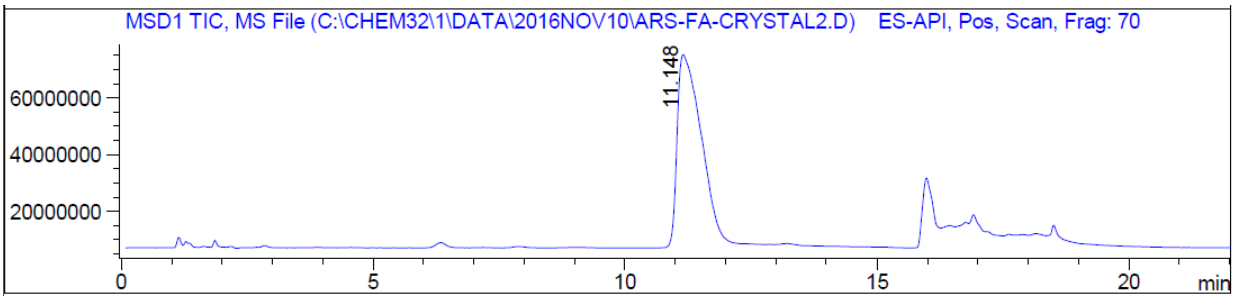
MSD1 TIC, MS File (C:\CHEM32\1\DATA\2016NOV10\ARS-FA-CRYSTAL2.D) ES-API, Pos, Scan, Frag: 70
11.148
60000000
40000000
20000000
0
5
10
15
20
min

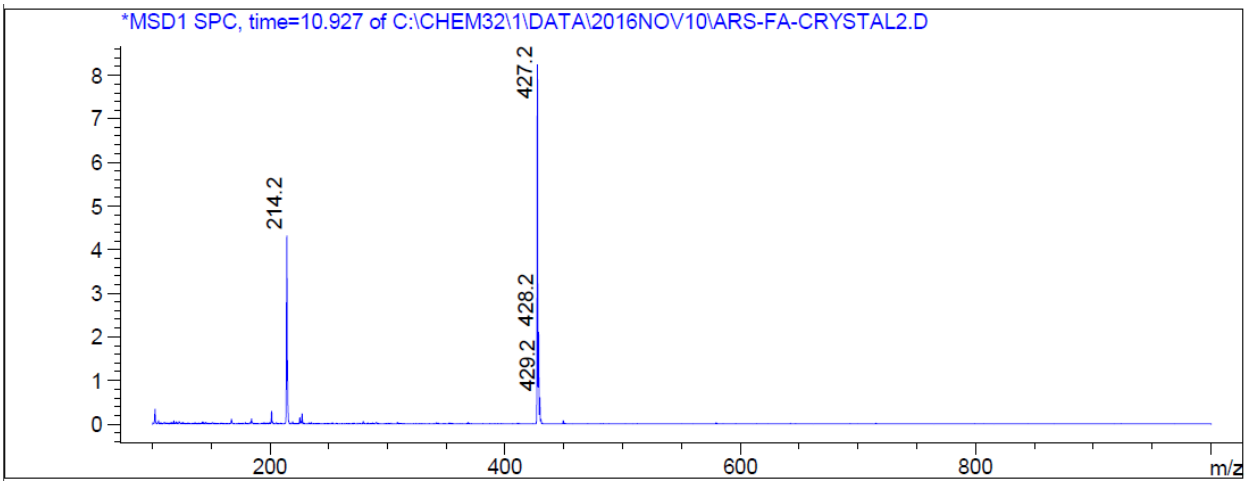
*MSD1 SPC, time=10.927 of C:\CHEM32\1\DATA\2016NOV10\ARS-FA-CRYSTAL2.D
427.2
214.2
428.2
429.2
8
7
6
5
4
3
2
1
0
200
400
600
800
m/z

Assignment of atoms by using 2D NMR:

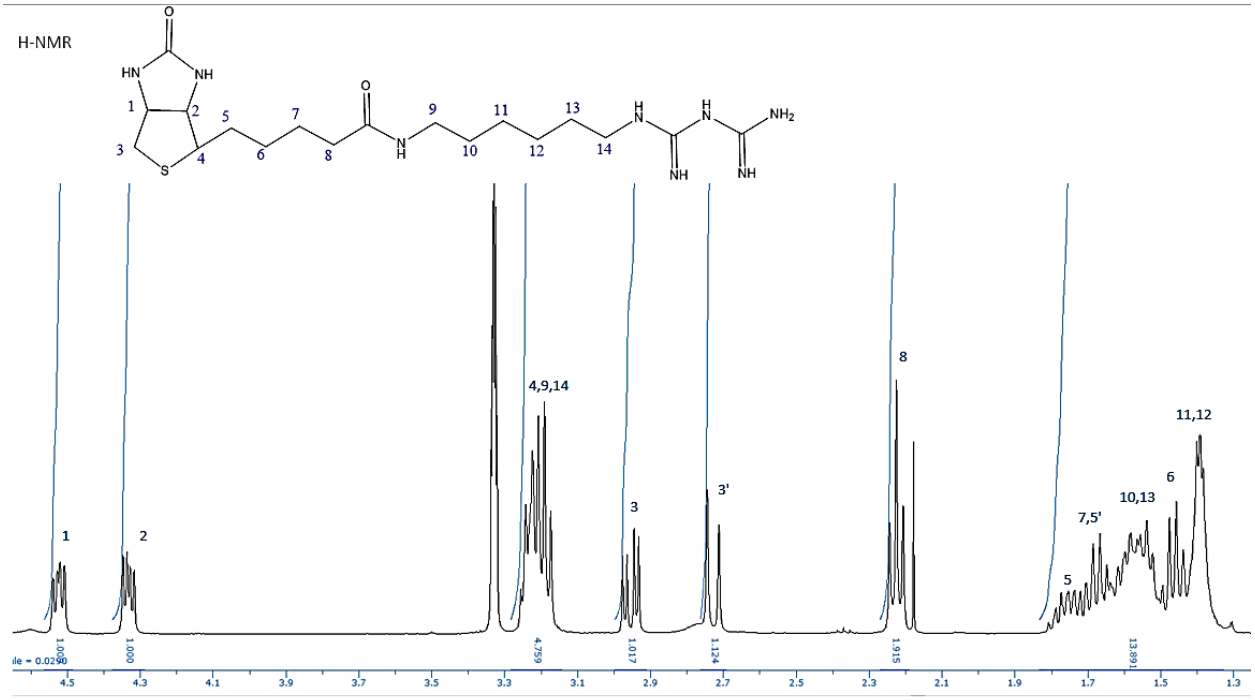

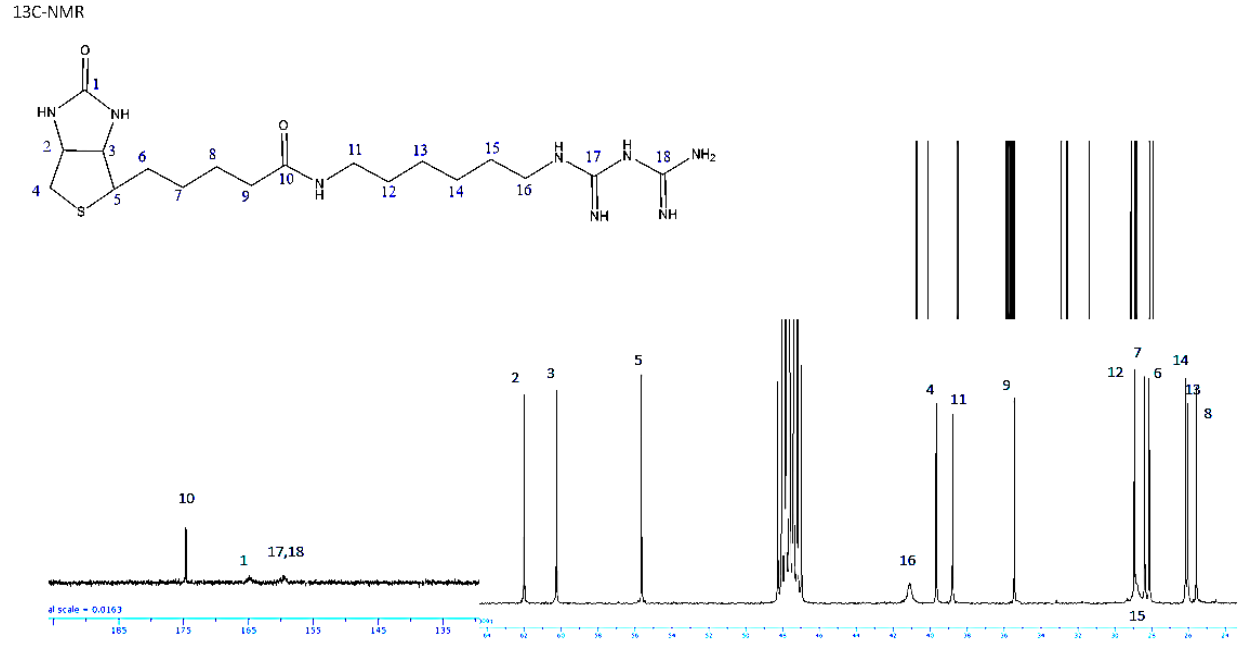

Elemental analysis

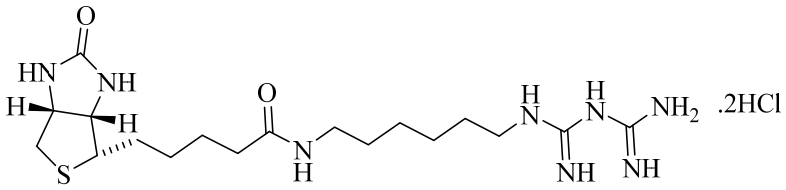

Dossier:	SCH96
Identification de l'échantillon:	ars-fa-52-1
Formule moléculaire:	C18H38N8O2S
Nom de chimiste:	farzaneh mohebali
Nom de responsable:	Schmitzer

Sample Name	% Nitrogen	% Carbon	% Hydrogen	% Sulphur
SCH96-1	22.07	43.77	7.56	7.40
SCH96-2	22.03	43.72	7.57	7.50

	% Nitrogen	**% Carbon**	**% Hydrogen**	**% Sulphur**
Moyenne	22.05	43.74	7.56	7.45
Théorie:	26.21	50.56	8.25	7.50

Technicienne:	Carlos Castro
Chimiste:	Francine Bélanger-Gariépy
Méthode utilisée:	161112E
Date d'analyse:	12-11-2016
Remarque:	sensitive sample; analyses were performed immediately after opening the sample container

Note: During the elemental analysis experiment, the neutral form of the biguanide has been considered for theoretical percentage of atoms. Theoretical percentages are matched with average percentage by considering two chloride binds to the biguanide group and respect to allowed tolerance for each atom.

Allowed tolerance in elemental analysis

	Nitrogen	carbon	Hydrogen	Sulphur
Tolerance limitation	±0.25	±0.3	±0.15	±1

Considering 2 chloride binds to the biguanide

	Nitrogen	carbon	Hydrogen	Sulphur
Theoretical	22.43	43.28	7.26	6.41
Moyenne	22.05	43.74	7.56	7.45

6-((((amino(iminio)methyl)amino)(iminio)methyl)amino)hexan-1-aminium (2.6)

[1]HNMR

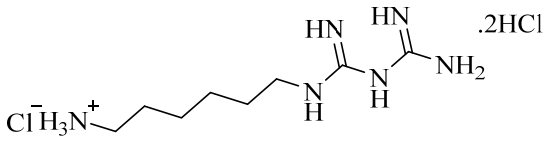

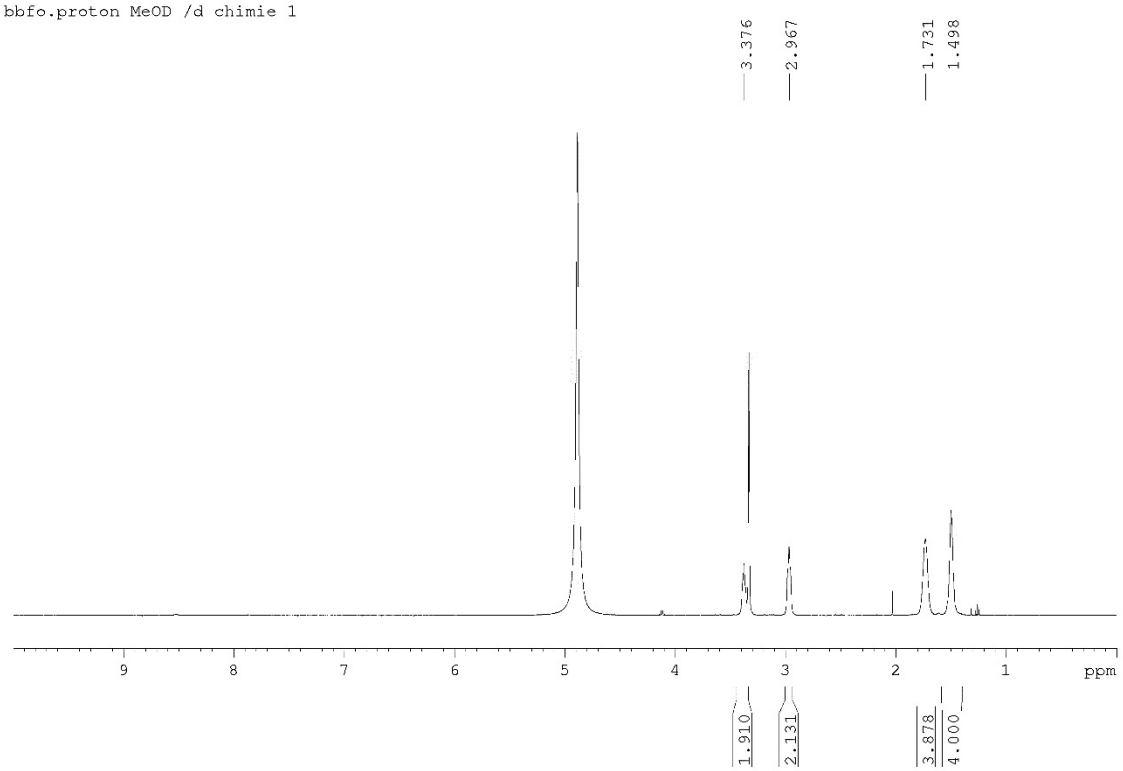

Note: the peaks are broad because of the highly hydrophilic nature of the molecule

^{13}CNMR

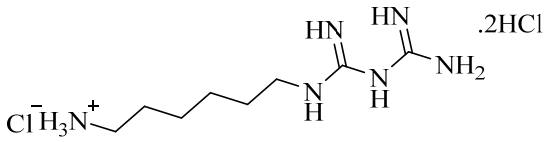
HN
HN
.2HCl
NH2
N
H
N
H
Cl
H3N+

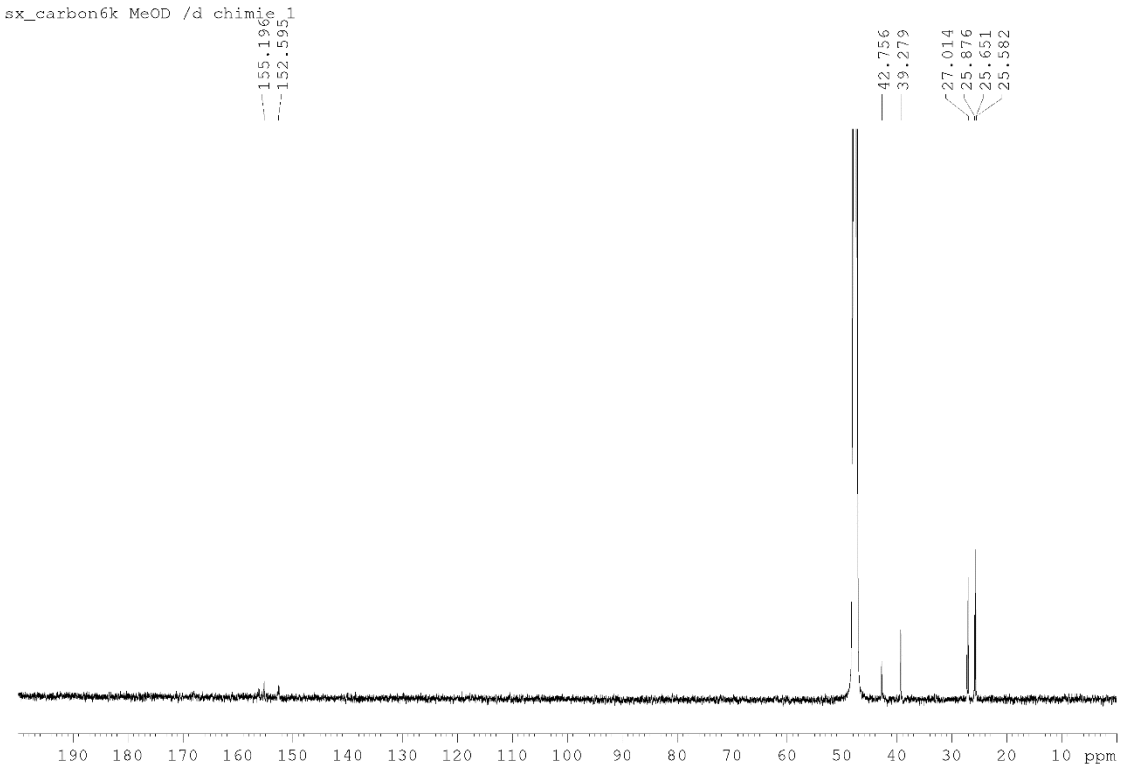
sx_carbon6k MeOD /d chimie 1
155.196
152.595
42.756
39.279
27.014
25.876
25.651
25.582
190 180 170 160 150 140 130 120 110 100 90 80 70 60 50 40 30 20 10 ppm

HSQC

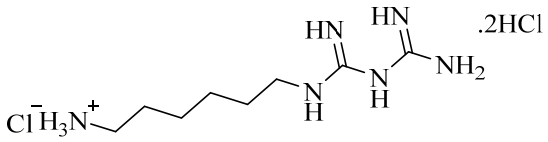
HN
HN
.2HCl
NH2
N
H
N
H
Cl⁻H3N+

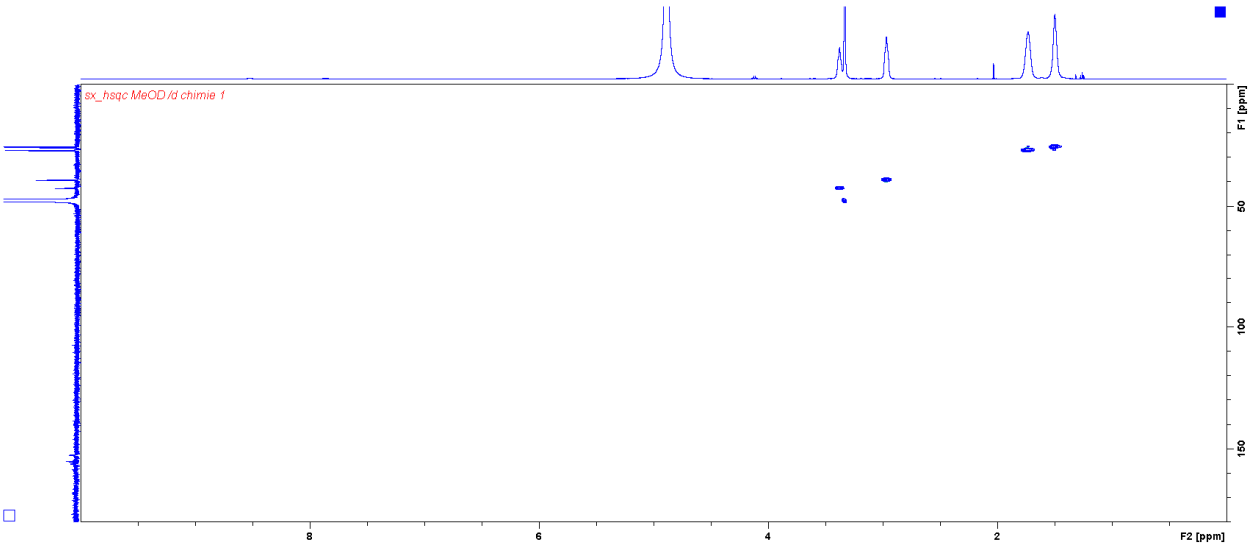
sx_hsqc MeOD fd chimie 1
F1 [ppm]
50
100
150
8
6
4
2
F2 [ppm]

Cosy

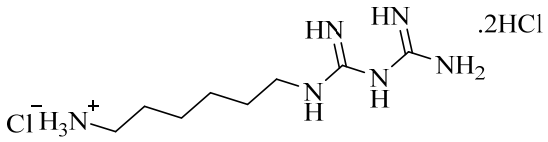
HN
HN
.2HCl
NH2
N
H
N
H
Cl⁻H3N+

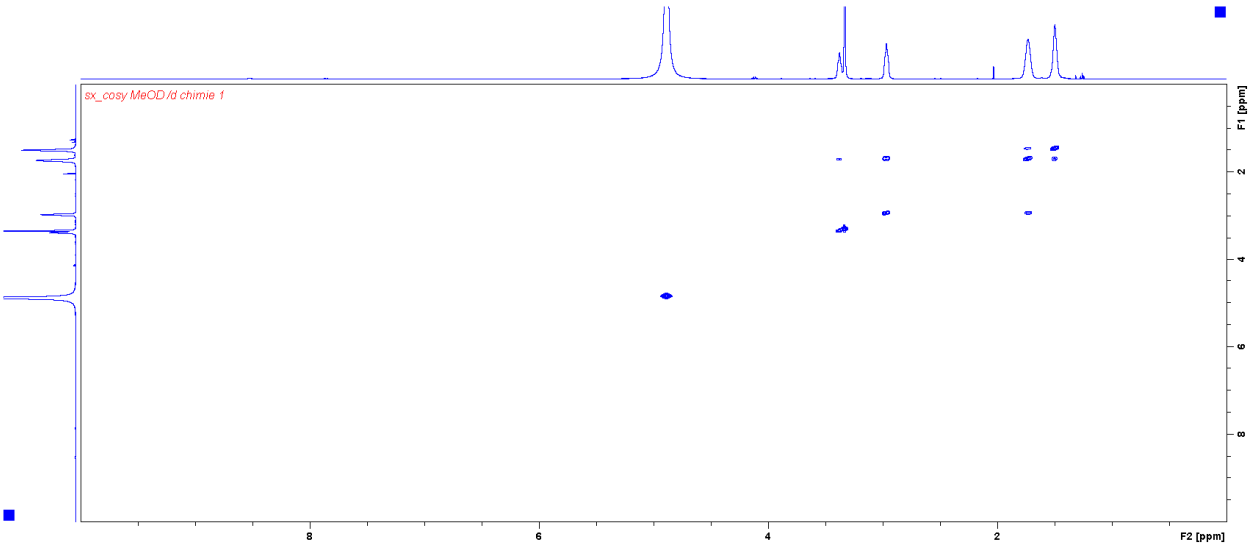
sx_cosy MeOD /d chimie 1
F1 [ppm]
F2 [ppm]
2
4
6
8
8
6
4
2

LC-MS conditions related to chapter 2

(Acq method, LC_20_95_15min_ACN, column, polar RP 30X2.00mm)

Solvent A: H2O.1%FA (Formic Acid)

Solvent B: ACN

	Time	%B	Flow	Max. Press
1	0.00	20.0	0.500	400
2	5.00	40.0	0.500	400
3	14.00	95.0	0.500	400
4	14.10	95.0	0.500	400
5	15	20.00	0.500	400

(Acq method, LC_20_95_15min_MeOH, column, Atlantis C18 3.9x100mm)

Solvent A: H2O.1%FA (Formic Acid)

Solvent B: MeOH

	Time	%B	Flow	Max. Press
1	0.00	20.0	0.500	400
2	5.00	40.0	0.500	400
3	13.00	95.0	0.500	400
4	14.20	95.0	0.500	400
5	15	20.00	0.500	400

(Acq method, LC_0_95_22min_ACN, column Luna 5µ PFP(2) 150x3.00mm)

Solvent A: H2O.1%FA (Formic Acid)

Solvent B: ACN

	Time	%B	Flow	Max. Press
1	0.00	0.0	0.500	400
2	5.00	5.0	0.500	400
3	12.00	8.0	0.500	400
4	13.00	95.0	0.500	400
5	15.00	95.0	0.500	400
6	16.00	0.0	0.500	400
7	22.00	0.0	0.500	400

(Acq method, LC_40_95_10min_MeOH, column, XSelect C18 4.6x100mm)

Solvent A: H2O.1%FA (Formic Acid)

Solvent B: MeOH

	Time	%B	Flow	Max. Press
1	0.00	40.0	0.500	400
2	8.00	95.0	0.500	400
3	10.00	95.0	0.500	400
4	10.20	40.0	0.500	400

(Acq method, LC_0_95_15min_MeOH, column, XSelect C18 4.6x100mm)

Solvent A: H2O.1%FA (Formic Acid)

Solvent B: MeOH

	Time	**%B**	**Flow**	**Max. Press**
1	0.00	0.0	0.500	400
2	9.00	8.0	0.500	400
3	10.00	95.0	0.500	400
4	14.10	95.0	0.500	400
5	15	0.00	0.500	400